ACS BIO & MED CHEM Au
AN OPEN ACCESS JOURNAL OF THE AMERICAN CHEMICAL SOCIETY

pubs.acs.org/biomedchemau

Review

Recent Advances in Discovery, Bioengineering, and Bioactivity-Evaluation of Ribosomally Synthesized and Post-translationally Modified Peptides

Guannan Zhong,[†] Zong-Jie Wang,[†] Fu Yan, Youming Zhang, and Liujie Huo*

Cite This: *ACS Bio Med Chem Au* 2023, 3, 1−31

Read Online

ACCESS | Metrics & More | Article Recommendations

ABSTRACT: Ribosomally synthesized and post-translationally modified peptides (RiPPs) are of increasing interest in natural products as well as drug discovery. This empowers not only the unique chemical structures and topologies in natural products but also the excellent bioactivities such as antibacteria, antifungi, antiviruses, and so on. Advances in genomics, bioinformatics, and chemical analytics have promoted the exponential increase of RiPPs as well as the evaluation of biological activities thereof. Furthermore, benefiting from their relatively simple and conserved biosynthetic logic, RiPPs are prone to be engineered to obtain diverse analogues that exhibit distinct physiological activities and are difficult to synthesize. This Review aims to systematically address the variety of biological activities and/or the mode of mechanisms of novel RiPPs discovered in the past decade, albeit the characteristics of selective structures and biosynthetic mechanisms are briefly covered as well. Almost one-half of the cases are involved in anti-Gram-positive bacteria. Meanwhile, an increasing number of RiPPs related to anti-Gram-negative bacteria, antitumor, antivirus, etc., are also discussed in detail. Last but not least, we sum up some disciplines of the RiPPs' biological activities to guide genome mining as well as drug discovery and optimization in the future.

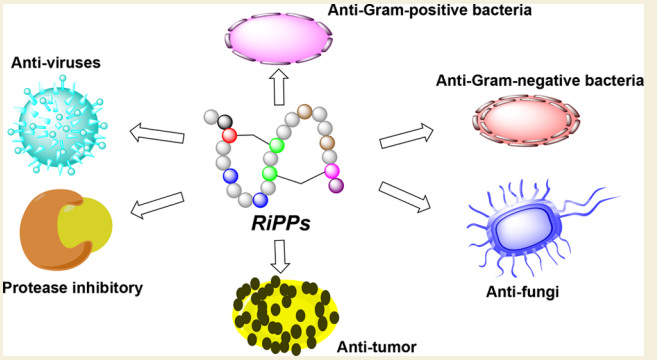

KEYWORDS: *Peptide, RiPPs, post-translational modifications, bioengineering, biological activities, anti-infective, antitumor, mode of mechanism, pharmaceuticals*

1. INTRODUCTION

There is an urgent need to identify novel therapeutic agents because of the potential development of tolerance or resistance to current anti-infectious agents. This concerns all the treatment of bacterial, fungal, and viral infections, as well as tumors and other incurable diseases.[1] Natural products have been of great interest for decades since they have been the most important source of potential drug leads and continue providing unique structural diversity for discovering novel lead compounds.[2] Polyketides, nonribosomal peptides, terpenoids, and alkaloids are four predominant groups of natural products explored in the last century. Nevertheless, advances in genomics, bioinformatics, and chemical analytics have paved the way for ribosomally synthesized and post-translationally modified peptides (RiPPs), a structurally diverse group of natural products with a broad spectrum of biological activities as well as mode of mechanisms.

The biosynthesis of RiPPs proceeds via ribosomally assembled precursor peptides that undergo post-translational modifications to gain their biological functions. Precursor peptides with a short length are usually constituted of an *N*-terminal leader peptide which recruits different post-translational modification (PTM) enzymes and a *C*-terminal core peptide with a sequence of amino acids that makes up the structural backbone of RiPPs. In some instances, the leader peptide (follower peptide) is attached at the *C*-terminus rather than the typically *N*-terminus of the precursor. In rare cases, a signal sequence or a recognition sequence could be found at the *N*-terminal of the precursors, respectively (Figure 1).

Generally, the leader peptide-dependent PTMs are highly promiscuous with different mutations in the core peptide, facilitating bioengineering efforts and structure−activity relationship (SAR) studies of RiPPs. Peptidases are needed to cleave the leader peptides of the precursors following the

Received: October 10, 2022
Revised: November 17, 2022
Accepted: November 22, 2022
Published: December 21, 2022

https://doi.org/10.1021/acsbiomedchemau.2c00062
ACS Bio Med Chem Au 2023, 3, 1−31

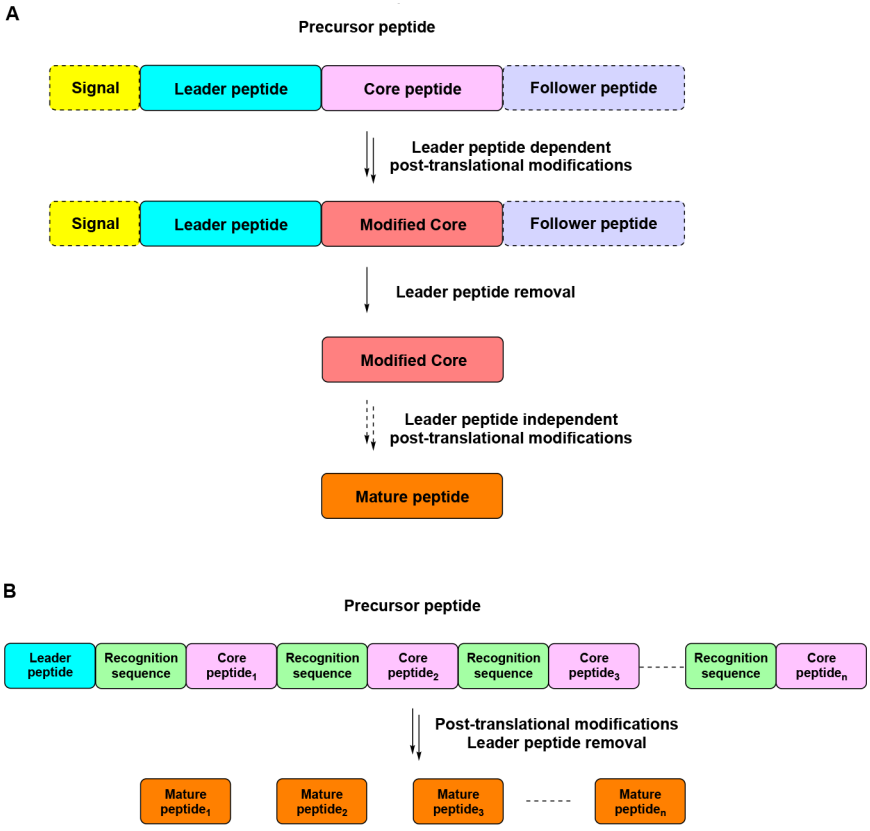

Figure 1. Biosynthetic route of RiPPs. (A) General biosynthetic pathway of RiPPs. The precursor peptide consists of a leader peptide and a core peptide. The core region is post-translationally modified in a leader peptide-dependent and (or) independent manner to generate the mature RiPP. (B) Multiple copies of the recognition sequences and the following core peptides are distributed in the precursor peptide in some RiPPs. The sequences of the core peptides can be highly diverse, which results in different RiPP products.

Table 1. Bioactive RiPPs and the (Proposed) Targets Thereof Reported in the Past Decade

RiPP compound	RiPP class	biological activity	(proposed) target	ref
Homicorcin	lanthipeptide	anti-Gram-positive	cytoplasmic membrane	ref 46
Bicereucin	lanthipeptide	anti-Gram-positive	the outer surface of the bacterial cell	ref 49
Ruminococcin C1	sactipeptide	anti-Gram-positive	ATP synthesis	refs 62−64
Huazacin/Thuricin Z	sactipeptide	anti-Gram-positive	bacterial cell membrane	refs 66, 67
Hyicin 4244	sactipeptide	anti-Gram-positive	staphylococcal biofilm	ref 70
Arcumycin	lasso peptide	anti-Gram-positive	bacterial cell wall, lipid II	ref 83
Cacaoidin	lanthidin	anti-Gram-positive	bacterial cell wall, lipid II	ref 93
$YydF_{33-49DD}$	epipeptide	anti-Gram-positive	bacterial cell membrane	ref 96
Klebsazolicin/Phazolicin	LAP	anti-Gram-negative	the peptide exit tunnel of 70S ribosome	refs 111, 112
Darobactins	darobactins	anti-Gram-negative	BamA, the central component of complex for both folding and insertion of outer membrane proteins	refs103−108
Dynobactin A	dynobactins	anti-Gram-negative	BamA, the central component of complex for both folding and insertion of outer membrane proteins	ref 109
Citrocin/Acinetodin/ Klebsidin	lasso peptide	anti-Gram-negative	RNA polymerase	refs 113, 115
Aeronamide A	proteusins	antitumor activity	Cell membrane (pore-forming)	ref 138
XY3-3	lanthipeptide	antiviral activity	UEV domain of the human TSG101 protein	ref 162
Stlassin	lasso peptide	antagonistic activity	Toll-like receptor 4 (TLR4)	ref 168

https://doi.org/10.1021/acsbiomedchemau.2c00062
ACS Bio Med Chem Au 2023, 3, 1−31

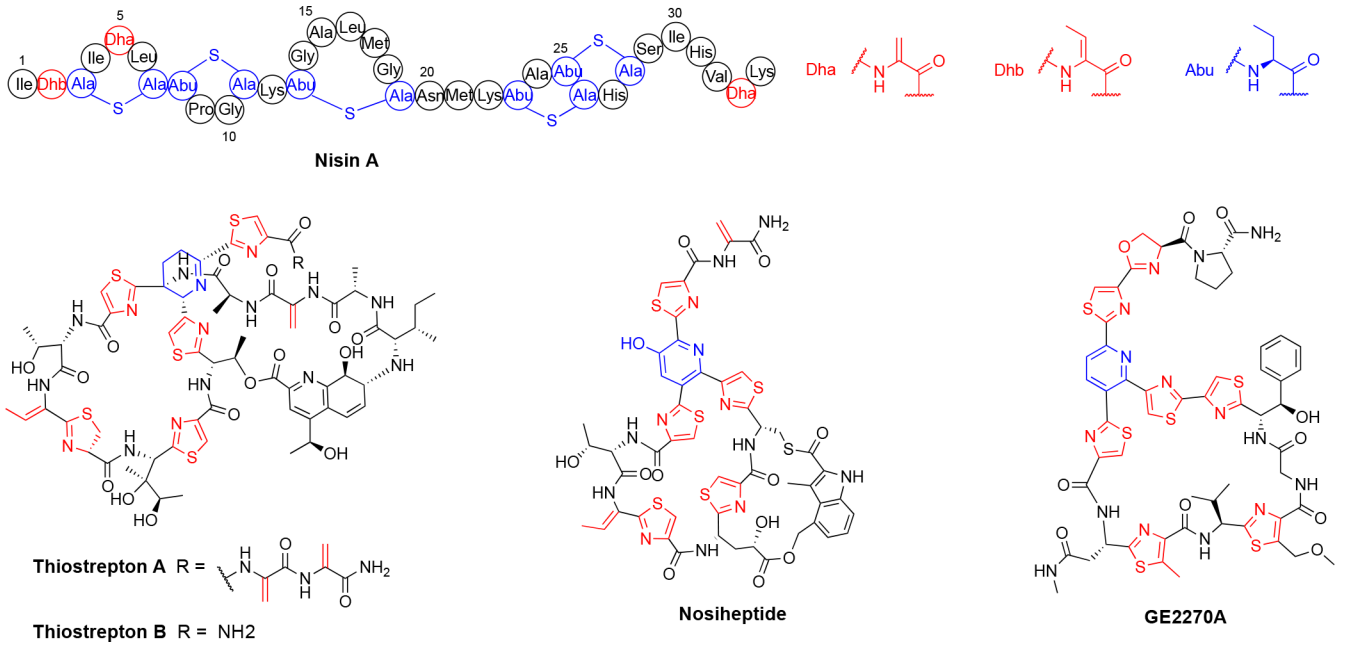

Figure 2. Structures of nisin A, thiostreptons, nosiheptide, and GE2270A, the RiPPs applied in commercial/clinical trials. The class-defining PTMs are highlighted in blue, and other PTMs are highlighted in red.

leader peptide-dependent PTMs and release the modified core peptides, which could be exported to the extra cell as mature peptides or be further modified by leader peptide-independent PTM enzymes prior to export (Figure 1). As detailed and comprehensive reviews have summarized the novel structural scaffolds, the biosynthetic mechanisms and corresponding intriguing PTM enzymes,[3,4] in this review we mainly focus on the diverse biological activities, the (proposed) mode of mechanisms of selective RiPPs, and the bioengineered derivatives in the past decade (Table 1).

Preliminary to the main text, the characteristics of the major classes of RiPPs mentioned in this Review are selectively introduced briefly.

Lanthipeptides represent the largest class and one of the well-characterized classes of the RiPP family. Their characteristic is the presence of lanthionine (Lan) and/or methyllanthionine (MeLan) thioether bridged amino acids that create a high thermal, chemical, and proteolytic stability. The formation of Lan and MeLan requires the dehydration of Ser and Thr residues to 2,3-didehydroalanine (Dha) and 2,3-didehydrobutyrine (Dhb), respectively. Then the hydrosulfide group of Cys residue undergoes a Michael-type addition to the nascent Dha or Dhb to produce Lan or MeLan, respectively.[5] According to the differences between the (Me)Lan biosynthetic enzymes, lanthipeptides are subdivided into five classes at present.[4,6,7] For Class I lanthipeptide, dehydration and cyclization reactions are catalyzed by dehydratase LanB and a zinc-dependent cyclase LanC, respectively.[8,9] Biosynthetic enzymes of class II, III and IV are all bifunctional enzymes termed LanM (Class II), LanKC (Class III), and LanL (Class IV).[6] Recently, a new lanthipeptide termed lexapeptide was identified and proved to be biosynthesized by a trienzyme cascade termed LxmK, LxmX, and LxmY.[7] Lexapeptide was assigned as the first member of Class V lanthipeptide. With respect to the biosynthetic mechanism, Class I LanB dehydratase employs glutamyl-tRNA to activate the side chains of Ser and/or Thr residues followed by glutamate elimination,[8,10] whereas class II–IV dehydratase domain of the biosynthetic enzymes utilize NTPs to phosphorylate Ser and/or Thr residues prior to dephosphorylation.[6,11,12] Except for Lan and MeLan, it is noteworthy that an additional carbon–carbon cross-link termed (methyl)-labionin ((Me)Lab) could be formed by a subgroup of LanKC enzymes. The Lab is generated putatively by the attack of the enolate intermediate onto another dehydroalanine located in the core peptide.[13,14]

Sulfur to α-carbon cross-linked peptides (sactipeptides) and radical non-α-carbon thioether peptides (ranthipeptides) are also featured with one or more thioether bonds like the structurally similar lanthipeptides. The thioether bonds in sactipeptides and ranthipeptides are between the sulfur atom of a Cys residue and the α-carbon (sactipeptides) or β-/γ-carbon (ranthipeptides) of an acceptor residue. Superficial resemblance of the chemical structures of sactipeptides and ranthipeptides indicates resemblant biosynthetic pathways, as both of the biosynthetic gene clusters (BGCs) include a Cys-rich precursor peptide and a radical *S*-adenosylmethionine (SAM)-dependent enzyme that forms thioether linkages, which are distinguished from the Michael-type addition involved in the formation of β-thioether linkages to Dha/Dhb in lanthipeptides.[15,16]

Thiopeptides represent a group of highly modified RiPPs with a central pyridine ring, a core macrocyclic ring, both of which are formed via an unusual enzymatic [4 + 2] cycloaddition on two Dha-containing fragments, and a tail that is linked to the macrocyclic ring via the central pyridine. The thiopeptide macrocycle is further decorated with additional thiazole and/or (methyl)oxazole rings as well as multiple dehydrated amino acid residues.[17,18] LAPs are structurally similar to thiopeptides in having a full set of dehydroamino acids and thiazole and/or (methyl)oxazole rings, resulting from dehydration of Ser/Thr and cyclization of Cys and Ser (Thr) side chains on nonmacrocyclized natural products, which are different from thiopeptides and cyanobactins. The latter is also

https://doi.org/10.1021/acsbiomedchemau.2c00062
ACS Bio Med Chem Au 2023, 3, 1–31

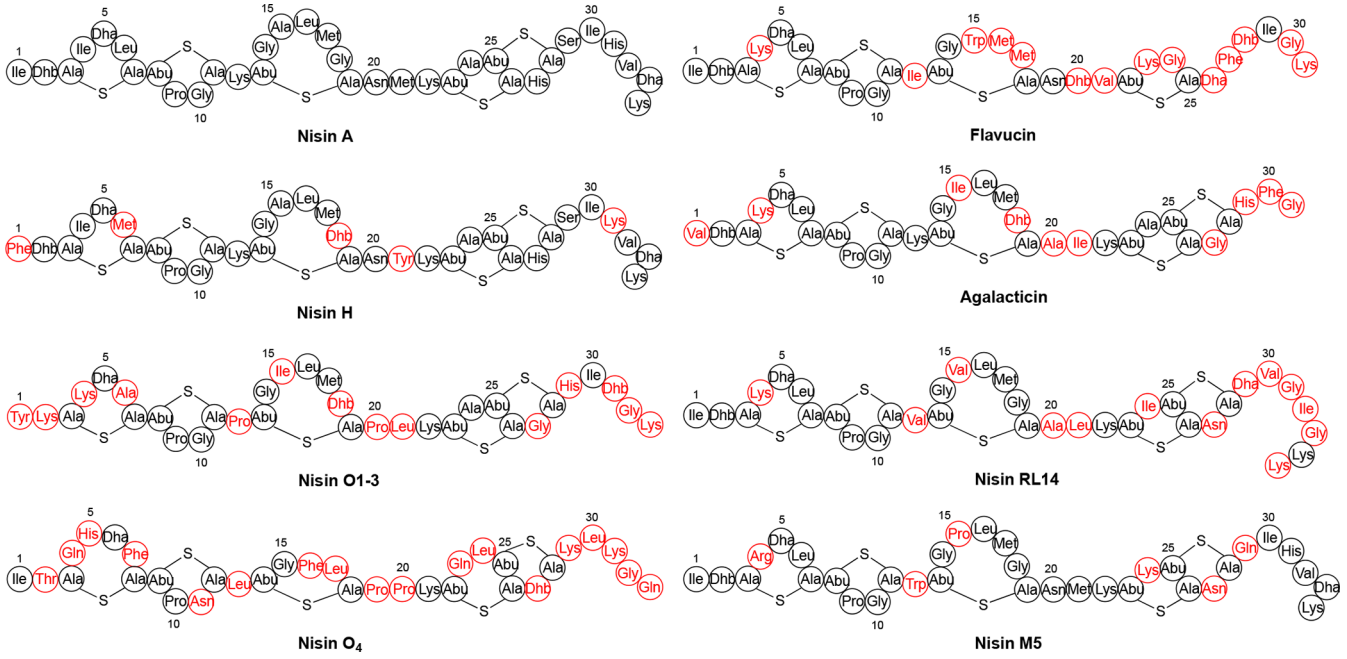

Figure 3. Representative structures of the bioactive nisin analogues. The distinct residues that vary from nisin A are highlighted in red.

structurally related to thiopeptides with multiple azole/azoline motifs, but their head-to-tail macrocyclic rings are produced via a protease-assisted lactamization process.[4]

Another two classes of RiPPs distinct from the above are lasso peptides and glycocins comprising no thioether linkage, dehydrated amino acids, or azol(in)e rings. Lasso peptides are a group of RiPPs with a characteristic lariat topology. The C-terminal tail threads through the macrolactam ring formed by the *N*-terminal amino group and the carboxylic acid side chain of aspartate or glutamate located in the 7−9 residues of the core peptide via an isopeptide bond. The lasso topology is stabilized by steric interactions above and below the ring and/or disulfide bridge(s).[19,20] Glycocins are post-translationally glycosylated bacteriocins that feature sugar moieties installed via glycosyltransferase on Ser, Thr, or Cys residues of precursor peptide and two nested disulfide bonds formed by two disulfide oxidoreductases that stabilize their unique helix−loop−helix structures.[21]

Overall, RiPPs have demonstrated diverse physiological functionalities and the potential for pharmaceuticals. Nisin (Figure 2) is the oldest and the most extensively characterized RiPP until now. This compound was identified in 1928, the same year as penicillin was discovered, and commercially marketed after 25 years. Since then, nisin has been approved as a safe food preservative to inhibit several food spoilage and food-borne pathogens without distinct observation of resistance. It hinders cell wall biosynthesis by binding to lipid II and damages the cell membrane, eventually leading to the cell death of sensitive bacteria.[22] In addition to nisin, two thiopeptides are currently used in commercials. Thiostrepton (Figure 2) has potent anti-Gram-positive activity and is a component in veterinary topical ointment to treat interdigital cysts and infected anal glands of dogs and cats.[18] A structurally similar thiopeptide, nosiheptide (Figure 2), is highly active against several Gram-positive bacteria resistant to other antibiotics and is widely added into feed additives to promote growth and feed conversion in pigs and chickens.[23] Besides, thiopeptide GE2270A (Figure 2) displays potent activity against Gram-positives, including methicillin-resistant staphylococci (MRSA), vancomycin-resistant enterococci (VRE), and group A streptococci.[24] Two semisynthetic analogues of GE2270A, i.e., LFF571 and CB-06-01 (now named NAI-Acne) have been completed Phase II clinical trials. LFF571 exhibits excellent activity against *Clostridium difficile* comparable with vancomycin,[25] but it was cut and discontinued in 2018.[9] NAI-Acne displays efficacy in treating *Propionibacterium acnes* with less disruption to other skin flora,[26] and is expected to be a human drug in the future.

In spite of valuable collective reviews focusing on RiPP biosynthetic mechanisms, intriguing/unique post-translationally modifying enzymes, as well as the novel structural scaffolds thereof,[3,4,6,27−32] relatively fewer summaries in regard to their diverse bioactivities, physiological/ecological functionalities, and/or mode of mechanism, are available in the literature.[33−36] Thus, this Review systematically covers the recent advances in bioactive RiPPs in terms of bioactivity and/or mode of mechanisms in the past decade. RiPPs exhibiting anti-Gram-positive bacteria, anti-Gram-negative bacteria, antitumor, antivirus, etc. activity are discussed in detail. Some disciplines of the RiPPs physiological activities are also summarized to guide genome mining as well as drug discovery and optimization in the future.

2. RiPPs AGAINST GRAM-POSITIVE BACTERIA

2.1. Lanthipeptides

Due to the excellent antimicrobial activity and demonstrated biosafety, several natural or bioengineered nisin variants have been uncovered during the past years. Recently, a homologue designated nisin H (Figure 3) was identified from a gut-derived strain *Streptococcus hyointestinalis* DPC6484. Nisin H has almost the same structure except for five mutations (Ile1Phe, Leu6Met, Gly18Dhb, Met21Tyr, and His31Lys) compared to the prototypical nisin A. It was effective against a series of Gram-positive bacteria but was less inhibitory than nisin A in the majority of instances except for *Staphylococcus aureus*

https://doi.org/10.1021/acsbiomedchemau.2c00062
ACS Bio Med Chem Au 2023, 3, 1−31

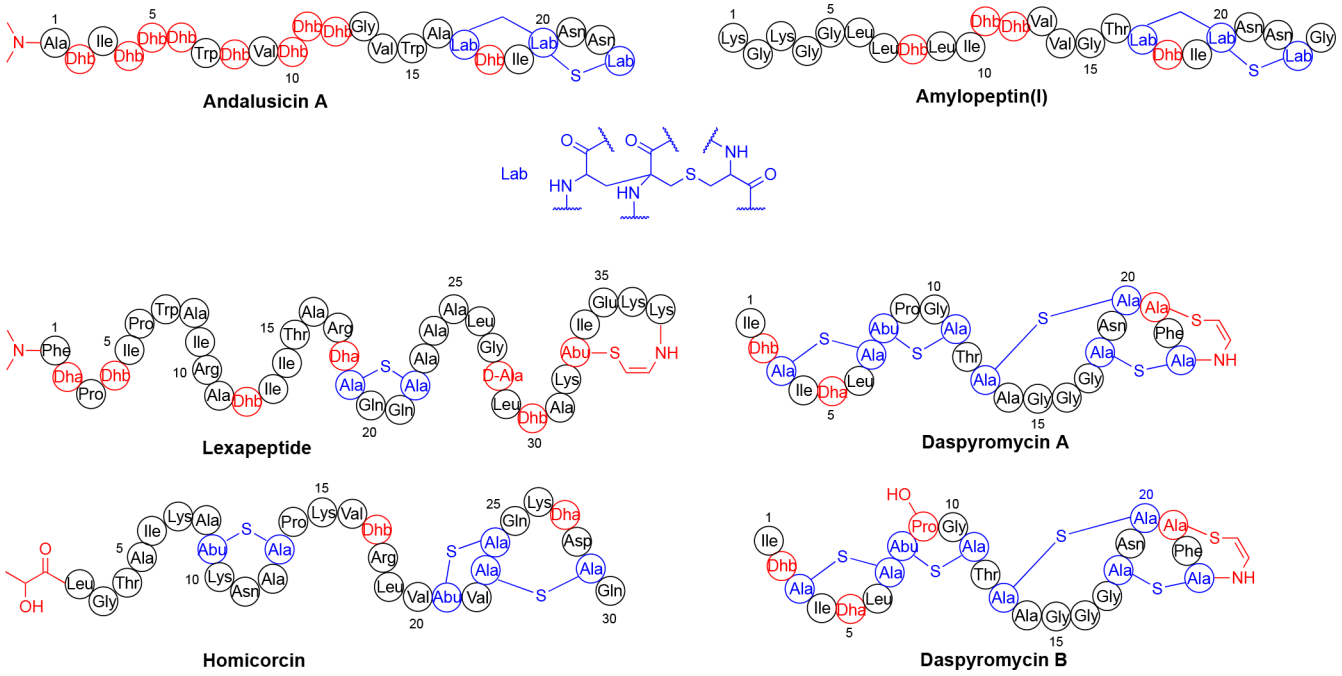

Figure 4. Structures of representatives of the single-component lantibiotics. The class-defining PTMs are highlighted in blue, with the other PTMs highlighted in red.

DPC5245, for which nisin H was more effective, and *Listeria innocua* DPC3572, for which the two peptides were equally effective.[37] The BGC of another nisin homologue containing four precursor genes was discovered from the dominant human gut bacterium *Blautia obeum* strain A2-162. Likely, the deduced products NsoA (nisin O) (Figure 3) was detrimental to *L. lactis* MG1614, *C. difficile*, an urgent threat for which new antibiotics are needed, and *Clostridium perfringens*, the third cause of foodborne infections in the United States according to the Centers for Disease Control and Prevention (CDC).[38,39]

Flavucin from *Corynebacterium lipophiloflavum* DSM 44291 and agalacticin from *Streptococcus agalactiae* ATCC 13813 are two lantibiotics unveiled using the promiscuous nisin modification machinery. They have been shown to have a broad substrate tolerance for diverse lantibiotic peptides fused to nisin leader peptide. Both sequences are partly similar to nisin, particularly the *N*-terminal region (Figure 3). Flavucin was less potent than nisin for most tested bacteria, but the vancomycin- and avoparcin-resistant *Enterococcus faecium* LMG 16003. Agalacticin only showed moderate activity against *E. faecium* LMG 16003 and *Listeria monocytogenes* LMG 10470.[40]

A similar strategy was used for mining potential nisin analogues in a cell-free protein synthesis (CFPS) platform. Four novel analogues (RL6, RL8, RL13, RL14; Figure 3) with antibacterial activity against *M. luteus*, clinical pathogenic strains of *Enterococcus faecalis*, *S. aureus*, and methicillin-resistant *S. aureus* (MRSA) were identified, with RL14 surpassing nisin against *M. luteus* and *E. faecalis*. Furthermore, another analogue M5 (Figure 3), with five mutations in the core peptide, was identified to effectively against Gram-negative *Escherichia coli* (mentioned in section 3.1).[41]

New-to-nature variants of lanthipeptides were generated by a combinatorial shuffling of peptide modules derived from 12 natural lantibiotics and processing by the nisin PTM machinery in *Lactococcus lactis*. The antimicrobial screening revealed more than 30 candidates against *Micrococcus flavus*, among which three nisin variants showed improved activities against some pathogenic reference strains than nisin and gallidermin. In addition to the antimicrobial activities, ten newly yielded lanthipeptides could bypass lantibiotic defense mechanisms. Half of them were less sensitive to the nisin immunity machinery, while the other half was insensitive to the nisin resistance protein (NSR) present in resistant pathogenic strains (exact structures not available for these variants).[42]

Andalusicin A (Figure 4) as a new family of class III lanthipeptides from *Bacillus thuringiensis* sv. *andalousiensis* NRRL B23139 was active against a panel of Gram-positive bacteria like *Bacillus cereus* ATCC 14579, *Bacillus mycoides* DSM 2048, *S. aureus* ATCC 25923, *Paenibacillus polymyxa* ATCC 842, and *Arthrobacter* sp. ATCC 21022, with closely related *Bacillus* strains being the most sensitive. This is striking since most class III and IV lanthipeptides have been reported to lack antimicrobial activities.[6] The dimethylation of andalusicin A is essential for the antimicrobial activities as andalusicin B without the dimethyl groups abolishes the activity against most of the tested bacteria.[43]

Another class III lanthipeptides amylopeptin(I) (Figure 4) from the Sprague−Dawley (SD) rats gut microbe *Bacillus amyloliquefaciens* displayed narrow antimicrobial activity against the rat gut-derived *Bacillus megaterium* R28, suggesting that this lantibiotic might be involved in the microbe−microbe interactions in the rat gut microbiota. The removal of the leader peptide is essential for maturation, and this is catalyzed by the S8 family protease AmyP, which represents a novel type of protease involved in class III lanthipeptide biosynthesis.[44]

Lexapeptide (Figure 4) is the founding member of a novel class V lanthipeptides, considering the unique trienzyme cascade responsible for the Lan biosynthesis. This lantibiotic and its derivatives exhibited more effective antimicrobial activities against several Gram-positive bacteria than nisin and vancomycin, particularly for the methicillin-resistant *S.*

https://doi.org/10.1021/acsbiomedchemau.2c00062
ACS Bio Med Chem Au 2023, 3, 1−31

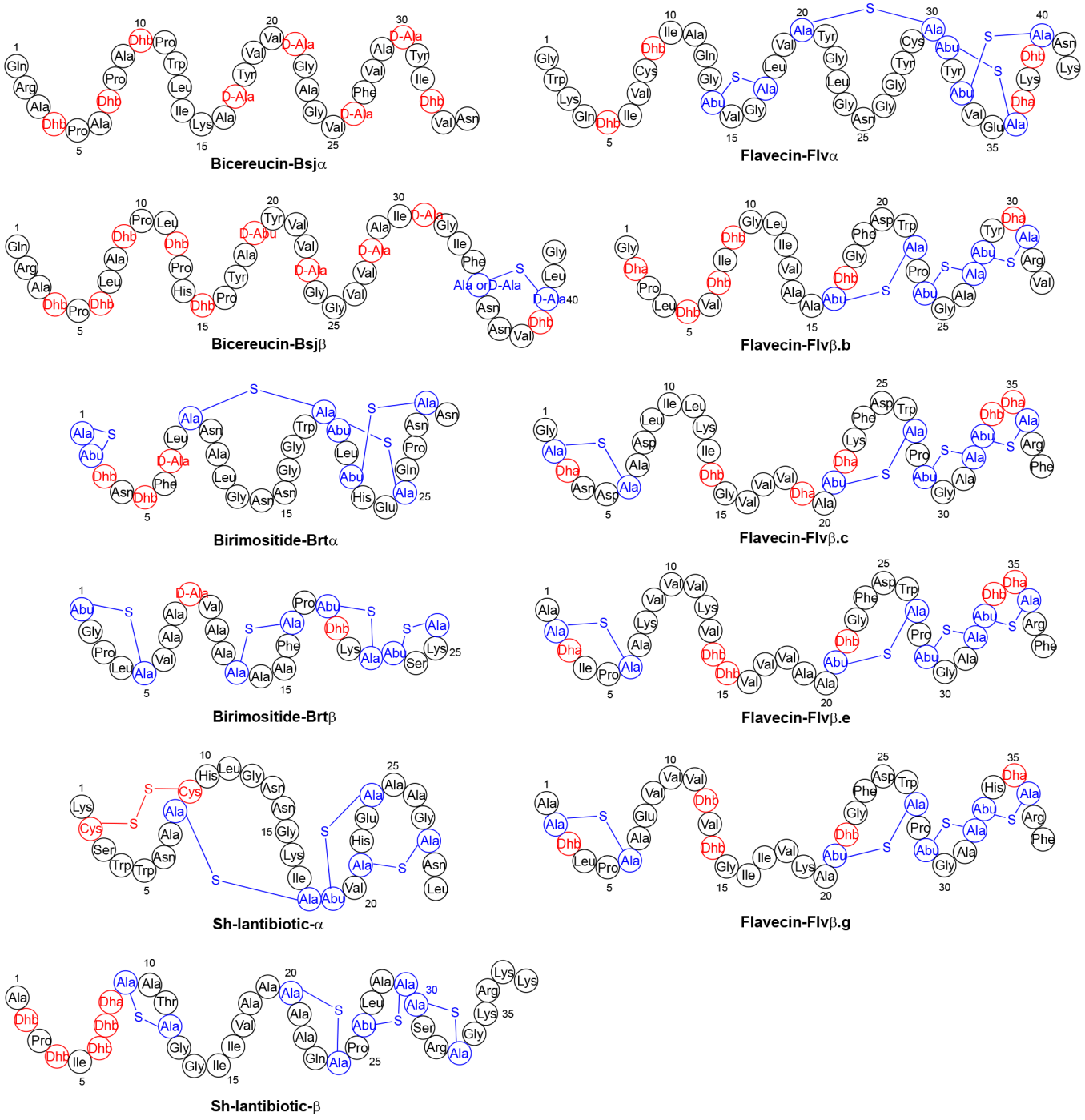

Figure 5. Structures of representatives of the two-component lantibiotics. The class-defining PTMs are highlighted in blue, with the other PTMs highlighted in red.

aureus (MRSA) and *Staphylococcus epidermidis* (MRSE), *E. faecalis* and *Mycobacterium smegmatis* mc2155. A rare D-Ala modification (D-Ala28) installed by an $F_{420}H_2$-dependent reductase termed LanJc significantly enhanced the antimicrobial activity against *S. aureus* ATCC 29213, *Micrococcus luteus*, and *M. smegmatis* mc2155 compared to its L-isomer.[7] It is worth mentioning that another "class V" lanthipeptide-pristinin that differs from lexapeptide was reported almost simultaneously. The formations of Lan and MeLan in pristinin have not been elucidated yet, but are distinct from the classical lanthipeptides, representing a novel subfamily of lanthipeptides.[45]

Homicorcin (Figure 4) from a jute endophyte *Staphylococcus hominis* strain MBL_AB63 showed promising antimicrobial activity against all the Gram-positive bacteria tested, inclusive of *Staphylococcus simulans* 22, *S. aureus* SG511, *Staphylococcus carnosus* TM300, *M. luteus* ATCC1856, *M. luteus* DSM1790, *L. lactis* NCTC497, *Bacillus subtilis* 168 and methicillin-resistant *S. aureus* (MRSA), and methicillin sensitive *S. aureus* (MSSA1), but was less potent than nisin A against the tested strains. It exerted bactericidal activity against susceptible strains by disrupting the integrity of the cytoplasmic membrane through pore formation to dissipate the proton motive force

https://doi.org/10.1021/acsbiomedchemau.2c00062
ACS Bio Med Chem Au 2023, 3, 1−31

(PMF) as observed under field emission-scanning electron microscopy (FE-SEM).[46]

Daspyromycin A and B (Figure 4) strongly suppressed the growth of Gram-positive bacteria like *M. luteus* ATCC 4698, *Staphylococcus capitis* W7, *S. aureus* LV-B1, *B. subtilis* ATCC 6051, and the Gram-negative bacteria including *Acidovorax avenae*, *Pseudomonas syringae*, and *Xanthomonas oryzae*. This activity is exceptional as most of the lanthipeptides are only active toward Gram-positive bacteria. In addition, daspyromycin A was particularly active against methicillin-resistant *S. aureus* (MRSA) and vancomycin-resistant *Enterococci* (VRE). Compared to daspyromycin A, daspyromycin B has an extra hydroxyl group located at the C-4 position of Pro9 and is less active against bacteria. The hydroxyl group is added via a hydroxylase encoded in the genome of the heterologous hosts and is believed as a detoxification step during the heterologous production.[47]

Apart from the aforementioned single-component lantibiotics, the other subclass is the two-component lantibiotics employing two lanthipeptides which are post-translationally modified individually to generate two different products acting in synergy for antibacterial activity.[48] One example is the bicereucin (Figure 5) from *B. cereus* SJ1. It is noted that one of the two peptides (Bsjα) lacks any cysteines and is not a lanthipeptide. The optimal molar ratio between Bsjα and Bsjβ is 2:1, about 50−100 lower than their independent minimal inhibitory concentrations (MICs). Bicereucin showed antimicrobial activities against a range of Gram-positive bacteria, such as *B. subtilis* ATCC6633, *L. lactis* CNRZ 481, *S. epidermidis* 15x, *Streptococcus mutans* ATCC 25175, *M. luteus* ATCC 4698, methicillin-resistant *S. aureus* Rosenbach ATCC BAA-1717, and vancomycin-resistant *E. faecium* ATCC 700221. The Lan in Bsjβ is crucial for its activity as the Bsjβ-C40A variant dramatically drops in inhibitory activity. It was suggested that Bsjα bound a target on the outer surface of the bacterial cell, and Bsjβ performed its synergistic effect for antimicrobial activity. Besides, bicereucin also exhibited weak synergistic hemolytic activity against rabbit red blood cells.[49]

The genome of *Ruminococcus flavefaciens* FD-1 encoded the lanthipeptide BGC of flavecins (hereinafter *flv*), which comprised four highly conserved copies with the same core peptide (Flvα.*x*, where *x* = a−d) and a diverse set of eight additional peptides (Flvβ.*x*, where *x* = a−h) (Figure 5). Some of the Flvβ.*x* did not act synergistically with Flvα against *M. luteus* DSM 1790, such as Δ1-Flvβ.c and Δ1-Flvβ.e. In contrast, the antimicrobial activities of Flvβ.b and Δ1-Flvβ.g were synergistically enhanced by Δ2-Flvα.a that was characteristic of two-component lantibiotics. Weak antimicrobial activity was also observed against *Ruminococcus albus* 7 and *R. flavefaciens* C94. The remainder of the Flvβ.*x* did not display antimicrobial activity separately or combined with Δ2-Flva.a and are not considered lantibiotics.[50]

Roseocin isolated from *Streptomyces roseosporus* NRRL 11379 is the first two-component lantibiotics from a non-*Firmicute*, though the structure of roseocin has not been fully characterized. The full-length RosA1 and RosA2 modified peptides alone or in combination show no antimicrobial activity. Contrarily, they displayed synergistic antimicrobial activity against *L. monocytogenes* MTCC 839 and VRE after the treatment of GluC to remove most of the leader peptides and even active against methicillin-resistant *S. aureus* ATCC 43300 with the treatment of proteinase K, as the latter treatment is much closer to the native core peptide predicted in silico.[51]

Almost simultaneously, another two-component lantibiotic from Actinobacteria designated birimositide (Figure 5) was identified from *Streptomyces rimosus* subsp. *rimosus* WC3908. It was screened against *L. lactis* sp. *cremoris* and *M. luteus* ATCC 4698.[52]

Sh-lantibiotic-α and *Sh*-lantibiotic-β (Figure 5) are two lanthipeptides isolated from human skin commensal bacteria *S. hominis* A9. These Sh-lantibiotic peptides selectively inhibit multiple strains of *S. aureus*, including *S. aureus* ATCC 35556, methicillin-resistant *S. aureus* (MRSA) strain USA 300 and Sanger252, and clinical isolates from subjects with atopic dermatitis, but is tolerant of other species frequently isolated from normal human skin. It is unclear whether the two lanthipeptides act synergistically or not, whereas each of the *Sh*-lantibiotics synergized with the cathelicidin family human antimicrobial peptide LL-37.[53]

Other lantibiotics that are active against Gram-positive bacteria include BP_{SCSK} (Figure 6), which had a narrower

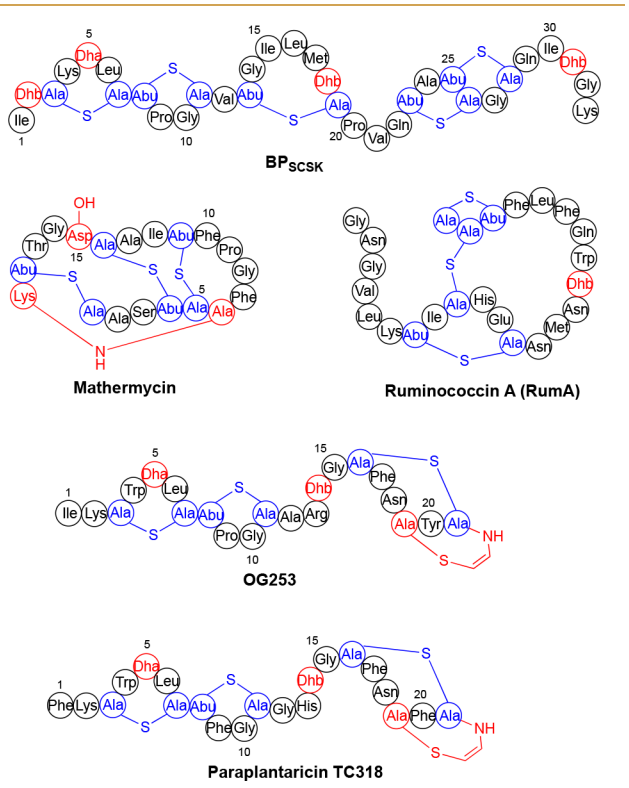

Figure 6. Structures of some other lantibiotics against Gram-positive bacteria. The class-defining PTMs are highlighted in blue, with the other PTMs highlighted in red.

spectrum of activity that targeted VRE while preserving commensal bacteria,[54] mathermycin (Figure 6), a congener of cinnamycin against *B. subtilis* LH45,[55] ruminococcin A (RumA, Figure 6) against *B. subtilis* ATCC 6633,[56] OG253 (mutacin 1140, Phe1Ile, Figure 6), a lead compound due to the superior *in vivo* efficacy along with an apparent lack of relapse against *C. difficile*,[57] and paraplantaricin TC318 (Figure 6), another mutacin 1140 analogue against various pathogenic and spoilage bacteria such as *B. cereus*, *Clostridium sporogenes*, *E. faecalis*, *L. monocytogenes*, *Salmonella enterica* ser, and *S. aureus*.[58]

A variation of class-III lanthipeptides is the lipolanthines, lipid moieties connected with the *N*-terminus of RiPPs. Based

https://doi.org/10.1021/acsbiomedchemau.2c00062
ACS Bio Med Chem Au 2023, 3, 1−31

on the presence or not of the *lanD* gene (encoding cysteine decarboxylase) and the encoded polyketide synthase (PKS) enzymes, lipolanthines were divided into four subtypes and characterized as a hybrid of RiPPs, polyketides, NRPs, and polysaccharides.[59] The founding member is microvionin (Figure 7) containing a bicyclic octapeptide formed by a

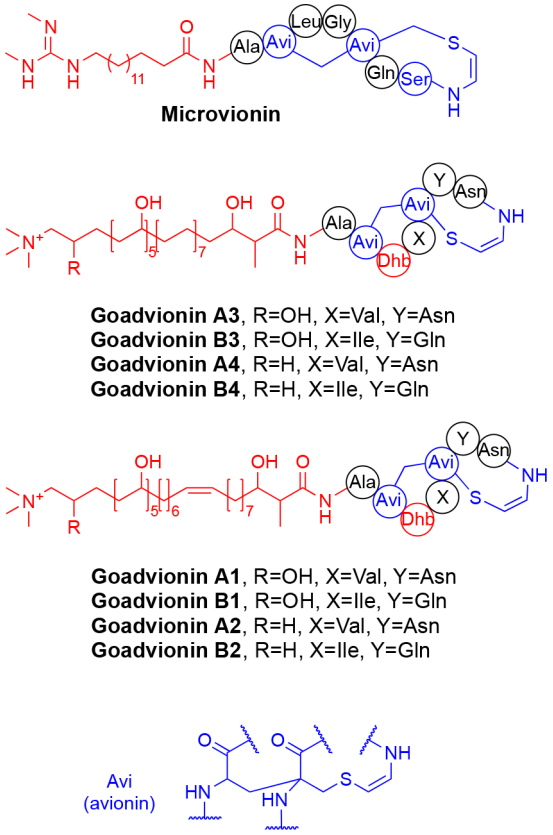

Figure 7. Structure of the lipolanthines. The class-defining PTMs are highlighted in blue, and other PTMs, including the lipid moieties, are highlighted in red.

hybrid aminovinylcysteine (AviCys)-labionin moiety (termed avionin) with an *N*-terminal PKS-derived dimethyl guanidino fatty acid. Microvionin exhibited antibacterial effects with MICs (MICs are given in parentheses, the same below) for MRSA (<0.46 μg/mL), MSSA (<0.1 μg/mL) and *Streptococcus pneumoniae* (<0.15 μg/mL).[60] The other bioactive lipolanthines discovered so far are goadvionins (Figure 7), consisting of a polyfunctional C_{32} fatty acid with a polar ammonium headgroup and an eight-residue RiPP with an avionin structure. Goadvionins showed antimicrobial activity against *Streptomyces* like *Streptomyces* sp. TP-A0584, *S. avermitilis* MA-4680, *S. lividans* TK23, *S. coelicolor* A3(2), *S. albus* J1074, *S. griseus* IFO13350 and *M. smegmatis*, *B. subtilis* ATCC6633, *M. luteus*, and *S. aureus* 209P JC-1. The MICs of goadvionin B2 against the last three sensitive strains were 3.2, 3.2, and 6.4 μg/mL, respectively.[61]

2.2. Sactipeptides

Ruminococcin C1 (RumC1, Figure 8), purified from the cecal contents of rats monoassociated with *Ruminococcus gnavus* E1, carries four sulfur to α-carbon thioether cross-links, folding the peptide in a unique double hairpin-like structure, distinct from most sactipeptides with ring-within-a-ring topologies, or rather single hairpin-like structures.[62−64] This sactipeptide undergoes

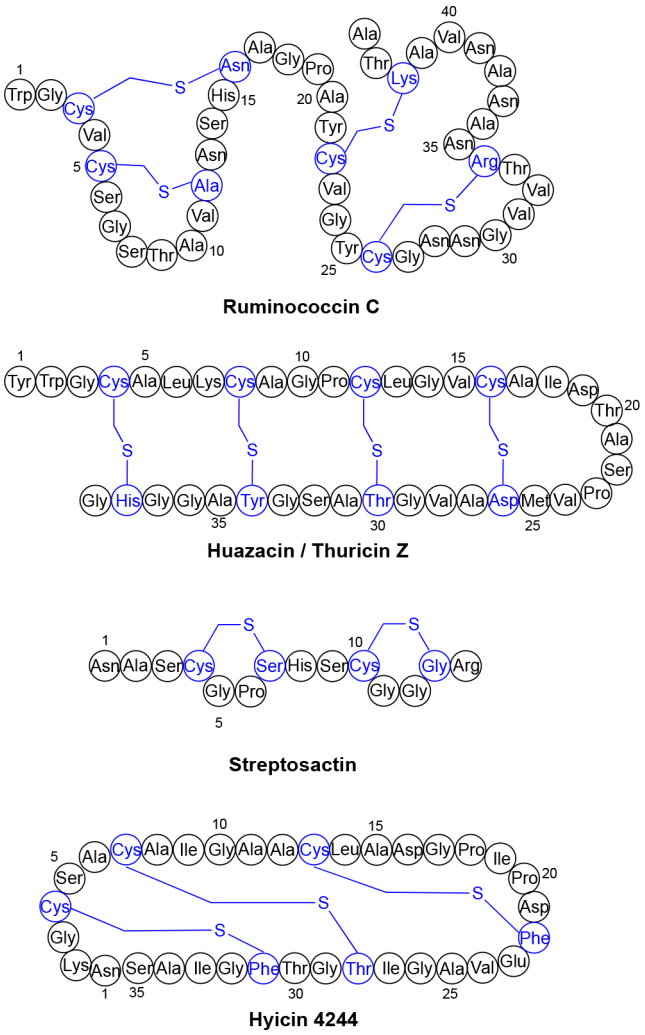

Figure 8. Structure of representatives of sactipeptides against Gram-positive bacteria. The thioether-bridged residues are highlighted in blue.

a two-step cleavage process to maturation, involving a monofunctional Zn-metallopeptidase from the symbiont (i.e., RumPc) and a serine protease from the host organism (i.e., trypsin).[63] RumC1 exerted antimicrobial activity toward Gram-positive *Clostridium* species, including *Clostridium coccoides*, *C. perfringens*, *C. difficile*, and *Clostridium botulinum*, a pathogen responsible for foodborne botulism (via a preformed toxin), infant botulism (intestinal infection via a toxin-forming *C. botulinum*), and wound botulism.

Moreover, RumC1 was also active against *B. cereus*, *L. monocytogenes*, *S. aureus*, *E. faecium*, vancomycin-resistant *E. faecalis* (VRE), nisin-resistant *B. subtilis*, methicillin-resistant *S. aureus* (MRSA) as well as a clinical *S. pneumoniae* strain responsible of multiple types of infection.[63−65] The Gram-negative *E. coli* was also reported to be suppressed by RumC1 (mentioned in section 3.3).[62] And not only that, RumC1 exhibits a selective antifungal activity against the growth of *Heterobasidion annosum* BRFM 524 at 12.5 μM, a pathogen responsible for conifer diseases in the forest industry.[65] The minimal bacteriostatic concentration (MBC) values are identical to MICs for most strains, indicating that RumC1 is bactericidal rather than bacteriostatic. The antimicrobial activity of RumC1 likely derives from the inhibition of the

https://doi.org/10.1021/acsbiomedchemau.2c00062
ACS Bio Med Chem Au 2023, 3, 1−31

ATP synthesis to block the synthetic pathways of DNA, RNA, proteins, and peptidoglycan, which is distinct from most of the bacteriocins targeting cell membranes.[64] In addition to its prominent bioactivity, the thioether network leading to a compact structure of RumC1 confers high resistance to physicochemical treatments such as acidic or basic pH, elevated temperature, high salt concentrations, and the physiological but harsh conditions encountered in blood or the digestive tract, validating the potency of RumC1 as a drug-lead.[64]

Conversely, other reported sactipeptides typically have a narrow spectrum of activity toward Gram-positive bacteria. Huazacin, also named thuricin Z (Figure 8) from *B. thuringiensis* sv *huazhongensis*, was active against *L. monocytogenes* 4b F2365 and several *B. cereus* strains with MICs of 4 μM and 2−8 μM, respectively.[66,67] Multianalyses involving confocal laser scanning microscopy, ultrathin-sectioning transmission electron microscopy, scanning electron microscopy, and large-unilamellar-vesicle-based fluorescence analysis unveiled that huazacin targets the bacterial cell membrane and induces membrane permeabilization.[67] Another hallmark of huazacin is the BGC containing two precursor peptide genes and two sactionine synthetic genes, which is reminiscent of the two-component sactipeptide thuricin CD.[68] Nonetheless, the two copies of precursor peptide genes in the huazacin BGC encoding an identical precursor peptide and the two sactionine synthases appear to be modified independently with each other.[67]

Streptosactin (Figure 8) was isolated from *Streptococcus thermophilus* JIM 8232 and represented the first sactipeptide of streptococcal origin. The thioether cross-links in streptosactin are unnested, with the mercapto donors and acceptors alternating along the core peptide, a structure akin to the double hairpin in RumC1. Streptosactin acts as a fratricidal reagent to potently suppress the producing host and its closest relatives like *S. thermophilus* LMD-9 and *S. thermophilus* LMG 18311, which also carry the BGC of streptosactin.[69]

Hyicin 4244 (Figure 8) from *Staphylococcus hyicus* 4244 is the first sactibiotic to be described in staphylococci, albeit not isolated for detailed structural characterization. It had a bactericidal mode of action against staphylococcal isolates from either human infections or bovine mastitis, including *S. aureus*, *S. epidermidis*, *S. hominis*, *S. saprophyticus*, and *S. simulans*, by preventing staphylococcal biofilm-formation or killing of staphylococcal cells in preformed biofilms to reduced cell proliferation and viability.[70]

2.3. Thiopeptides

Saalfelduracin (Figure 9) from *Amycolatopsis saalfeldensis* NRRL B-24474 is a thiostrepton-like thiopeptide featuring a central piperidine and a rare thioamide moiety.[71] Heterologous expression experiments revealed that the thioamide moiety is installed post-translationally by the combined action of the TfuA and YcaO pair, which reconciled the subsequent research on thioamidation in thiovarsolin,[72] thioviridamides[73] and methyl-coenzyme M reductases from most of the methanogen.[74] Saalfelduracin displayed strongly growth inhibitory toward *Bacillus anthracis* str. Sterne and two drug-resistant Gram-positive pathogens VRE and MRSA, with approximately equivalent MICs to thiostrepton.[71]

The human skin commensal bacterium *Cutibacterium acnes* HL030PA1 is widely distributed across individuals and skin sites produce a berninamycin-like thiopeptide-cutimycin

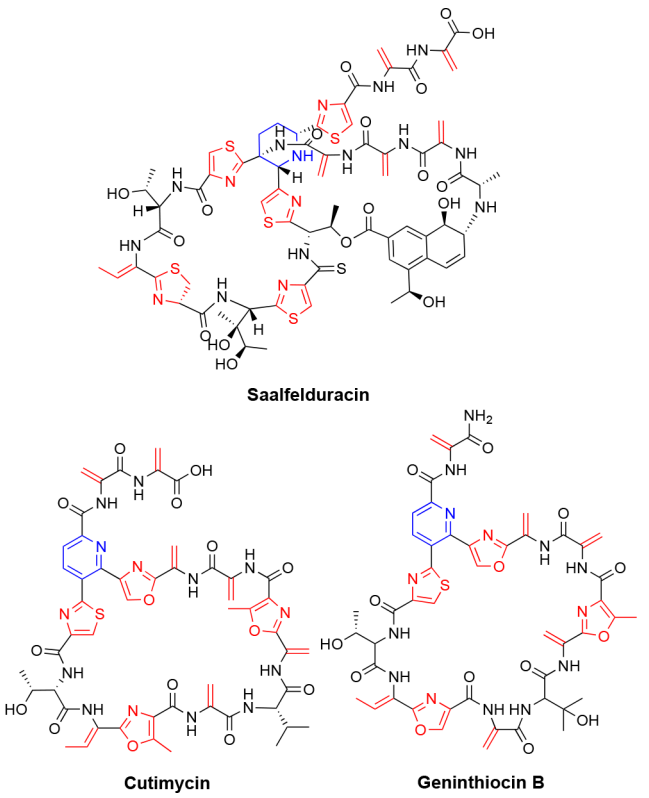

Figure 9. Structure of representatives of thiopeptides against Gram-positive bacteria. The central pyridine rings are highlighted in blue, with the other PTMs highlighted in red.

(Figure 9), which significantly inhibited the growth of *S. aureus* UAMS-1 and the MRSA strain *S. aureus* USA300 NRS384 as well as *S. epidermidis* W23144, *S. epidermidis* DSM2004 and *S. epidermidis* ATCC 35984 with a MIC lower (for the strains except for *S. epidermidis* ATCC 35984) or comparative (for *S. epidermidis* ATCC 35984) to berninamycin. Cutimycin favors the growth of resident skin Actinobacteria over staphylococcal species owing to the resistance of several other *C. acnes* strains and *Corynebacterium* species. The coculture of *C. acnes* further demonstrates this scenario with susceptible *Staphylococcus* strains increases cutimycin BGC transcription. Cutimycin is potentially applied to change the skin microbiota composition to prevent or treat skin diseases.[75] Another berninamycin-like thiopeptide-geninthiocin B (Figure 9), which lacks the C-terminal Dha-residue compared to geninthiocin, was isolated from *Streptomyces* sp. YIM 130001 with bioactivity against *B. subtilis*.[76]

2.4. Lasso Peptides

The number and position of disulfide linkage are used to categorize lasso peptides into four classes. Class IV with a disulfide bridge residing on the tail (resulting in "handcuff" topology) is newly identified. The founding member is LP2006 (Figure 10) from *Nocardiopsis alba* NRRL B-24146. It was active against *E. faecium* (VRE), *B. subtilis*, *B. anthracis*, and *M. smegmatis* that is a strain used to develop and test treatments for tuberculosis.[77]

The class I lasso peptide siamycin I (MS-271) was isolated as an anti-HIV, anti-MRSA, and anti-VRE compound from *Streptomyces*.[78,79] Inspired by the remarkable bioactivity, a natural siamycin I mutation (Ile17Val) named specialicin (Figure 10) was uncovered via genome mining.[80] Specialicin

https://doi.org/10.1021/acsbiomedchemau.2c00062
ACS Bio Med Chem Au 2023, 3, 1−31

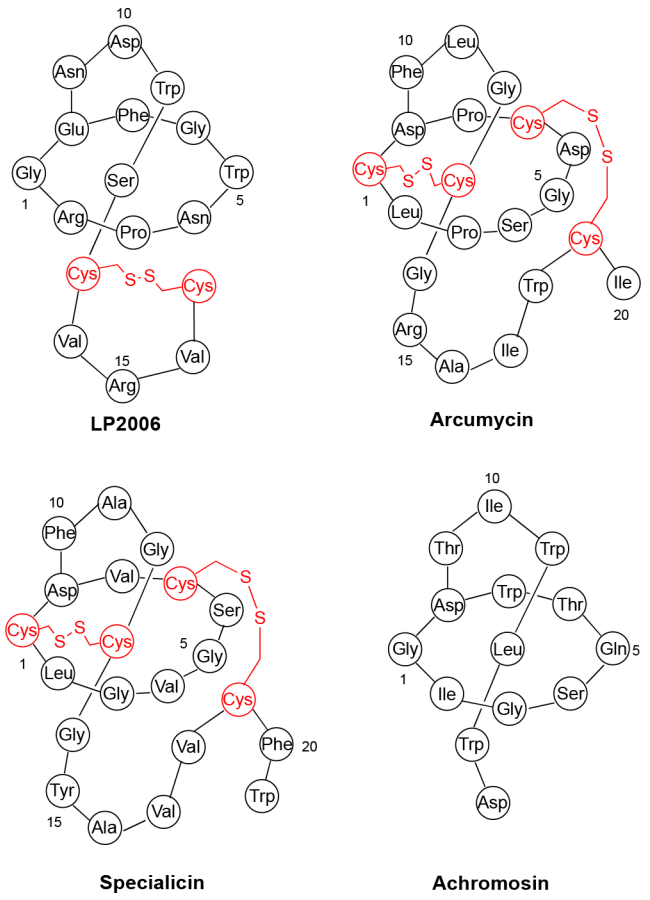

Figure 10. Structure of representatives of lasso peptides against Gram-positive bacteria. The disulfide bridged residues are highlighted in red.

also includes a *C*-terminal D-Trp residue and is suspected to be epimerized by the CapA family protein SpeH (a homologous protein of MslH that catalyzes the *C*-terminal D-Trp epimerization in siamycin I biosynthesis[81]) before cleavage of the leader peptide, due to the resemblance of the structures and BGCs between specialicin and siamycin I. In addition to its anti-HIV activity (see below), specialicin displays antibacterial activity against only *M. luteus* (MIC: 8 μg/mL) but no antibacterial activity against *S. aureus*, *B. subtilis*, and *E. coli*, *Pseudomonas aeruginosa*. The activity against MRSA and VRE was not tested.[80] The antibacterial activity of specialicin is reminiscent of class II lasso peptide achromosin (Figure 10) from *Streptomyces achromogenes* subsp. *achromogenes* NBRC12735, which only showed an inhibitory against *M. luteus* among a range of bacterial strains.[82]

Another siamycin I-like class I lasso peptide arcumycin (Figure 10) was uncovered from *Streptomyces* NRRL F-5639. This compound shares an overall 55% amino acid identity with both siamycin and sviceucin. It does not contain any D-amino acids correspondence to the fact that the BGC of arcumycin lacks the putative epimerases observed in the BGC of siamycin and sviceucin. Arcumycin induced the inhibition of multiple Gram-positive bacteria such as *B. subtilis* ATCC 6051 (4 μg/mL), *S. aureus* ATCC 25923 (8 μg/mL), and *M. luteus* ATCC 4698 (8 μg/mL) but was inactive against the Gram-negative bacteria. Treatment of the *B. subtilis* reporter strain with arcumycin illustrates that this molecule tampers with lipid II biosynthesis, a mode of action shared with siamycin I.[83]

2.5. Glycocins

The *S*-linked glycocin sublancin (Figure 11) is an antimicrobial peptide isolated from *B. subtilis* 168 containing 37 amino acids and exhibited bactericidal activity against an array of Gram-positive bacteria, including important pathogens such as *B. cereus*, *Streptococcus pyogenes*, *C. perfringens*, and MRSA.[84,85] Due to the flexibility and robustness of the leader peptide dependent PTMs of RiPPs, structure−activity relationships (SARs) were analyzed via reconstitution of the biosynthetic pathway in *E. coli* Shuffle, a strain expressing the disulfide bond isomerase DsbC to aid oxidative folding of Cys-rich proteins in the cytoplasm.[86] Both Asn31 and Arg33 in helix B might have an essential role in interacting with the target or delivery to the target since mutations of these sites led to a significant decrease in bioactivity. The positive charge was evaluated to be crucial as R33K displayed an almost identical activity, and residues bearing a positive charge at equivalent positions are highly conserved in a sequence alignment to sublancin. The aglycone and C22S variant showed the absence of growth inhibition, indicating that the sugar moiety is essential for the antimicrobial activity, or rather, sublancin is "glycoactive".[87]

The biosynthetic pathway of a sublancin type glycocin named pallidocin (Figure 11) from the thermophilic bacterium *Aeribacillus pallidus* 8 was reconstituted in *E. coli* BL21(DE3). The strain without additional DsbC in the cytoplasm could also form disulfide bonds automatically. Pallidocin exhibited high stability for high temperatures and a wide range of pH values. Admirable antibacterial activities against *B. cereus* ATCC 14579, *B. megaterium* DSM 319 (37 nM), and some thermophilic bacteria like *Geobacillus stearothermophilus* B4109, B4111, B4112, B4114 (246 pM), *Parageobacillus genomospecies* 1 NUB36187 (2.4 pM), *Parageobacillus toebii* B4110, B4162 (493 pM), *Parageobacillus caldoxylosilyticus* B4119 (985 pM), and *Caldibacillus debilis* B4165, could be observed. The *S*-glycosyltransferase PalS possesses a quite flexible substrate selectivity as PalS was able to modify the maturation of two other glycocins, Hyp1 (Figure 11) from *B. megaterium* BHG1.1 and Hyp2 from *Bacillus* sp. JCM19047. Hyp2 is inactive against all the strains tested, whereas Hyp1 was active against *Geobacillus* sp. B4113 and *G. stearothermophilus* B4163. Of note, both the disulfide bonds and glycosylations are essential for the antimicrobial activities of pallidocin and Hyp1.[88]

A plug-and-play pathway refactoring workflow established for natural product research was used to discover three sublancin-type glycocins, geocillicin, bacillicin CER074, and bacillicin BAG2O, as well as an enterocin 96-type glycocin listeriocytocin (Figure 11) with two successive glycosylations occurring on Ser60. Despite listeriocytocin lacking any antimicrobial activity, bacillicin CER074 and bacillicin BAG2O had a narrower antimicrobial spectrum against *B. cereus* ATCC 14579 with MICs much lower than sublancin, while geocillicin exhibited much weaker activity against the same indicator strain than sublancin. The bioactivity of bacillicin BAG2O is intriguing as it does not contain a positively charged residue corresponding to Arg33 of sublancin, which may imply that this glycocin has an altered target from sublancin.[21]

The glycocin F (GccF) type glycocin ASM1 (Figure 11) was isolated from *Lactobacillus plantarum* A-1 at nearly the same time as GccF, but its structure was yet fully characterized until recently. ASM1 has five amino acid substitutions in the flexible C-terminus compared to GccF. The peptide is diglycosylated

https://doi.org/10.1021/acsbiomedchemau.2c00062
ACS Bio Med Chem Au 2023, 3, 1−31

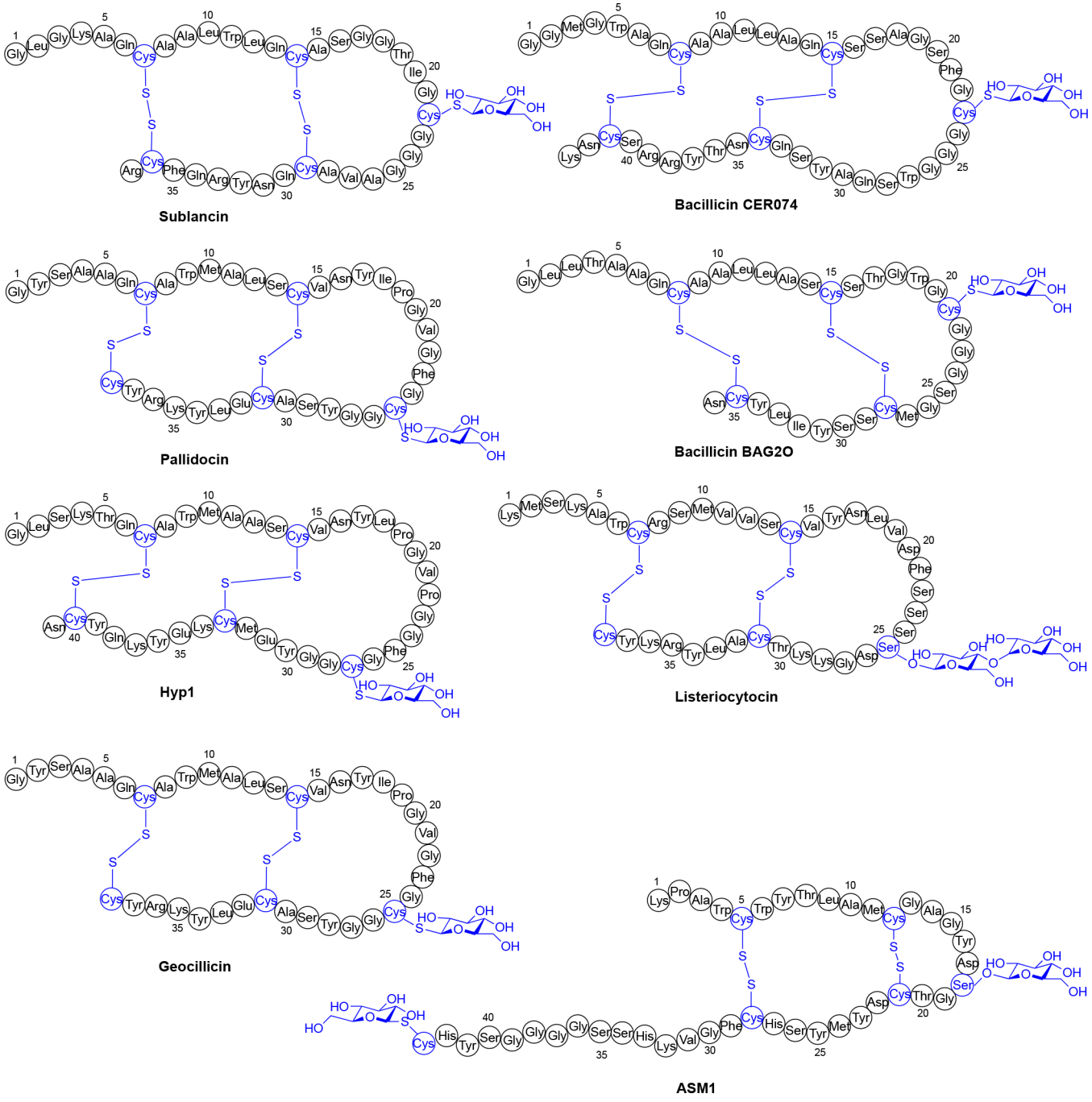

Figure 11. Structures of representatives of glycocins against Gram-positive bacteria. The class-defining disulfide bridges and glycosyls are highlighted in blue.

by two HexNAcs, with one *S*-linked to Cys43 and the other *O*-linked to Ser18, as is the case for GccF. ASM1 inhibited most *Lb. plantarum* strains to varying degrees except the known glycocin producers KW30 and A-1, and the plantaricin EF/JK indicator strain LP965. Inhibitions were also observed for *Lactobacillus acidophilus* NCFM, *Lb. plantarum* WCFS1, *Lactobacillus sakei* Lb790, *Lactobacillus brevis* LMG11437, *Lb. plantarum* NC8 and weak inhibition for *E. faecalis* V583.[89]

2.6. Others

Many other classes of RiPPs unveiled recently also exhibit potent anti-Gram-positive activity, most of which contain only one example in a certain class of RiPPs. Representatives are discussed in this section.

Linaridins are linear and dehydrated (arid) RiPPs with an unexplored diversity in nature discovered by bioinformatic studies. The maturation of linaridin involves dehydratases (and possibly dethiolases) by a set of enzymes with unknown biochemistry but distinct from lanthipeptide dehydratase-like enzymes.[90] Salinipeptin A−D (Figure 12) are type A linaridins isolated from the halotolerant *Streptomyces* sp. strain GSL-6C as analogues of cypemycin, the founding linaridin peptide that is active against *M. luteus* and mouse P388 leukemia cells.[91] Both cypemycin and salinipeptins include several Dhb residues and an AviCys ring in the C-terminus, whereas salinipeptins

https://doi.org/10.1021/acsbiomedchemau.2c00062
ACS Bio Med Chem Au 2023, 3, 1−31

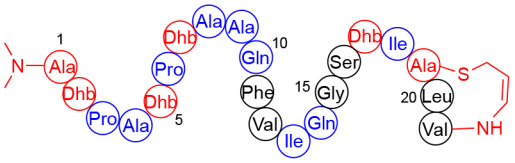

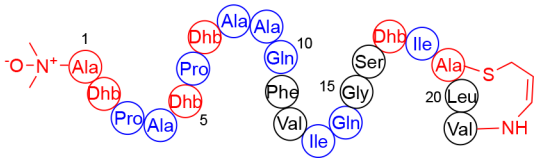

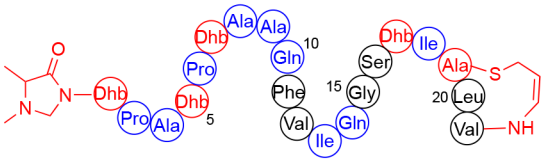

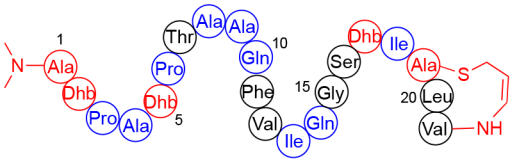

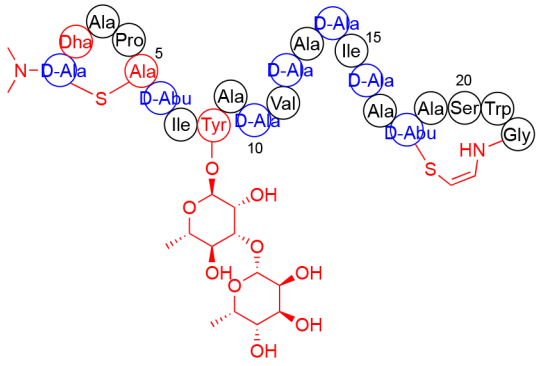

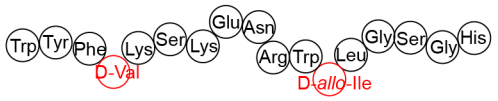

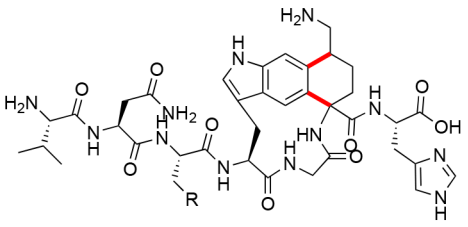

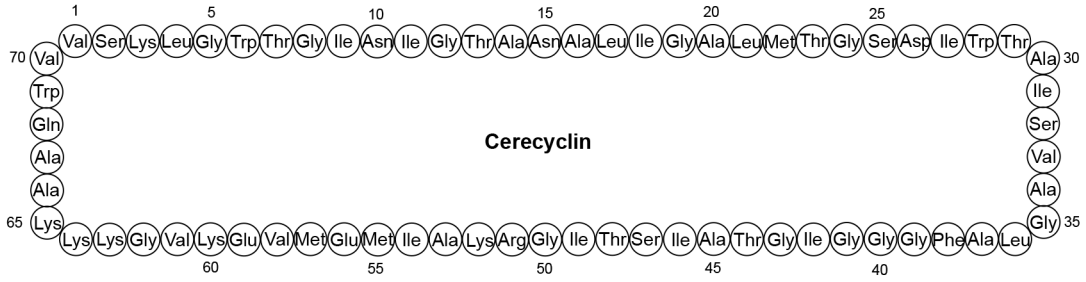

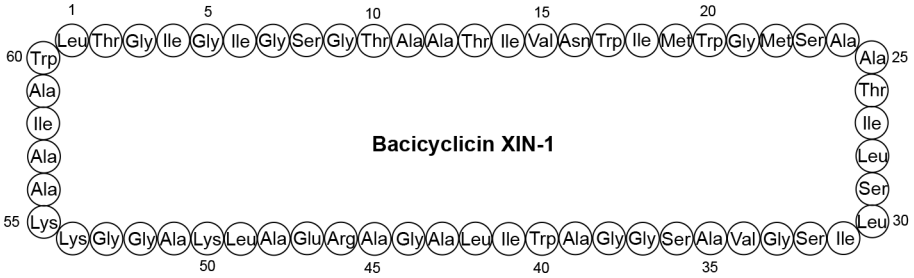

Figure 12. Other representative RiPPs against Gram-positive bacteria. The post-translationally modified amino acids and D-amino acids are highlighted in red and blue, respectively, with the proteinogenic amino acids drawn in black.

also feature multiple D-amino acids, even the unprecedented D-Pro and D-Ile residues.[92] This is confusing because no enzymes like radical SAM epimerase or oxidoreductase are encoded in the BGC of salinipeptins, and the formations of D-amino acids

https://doi.org/10.1021/acsbiomedchemau.2c00062
ACS Bio Med Chem Au 2023, 3, 1−31

remain elusive.[90] In addition to the *N*-terminal demethylation in salinipeptin A, further mysterious PTMs are found in salinipeptin B and salinipeptin C, with an *N*,*N*-dimethylalanine-*N*-oxide moiety in the former and a dimethylimidazolidin-4-one moiety in the latter. Salinipeptin A showed antibacterial activity against Group A *S. pyogenes* M1T1 with an LD_{50} of 12.5 μg/mL but is inactive against other tested bacterial.[92]

Cacaoidin (Figure 12) isolated from *Streptomyces cacaoi* CA-170360 combines outstanding structural features: a rare disaccharide β-6-deoxygulopyranosyl-(1 → 3)-α-rhamnopyranoside moiety attached to the phenolic oxygen of Tyr8, a high number of D-amino acids including two remarkable D-aminobutyric acid (Abu) residues, and particularly, an unprecedented *N*,*N*-dimethyl lanthionine system (NMe_2Ala-S-Ala) first identified within RiPPs. As mentioned above, (Me)Lan ring and terminal *N*-methylation are specific features of lanthipeptides and linaridins, making cacaoidin a novel RiPP class possessing the structural features of both lanthipeptides and linaridins, therefore termed lanthidins.[93] Induction of LiaRS bioreporter, specifically and strongly induced by antibiotics that target the cell wall,[94] was confirmed for cacaoidin, and it could be antagonized of the LiaRS stress response by the addition of purified Lipid II. These results strongly suggest that cacaoidin targets Lipid II and further impedes the cell envelope integrity to suppress the growth of susceptive strains, with potent activity against *Staphylococcus simulans* 22 (MIC 0.25 μg/mL), the clinically isolated MRSA MB5393 (MIC 0.5 μg/mL), and moderate activity against *B. subtilis* 168 and a set of *C. difficile* strains.[93]

LiaRS regulation screening for *B. subtilis* disclosed YydF (Figure 12), a novel class of RiPPs termed epipeptides with D-amino acids as the sole PTMs catalyzed by a radical SAM epimerase. The precursor peptide of YydF is first epimerized by the radical SAM enzyme (YydG) to obtain a D-Val and a D-*allo*-Ile in positions 36 and 44, respectively, processed by the membrane protease (YydH) and then exported by the ABC transporter (YydIJ) and requires no other post-translational modification. The matured peptide $YydF_{33-49DD}$ proved to be a more potent inhibitor leading to the total inhibition of *B. subtilis* growth with a MIC < 2 μg/mL. The peptide with an identical sequence but devoid of D-amino acid residues lost the activity toward *B. subtilis* completely, which is indicative of the importance of the D-amino acid residues.[95] Further studies demonstrated that $YydF_{33-49DD}$ targets the cell envelope, triggers membrane depolarization, permeabilization, rigidification, and additionally lipid domain formation to block cell wall synthesis, thereby ultimately resulting in cell death.[96]

Tryglysin A from *Streptococcus ferus* DSM 20646 and tryglysin B from *S. mutans* UA159 (Figure 12) carry an unprecedented tetrahydro[5,6]benzindole modification via two C−C bonds cross-links between Trp and Lys residues. A single radical SAM enzyme is responsible for the regio- and stereospecific cyclization of unactivated carbons.[97] Both tryglysins displayed bacteriostatic activities against their producing strains and the competing species, including *Streptococcus mitis*, *Streptococcus oralis*, *S. pneumoniae*, and several other streptococcal species. This raises the possibility that tryglysins are fratricidal agents as well.[98]

Circular bacteriocins cerecyclin and bacicyclicin XIN-1 (Figure 12) were isolated from *B. cereus* DDD103 and *Bacillus* sp. Xin1, respectively. They are incredibly stable under acidic and high temperatures but less stable in neutral or alkaline conditions. They exhibited inhibition of *B. cereus* spore outgrowth and a broad antimicrobial spectrum against Gram-positive bacteria, including *B. cereus*, *E. faecalis*, and *L. monocytogenes*. In contrast, no antimicrobial activity is detected against Gram-negative bacteria. Hemolysis of red blood cells (RBCs) was observed for neither of them at different concentrations, further implying the potential of circular bacteriocins as promising biopreservatives. A bit difference is that cerecyclin also significantly inhibited the growth of *B. amyloliquefaciens*, *Bacillus firmus*, *B. subtilis*, *B. pumilus*, while bacicyclicin XIN-1 strongly suppressed the growth of *S. aureus*, *E. faecium*, *S. epidermidis*, *S. pyogenes*, and *S. pneumoniae* as well.[99,100]

Enterocin Gr17 was isolated from *E. faecalis* Gr17, a novel bacteriocin-producing strain from the Chinese traditional low-salt fermented whole fish product Suan yu. The entire amino acid sequence was determined as RSYGNGVYCNNSKCWV-NWGEAKENIIGIVISGWATGLAGMGR with a disulfide bond, although the detailed structure remains obscure. It displayed potent antibacterial activity against Gram-positive bacteria such as *L. monocytogenes*, *S. aureus*, *B. subtilis*, *B. cereus*, and *E. faecalis* and poor activity against Gram-negative bacteria like *E. coli*, *Salmonella enteritidis*, *Brochothrix thermosphacta*, *P. aeruginosa*, *Pseudomonas fluorescens*, and *Cronobacter sakazakii* (mentioned in section 3.4).[101] In addition, it is also active against the pathogenic yeast *Candida albicans* (mentioned in section 4).[101]

Another structurally uncharacterized bacteriocin is lactolisterin BU with a molecular mass of 5160.94 Da and an internal fragment AVSWAWQH, isolated from *L. lactis* subsp. *lactis* bv. diacetylactis BGBU1-4. It was active against various Gram-positive bacteria, with the MICs in the micromolar range, embracing several *L. lactis* strains, *Lactobacillus casei* BGHN14, *L. monocytogenes* ATCC 19111, *S. aureus* ATCC 25923, *S. pyogenes*, *S. pneumoniae*, *E. faecalis* ATCC 29212, and *E. faecalis* BGZLS10-27. Curiously, lactolisterin BU even exhibited comparable antimicrobial activity against its producers. Because of the relative thermostability and inhibitions of substantial food spoilage and foodborne pathogens, lactolisterin BU is another desirable candidate for application in the food industry.[102]

3. RiPPs AGAINST GRAM-NEGATIVE BACTERIA

3.1. Darobactins/Dynobactins

Darobactin A (Figure 13) was identified from the concentrated extract of *Photorhabdus khanii* HGB1456, a Photorhabdus symbiont of entomopathogenic nematode microbiomes and strain *P. khanii* DSM 3369 with a higher yield was used to isolate darobactin A. Structural elucidation showed that darobactin A is a modified heptapeptide (WNWSKSF) with an ether link between C7 indole of W^1 and the β-carbon of W^3, and a carbon−carbon bond between the C6 indole of W^3 and the β-carbon of K^5. Bioinformatic analysis, knockout experiment, and heterologous expression suggested that it was synthesized through a ribosomal pathway. Darobactin A exhibited potent activity against a series of Gram-negative bacteria, with IC_{50} values ranging from 2 to 64 μg/mL. Especially for some drug-resistant clinical isolates, it also showed promising inhibitory activity. Notably, this new peptide has little effect on gut commensals, and the virulence of the darobactin A-resistant strain is significantly reduced. Animal experiments showed that darobactin could effectively protect animals infected with pathogens. The target of

https://doi.org/10.1021/acsbiomedchemau.2c00062
ACS Bio Med Chem Au 2023, 3, 1−31

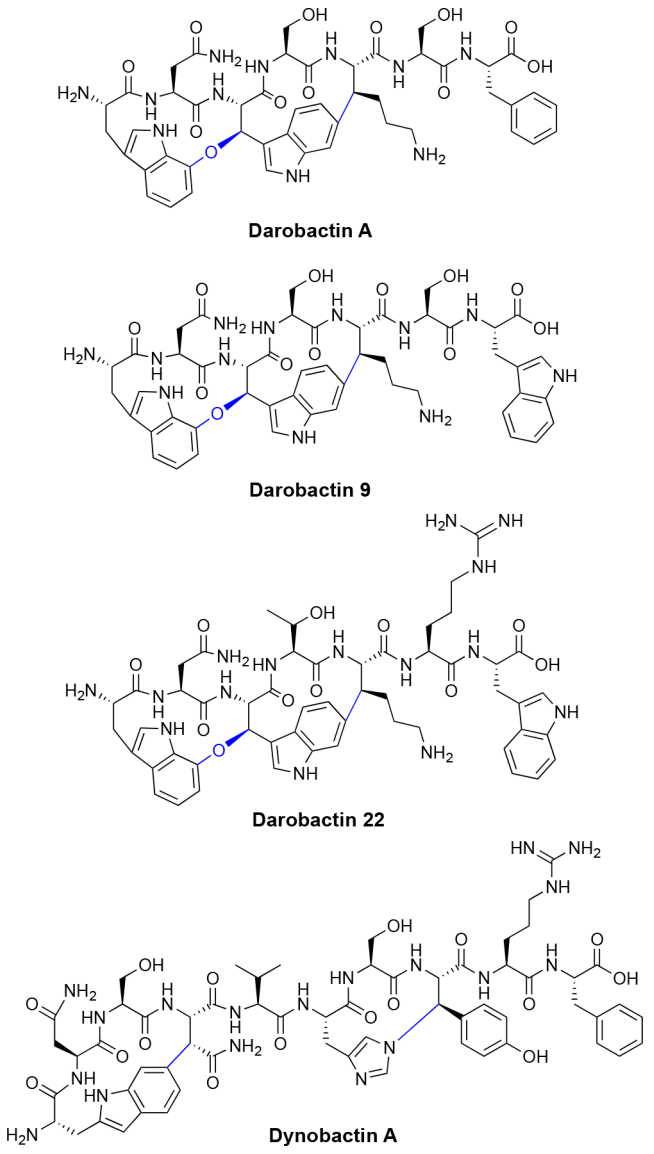

Figure 13. Structures of darobactins. The class-defining PTMs are highlighted in blue.

darobactin A was identified as BamA, an essential component for folding and inserting outer membrane proteins.[103] The structure of the darobactin-BamA complex suggested the peptide could mimic the *C*-terminal β-signal of native BamA substrates and seal the lateral gate.[104] The detail of how darobactin affects the mechanical, kinetic, and energetic properties of BamA was tested by dynamic single-molecule force spectroscopy.[105] The yield of darobactin A reached 13.4 mg/L by expressing the synthetically engineered gene cluster in *E. coli*, 13 new non-natural derivatives and four predicted products (darobactins B, C, D, and E) were obtained by engineering the core peptides of darobactin A. Among them, darobactin 9 (Figure 13) exhibited improved activity against *P. aeruginosa* and *Acinetobacter baumannii* with MICs of 0.125 and 1−2 μg/mL, respectively, as well as potent activity against MDR clinical isolates of *E. coli* (1−2 μg/mL) and *K. pneumoniae* (1−4 μg/mL).[106] In addition to darobactins B-E, another natural member F was also generated by mutasynthetic derivatization of a heterologous expression system, among which darobactin B, D, and E were isolated and also exhibited anti-Gram-negative activity.[107] Lately, guided by the Bam complex-darobactin 9 structures generated by cryogenic electron microscopy (cryo-EM), 20 new darobactin variants were obtained using biosynthetic engineering.[108] Notably, one variant Darobactin 22 (WNWTKRW) (Figure 13) turned out to bind more tightly to BamA and surpass the antimicrobial activity of darobactin 9 against *Acinetobacter baumannii* up to 32-fold with MICs ranging from 0.0625 to 0.5 μg/mL, without observing toxic effects.[108]

Another recently reported novel RiPP dynobactin A (WNSNVHSYRF) (Figure 13), exhibiting potent anti-Gram-negative bacteria activity, was identified from *Photorhabdus australis* by computational analysis of BGCs distantly related to darobactins.[109] Despite possessing an unrelated structural scaffold to darobactins, dynobactin A performs antimicrobial activity also by binding to BamA. Although it obstructs the function of Bam complex at a lower IC_{50} value than darobactin A and B, the MIC values of dynobactin A were about 4-fold higher than darobactin A.[109] This might be attributed to the lower permeation of dynobactin A to the outer membrane. As a RiPP from the symbiont of nematode gut microbiome, dynobactin A showed no observed cytotoxicity at the concentration up to 1 mg/mL and protection for the mouse from *E. coli* infection in animal experiments, indicating that dynobactin A is potentially a promising lead for the development of antibiotic agent.[109]

3.2. Lanthipeptides

Lanthipeptides are famous for their anti-Gram-positive activity. However, some versatile members also possess activity against Gram-negative bacteria. Utilizing the strategy of high-throughput elicitor screening (HiTES) combined with biological activity assays, a novel lanthipeptide (GPITFGTT-CWGTPCPSANTVSC), designated cebulantin (Figure 14) was purified from the fermentation broth of *Saccharopolyspora cebuensis* supplemented with furosemide as an elicitor. It

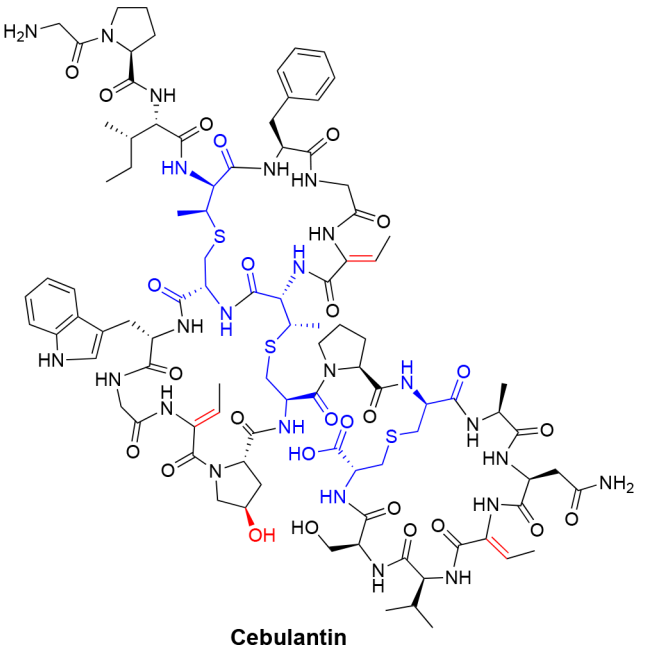

Figure 14. Structures of cebulantin with anti-Gram-negative activity. The class-defining PTMs are highlighted in blue, and other PTMs are highlighted in red.

https://doi.org/10.1021/acsbiomedchemau.2c00062
ACS Bio Med Chem Au 2023, 3, 1−31

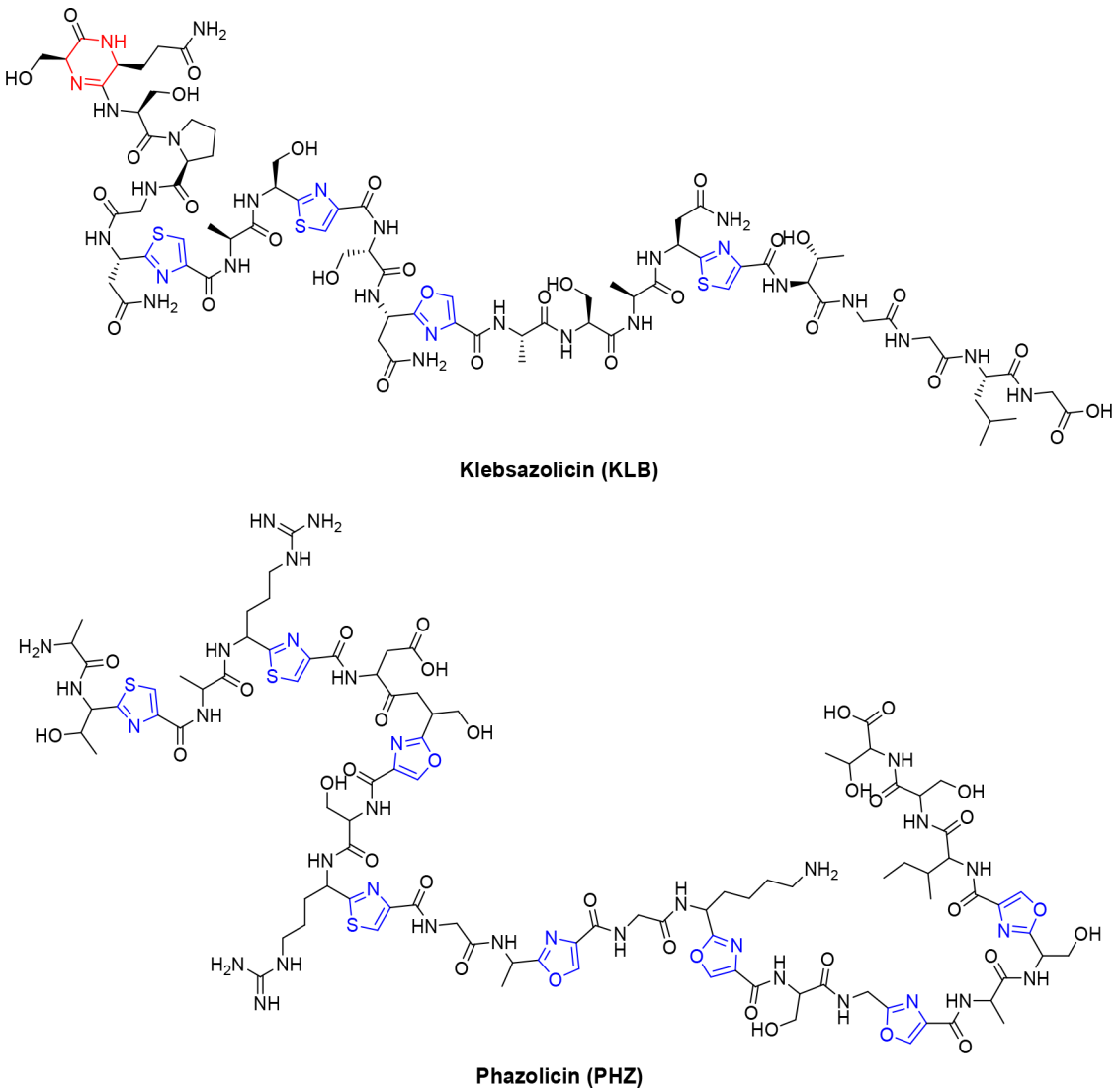

Figure 15. Structures of linear azol(in)e-containing peptides with anti-Gram-negative activity. The class-defining PTMs are highlighted in blue, and other PTMs are highlighted in red.

exhibited inhibitory activity against cell wall-weakened *E. coli* (Δ*lptD*) with an IC_{50} of 9.7 ± 0.4 μM; moreover, it also showed activity against several *Vibrio* strains with IC_{50}s ranging from 8.8 to 29.1 μM. Meanwhile, the activity of anti-Gram-positive bacteria was not detected.[110]

Compounds containing *C*-terminal 2-aminovinyl-cysteine (AviCys) usually exhibit strong bioactivities. Five strains with AviCys containing lanthipeptide BGCs were obtained through a genomic approach, and one showed potent antibacterial activity. To overcome the low yield of active components, the cosmid covering the intact BGC was expressed successfully in heterologous host *S. albus* J1074. Daspyromycin A (ITSISLCTPGCTSAGGGSNCSFCC, Figure 4) and its hydroxylated analog daspyromycin B, together with two degraded products, daspyromycins C and D, were isolated and characterized. Apart from the activity against Gram-positive bacteria, daspyromycin A and B also exhibited potent antibacterial activity against Gram-negative bacteria with MIC values of 4 and 16 μg/mL against *A. avenae* ATCC 19307, 4, and 32 μg/mL against *P. syringa*e ATCC-BAA-2502 and 2 and 4 μg/mL against *X. oryzae* ATCC 35933.[47]

Combining the cell-free protein synthesis (CFPS) platform with library screening, a mutant of nisin named M5 (I4R, K12W, A15P, A24K, and S29Q, Figure 3) exhibited higher inhibitory activity to *E. coli* with EDTA than nisin Z or S29A.[41]

3.3. Linear Azol(in)e-Containing Peptides (LAPs)

A thiazole/oxazole-modified microcin BGC was identified in the genome of *Klebsiella pneumoniae* subsp. *ozaenae* ATCC 11296 by genome mining. A new RiPP with three thiazoles, one oxazole, and one unique *N*-terminal amidine ring, named klebsazolicin (KLB, SQSPGNCASCSNSASANCTGGLG, Figure 15), was purified and characterized. It could inhibit the growth of Gram-negative bacteria, including *E. coli*, *K. pneumoniae*, and *Yersinia pseudotuberculosis*, with MICs ranging from 16 to 65 μM, while no inhibitory activity was detected against other tested Gram-negative or -positive strains. The narrow spectrum of KLB may be related to the cellular membrane proteins such as OmpF or SbmA, which could help KLB enter cells. Biochemical studies and structural analysis suggested that KLB could inhibit 70S ribosome by binding in the peptide exit tunnel in a compact conformation. Besides, a set of KLB mutants were obtained by engineering, which could

https://doi.org/10.1021/acsbiomedchemau.2c00062
ACS Bio Med Chem Au 2023, 3, 1−31

not only help to analyze the structure−activity relationship (SAR) but also serve as a starting point for developing new bioactive compounds.[111]

Another BGC of LAP similar to KLB was found in the genome of *Rhizobium* sp. Pop5 by genome mining and its products, phazolicin (PHZ, Figure 15), A-PHZ, and TA-PHZ were identified in the medium cultivated strain Pop5, which included three thiazole and five oxazole cycles. The PHZ showed inhibitory activity to some members of genera *Rhizobium*, *Sinorhizobium*, and *Azorhizobium* with MICs of 0.125−1 μM. Similar to KLB, PHZ also inhibited the growth of the targeted strain by binding in the peptide exit tunnel to interfere with the elongation step of protein synthesis.[112]

3.4. Sactipeptides

Ruminococcin (Figure 8) presented in section 2.2 could also induce a lag phase of the *E. coli* growth curve, suggesting that it also acted on Gram-negative bacteria. As a compound against both Gram-positive and -negative strains, it may target other components rather than the cell envelope. Meanwhile, it also could contribute to shaping the gut ecosystem.[62]

3.5. Lasso Peptides

Citrocin (Figure 16) is a 19-amino acid-long antimicrobial lasso peptide (GGVGKIIEYFIGGGVGRYG) isolated from *Citrobacter braakii*. The corresponding codon-optimized and refactored biosynthetic gene cluster was expressed successfully in the heterologous host *E. coli*. Citrocin is thermostable and exhibited moderate activity against *E. coli* and *Citrobacter* strains with IC_{50} values of 16−125 μM and some weak activity against *Salmonella* Newport with an IC_{50} value of 1000 μM. It exhibited more potent inhibitory activity against RNA polymerase (RNAP) of *E. coli* than microcin J25 (MccJ25) *in vitro*, while the activity against *E. coli* is weaker than MccJ25, which may attribute to the different uptake mechanisms. In addition, the authors found that Arg-17 is essential for both thermostability and antibacterial activity.[113] A structure similar to lasso peptide termed ubonodin with a compelling 18aa loop and a short 2aa tail was isolated from *Burkholderia ubonensis* MSMB2207. This lasso peptide is thermosensitive as it contains multiple Asp residues and degrades into various peptide fragments at 95 °C for 2 h. Ubonodin inhibits transcription initiation of the *E. coli* RNA polymerase and has potent activity against *Burkholderia cepacia*, *Burkholderia multivorans*, *Burkholderia mallei*, and poorly activity against *Burkholderia thailandensis*.[114]

Acinetodin (Figure 16) was isolated from the supernatant of *Acinetobacter gyllenbergii* CIP 110306, and klebsidin (Figure 16) was obtained by expressing the gene cluster from *K. pneumoniae* 4541−2 in *E. coli*. Both are lasso peptides and could inhibit transcript elongation of the RNA polymerase of *E. coli*. Acinetodin and klebsidin showed no or weak inhibitory activity against tested strains. However, the *E. coli* expressing FhuA became sensitive to acinetodin, which indicated the inability to permeate bacterial cells limited their activity.[115]

3.6. Others

Enterocin Gr17 presented in section 2.6 also exhibited poor antibacterial activity against Gram-negative bacteria, including *E. coli*, *S. enteritidis*, *Brochothrix thermosphacta*, *P. aeruginosa*, *P. fluorescens*, and *Cronobacter sakazakii*.[101]

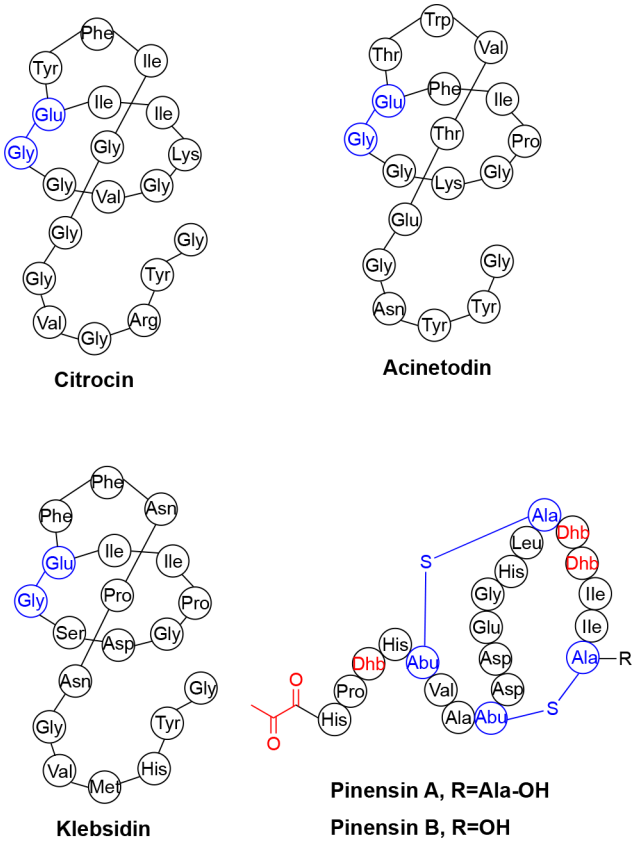

Figure 16. Structures of lasso peptide with anti-Gram-negative activity and pinensins with antifungal activity. The class-defining PTMs are highlighted in blue, and other PTMs are highlighted in red.

4. ANTIFUNGAL RiPPs

The first reported antifungal RiPPs are pinensin A and B (Figure 16) isolated from *Chitinophaga pinensis* DSM 28390 (= DSM 2588), a limited exploration group belonging to Bacteroidetes. Pinensin A and B are derivatized from one precursor peptide, and they differentiate each other with the last amide acid at *C*-terminal. The 1:1 mixture of A and B displayed broad-spectrum antifungal activity with the MICs against yeasts and filamentous fungi ranging from 2.1 to 4.2 mg/mL, similar to first-line antifungal drugs, such as nystatin and amphotericin B_1.[116] In addition, they also showed weakly antibacterial and cytotoxic activities. However, the structures of pinensins are relatively simple. Only two methyllanthionine rings and one pyruvyl group at *N*-terminal were detected. Although the mode of mechanism of pinensins remains ambiguous, the discovery of antifungal lantibiotics encourages researchers to explore more antifungal RiPPs, which will be beneficial to the treatment of fungal infections.

In addition to pinensins, other RiPPs also exhibited some antifungal activity, such as ruminococcin C[65] (mentioned in section 2.2) and enterocin Gr17 (mentioned in section 2.6).[101]

5. ANTITUMOR RiPPs

5.1. Thioviridamide-like RiPP

Thioviridamide (Figure 17) derived from core peptide SVMAAAASIALHC with five contiguous thioamide groups was first identified from *Streptomyces olivoviridis* by Shin-ya and co-workers in 2006, which showed selective cytotoxicity against Ad12-3Y1 and E1A-3Y1 cells containing adenovirus E1A oncogene at 3.9 and 32 ng/mL respectively (Table 2). Ad12-3Y1 cells treated with thioviridamide showed chromatin

https://doi.org/10.1021/acsbiomedchemau.2c00062
ACS Bio Med Chem Au 2023, 3, 1−31

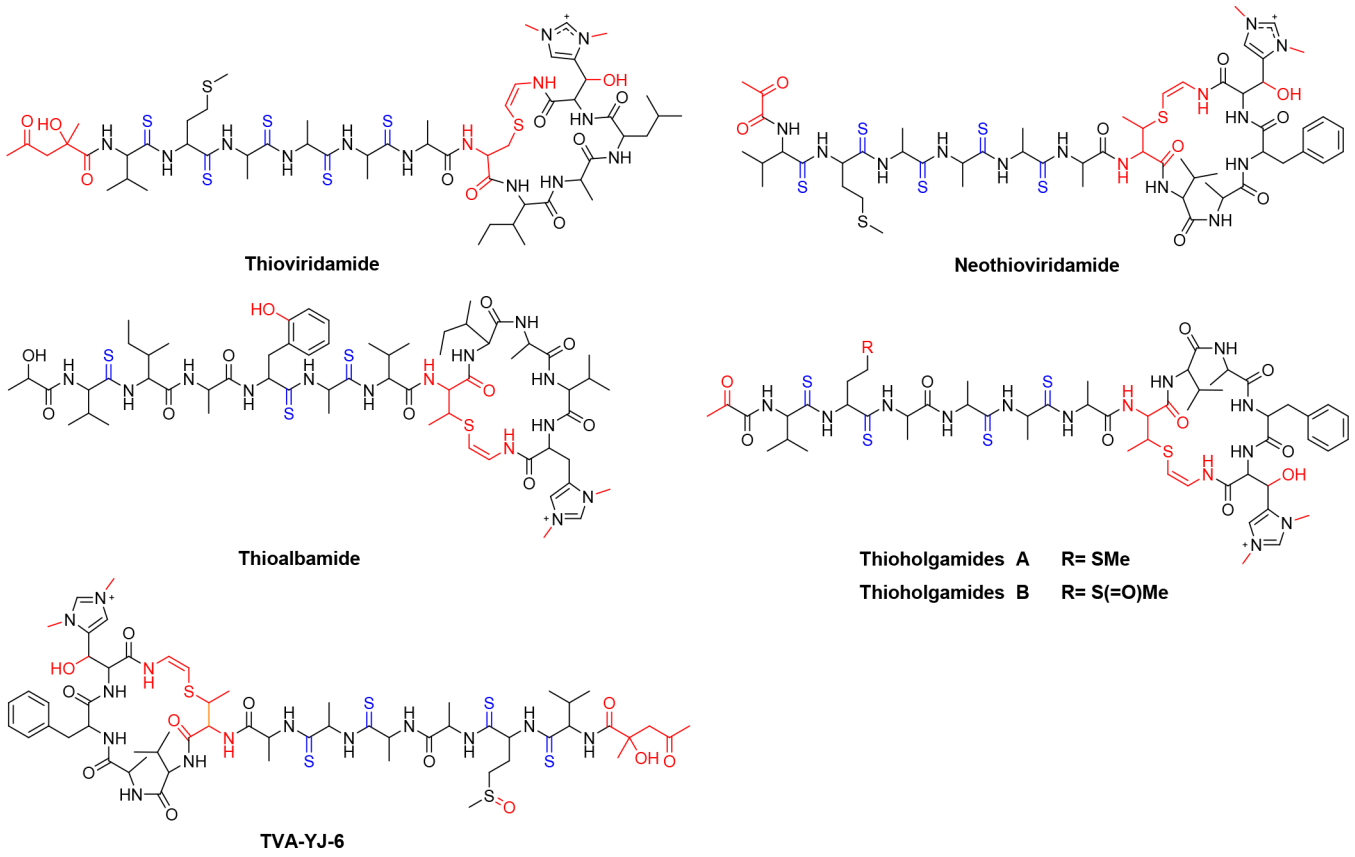

Figure 17. Structures of thioviridamide-like RiPPs with antitumor activity. The class-defining PTMs are highlighted in blue, and other PTMs are highlighted in red.

condensation and nuclear fragmentation, typical traits of apoptosis.[117,118] More interestingly, the apoptosis resulting from thioviridamide is dependent on E1A, which makes it a promising antitumor agent against tumor cells expressing E1A-like oncogenes.[117] Furthermore, more thioviridamide-like molecules (TLMs) featuring a series of thioamide groups with potent cytotoxicity were reported. Heterologous expression of the biosynthetic gene cluster of thioviridamide produced a novel derivative, JBIR-140, which possesses a lactyl moiety instead of a 2-hydroxy-2-methyl-4-oxopentanoyl group in thioviridamide. The cytotoxic activities of JBIR-140 are about two to three times higher than thioviridamide with tested cell lines (human ovarian adenocarcinoma SKOV-3, malignant pleural mesothelioma Meso-1, and Jurkat cells) (Table 2).[119] During efforts to generate polythioamide RiPPs, neothioviridamide (Figure 17) was obtained by employing heterologous expression, which shares a similar core peptide (SVMAAAATVAFHC) with thioviridamide. It exhibited cytotoxic activities against cancer cell lines SKOV-3, Meso-1, and Jurkat with IC_{50} values of 2.1, 0.7, and 0.4 μM, respectively (Table 2).[120]

Truman and co-workers pointed out that the unusual *N*-terminal modification may be generated during extraction. Their report identified three TLMs from selected actinomycetes based on genomic data analysis. And one of them, isolated from *Amycolatopsis alba* DSM 44262, designated thioalbamide (SVIGFAVTIAVHC, Figure 17), possesses a potent antitumor activity with considerable selectivity. The IC_{50} values of thioalbamide against tested cancer cell lines range from 48 to 72 nM, an order of magnitude more potent than clinically used doxorubicin. Meanwhile, the value toward a noncancerous epithelial cell line is 0.302 μM, similar to doxorubicin (0.343 μM) (Table 2).[121] Further research suggested that thioalbamide could induce mitochondrial dysfunction, oxidative stress, and apoptotic cell death of breast cancer cell lines. Similar to reported results, the antiproliferative activity of thioalbamide to selected breast cancer cell lines is more potent than doxorubicin (IC_{50} values ranging from 54 to 75 nM versus 154 to 1170 nM) while they showed similar cytotoxic activity to noncancerous cell lines (Table 2). More importantly, it could disturb the propagation of breast cancer stem cells.[122] With a similar ideology, two TLMs (thioholgamides A and B, Figure 17) from *Streptomyces malaysiense* DSM 100712 were purified and structurally characterized. They share a similar core peptide sequence (SVMAAAATVAFHC) with thioviridamide, and thioholgamide A exhibited superior cytotoxic activities than thioviridamide and JBIR-140. The IC_{50} values of thioholgamide A against SKOV-3 and Jurkat cell lines are 2.49 and 0.53 μM, respectively, four to ten times lower than JBIR-140. As to other tested cell lines, including HCT-116, KB-3.1, SW480, and U937, the IC_{50} values of thioholgamide A ranged from 0.03 to 2.19 μM, while the cytotoxic activity of thioholgamide B is 10-fold lower (Table 2).[123] Overexpression of the newly identified TLMs gene cluster in *Streptomyces* sp. NRRL S-87, three novel analogues of thioviridamide, TVA-YJ-4, TVA-YJ-5, and TVA-YJ-6 (Figure 17), shared identical core peptide with thioholgamides, were detected. However, the cytotoxic activity of newly discovered analogues is reduced than the parental thioholgamides A (TVA-YJ-2), with the IC_{50} values against selected cancerous

https://doi.org/10.1021/acsbiomedchemau.2c00062
ACS Bio Med Chem Au 2023, 3, 1−31

Table 2. IC_{50} (μM) Values of Antitumor RiPPs against Various Cell Lines in This Review

cell lines	Thioviridamide	JBIR-140	Thioalbamide	Doxorubicin	Thioholgamide A	Thioholgamide B	TVA-YJ-4	TVA-YJ-5	Neothioviridamide	Aurantizolicin	Curacozole	Aeronamide A	Gymnopeptide A	Gymnopeptide B
SKOV-3	38.0	10.8			2.49	20.89			2.1					
Meso-1	27.8	14.3							0.7					
Jurkat	12.5	5.4			0.53	5.23			0.4	0.217				
A549			0.048	0.712									0.0265	0.0185
MCF7			0.059	0.878	0.30		0.83	4.98						
MDA-MB-231			0.072	1.174									0.0374	0.0307
MDA-MB-468			0.054	0.362										
T47D			0.075	0.536										
SKBR3			0.074	0.154										
HeLa			0.050	0.644						0.209		0.0015	0.0884	0.0425
PA-TU-8988T			0.065	0.630										
MCF 10A			0.302	0.343										
BJ-hTERT			0.321	0.360										
HCT-116					0.03	0.51					0.009			
KB-3.1					0.54	4.49								
SW480					0.11	12.17								
U937					2.19	16.94								
HL60					0.60		1.47	0.61						
H1299					1.12		5.02	5.08						
LOVO					0.94		1.18	1.93						
A431													0.0664	0.0443
T47													0.018	0.014

https://doi.org/10.1021/acsbiomedchemau.2c00062
ACS Bio Med Chem Au 2023, 3, 1−31

cell lines ranging from 0.6 to 5.1 μM, while the values of thioholgamides A are between 0.3 and 1.2 μM (Table 2).[124]

5.2. Poly(thi)azole Cyclopeptides

Poly(thi)azole cyclopeptides biosynthesized by the RiPPs pathway usually exhibit potent cytotoxicity. Since telomerase inhibitor telomestatin was discovered from *Streptomyces anulatus*,[125] more and more members were purified and characterized in the following two decades, including YM-216391,[126,127] mechercharmycin A (MCM-A) and its linear congener MCM-B,[128] urukthapelstatin,[129,130] aurantizolicin and its deritative[131,132] and curacozole.[133] Assisted by genomic data, bio- and cheminformatic platform, aurantizolicin (Figure 18) was detected from *Streptomyces aurantiacus* JA 4570 in one of 20 media conditions. However, the yield of aurantizolicin was extremely low, and the corresponding bioactivity was not evaluated.[131] The aurantizolicin shares a similar core peptide sequence (FIIGSSCC versus FIVGSSSC) with YM-216391, combining a highly effective heterologous expression system with precursor peptide engineering, the group of Tang obtained aurantizolicin and its derivative (FIVGSSCC) with high yield. The derivative exhibited improved antitumor activity with IC_{50} values against HeLa and Jurkat cell lines at 119 and 62.2 nM, respectively, lower than aurantizolicin (209 and 217 nM) and YM-216391 (502 and 112 nM) (Table 2).[132] Curacozole (Figure 18) was isolated from *Streptomyces curacoi* by genome mining in 2018 which also shares a similar core peptide (FIIGSTCC) with YM-216391 and showed highly toxic toward HCT116 and HOS cancer cell lines with IC_{50} values at 8.6 and 10.5 nM respectively (Table 2).[133] Two novel congeners MCM 17 and 18 (Figure 18) were obtained by expressing engineered mechercharmycin pathway in heterologous host *B. subtilis* TG1111 and exhibited comparable cytotoxicity against Jurkat cell lines.[134]

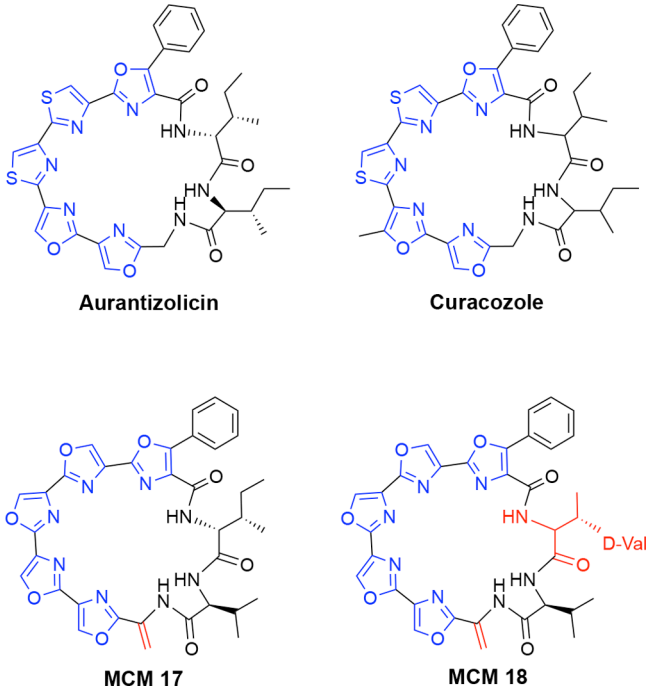

Figure 18. Structures of poly(thi)azole cyclopeptides with antitumor activity. The class-defining PTMs are highlighted in blue, and other PTMs are highlighted in red.

5.3. Proteusins

Proteusins are a new family of RiPPs characterized by β-helix and numerous nonproteinogenic amino acids. Polytheonamides, the first isolated proteusin constituted by 48 residues, were believed to be biosynthesized by nonribosomal peptide synthetase before their gene cluster was identified from the library of *T. swinhoei* total DNA. Further analysis suggested the gene cluster may source from uncultivated bacterial symbionts.[135] Polytheonamides are highly cytotoxic with IC_{50} against L1210 below 4 ng/mL, against P388 at 1.4 ng/mL, and HeLa at 2.9 ng/mL.[136,137] Given the potent cytotoxicity and difficulty in chemical syntheses, Piel's group found a homologous gene cluster in cultivable Betaproteobacterium *Microvirgula aerodenitrificans* DSM 15089 by genome mining, and its product, named aeronamide A (Figure 19), was obtained by a "tagged-bait" strategy. Although lacking the *tert*-butyl moiety, which has been implicated as a cytotoxicity determinant of polytheonamides, aeronamide A exhibited unexpected potent cytotoxicity with IC_{50} against HeLa at 1.48 nM which is based on a similar pore-forming mechanism to polytheonamides.[138]

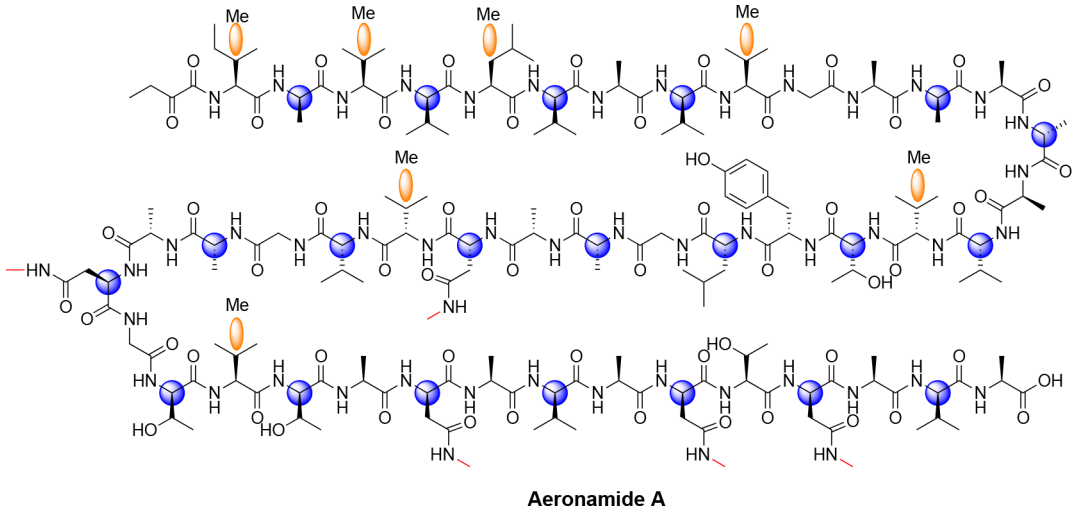

Figure 19. Structure of aeronamide A. Modified residues are labeled according to the legend below. The orange oval-shaped balloon indicates a methyl group localized to the corresponding residues, but the exact locations remain unknown.

https://doi.org/10.1021/acsbiomedchemau.2c00062
ACS Bio Med Chem Au 2023, 3, 1−31

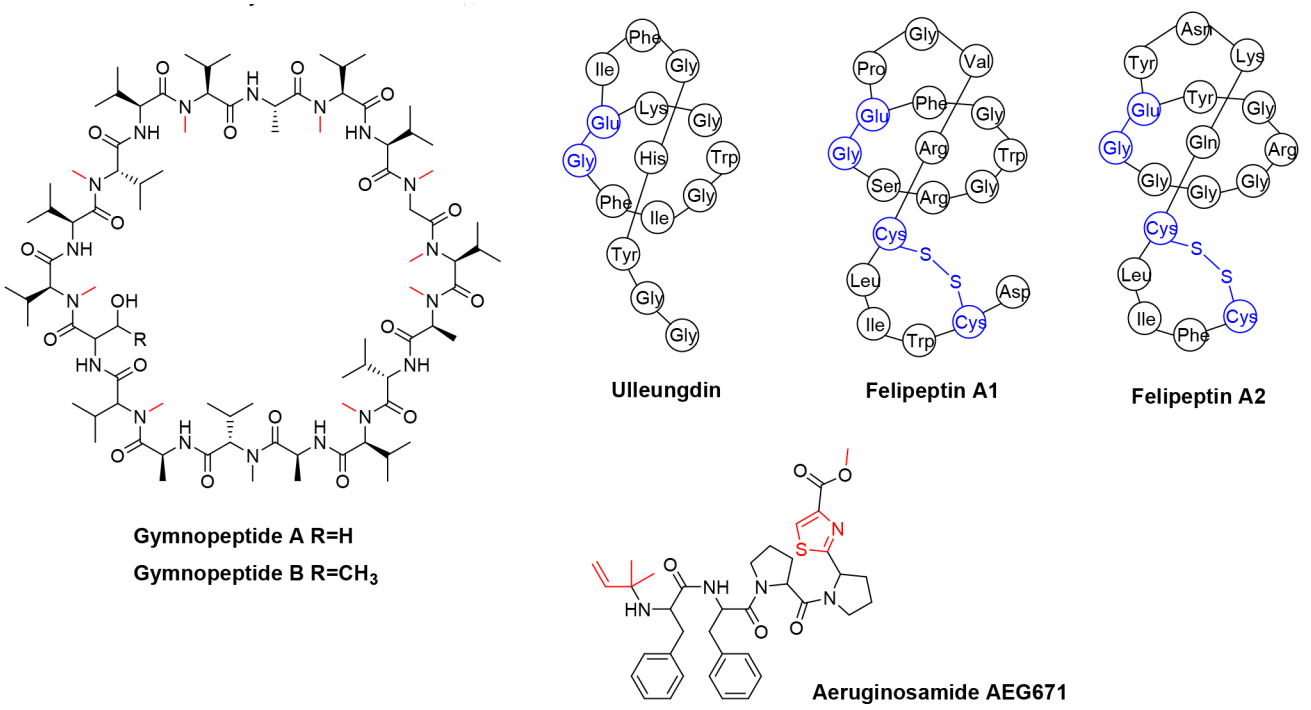

Figure 20. Structures of other RiPPs with antitumor activity. The class-defining PTMs are highlighted in blue, and other PTMs are highlighted in red.

5.4. Others

A novel lasso peptide was isolated from *Streptomyces* sp. KCB13F003 by genome mining and one strain many compounds (OSMAC) strategy. The compound designated ulleungdin (core peptide sequence GFIGWGKDIFGHYGG, Figure 20) showed inhibitory activity on cancer cell invasion and migration. The rate of A549 cells invaded through the tested membrane decreased by approximately 50% after treatment with 50 μM ulleungdin for 24 h. The migration and motility of the treated cells were also inhibited.[139] Another two lasso peptides named felipeptin A1 (GSRGWGFEPGVR-CLIWCD) and A2 (GGGGRGYEYNKQCLIFC) (Figure 20) were obtained by genome mining and heterologous expression. The mixture of these two lasso peptides could stimulate the proliferation of cancer cells by downregulating the tumor suppressor Rb.[140] Interestingly, the cancer cells treated with felipeptins are more sensitive to the chemotherapy drug doxorubicin. Furthermore, the DOX-resistant MCF7 cells became much more sensitive to doxorubicin after treating with felipeptins.[141]

Two highly *N*-methylated cyclic octadecapeptides, gymnopeptides A and B (Figure 20), were isolated from mushroom *Gymnopus fusipes*, and both showed potent antiproliferative activity on tested cancer cell lines. The IC_{50} values of gymnopeptide A against HeLa, A431, MCF7, MDA-MB-231, and T47A are 88.4 ± 3.3, 66.4 ± 4.1, 26.5 ± 3.2, 37.4 ± 2.2, and 18.0 ± 3.0 nM, respectively. Gymnopeptide B exhibited more potent cytotoxicity against the same cancer cell lines, with IC_{50} values of 42.5 ± 4.5, 44.3 ± 2.7, 18.5 ± 6.8, 30.7 ± 3.0 and 14.0 ± 2.2 nM, respectively, which are 2−3 orders of magnitude more efficient than cisplatin (Table 2).[142] Their biosynthetic pathway was subsequently identified through bioinformatic analysis and heterologous expression in *E. coli*.[143]

Eighteen new aeruginosamide (Figure 20) variants were detected in the crude extraction of cyanobacterium *Limnoraphis* CCNP1324. However, most of them were poorly separated. The chromatographically separated samples containing AEG681a and an unknown residue reduced the relative T47D cell viability to 4.2% ± 0.5% at 200 μg/mL.[144] In addition, salinipeptin A presented in section 2.6 also exhibited inhibitory activity against U87 and HCT-116 with LD_{50} of 15 μg/mL.[92]

6. PROTEASE INHIBITORY RiPPs

6.1. Microviridin-like RiPPs

Microviridin-like molecules which contain tricyclic scaffold constructed by intramolecular ω-ester and ω-amide bonds between TxKxPSD motifs are potent protease inhibitors. The first member of microviridin A was identified from the toxic cyanobacterium *Microcystis viridis* in 1990.[145] More and more microviridin-like molecules with protease inhibitory activity were isolated and characterized in the recent decade. Microviridin LH1667 (Figure 21) (YSTLKYPSDWEEY) was isolated from freeze-dried cells of *Microcystis* spp.. It could inhibit chymotrypsin with IC_{50} value at 2.8 μM and elastase at 20 nM, while no inhibitory activity to trypsin was detected at 45.5 μM.[146] The selectivity may relate to the amino acid at the 10th position from C-terminus.[147] Combining phylogenomic analysis and chemo-enzymatic synthesis, MdnA3, MdnA6, MdnA7, and MdnA8 (Figure 21) were obtained *in vitro*. MdnA3 and MdnA6 were acetylated tricyclic peptides which showed potent inhibitory activity to trypsin with IC_{50} values of 28.4 ± 4.0 nM and 21.5 ± 0.6 nM, respectively. Bicyclic MdnA7 and MdnA8 exhibited activity to elastase with IC_{50}s of 1.05 ± 0.20 and 21.85 ± 3.35 μM, respectively.[148] Microviridin M (YNVTLKYPSDWEEF, Figure 21) was obtained by expressing fosmid with gene *mdnA* or *mdnB* in *E. coli*. It is a tricyclic but not an *N*-acetylated microviridin variant which exhibited moderate inhibitory activity against elastase and subtilisin with IC_{50} values of 2.9 and 6.9 μM, respectively.[149]

https://doi.org/10.1021/acsbiomedchemau.2c00062
ACS Bio Med Chem Au 2023, 3, 1−31

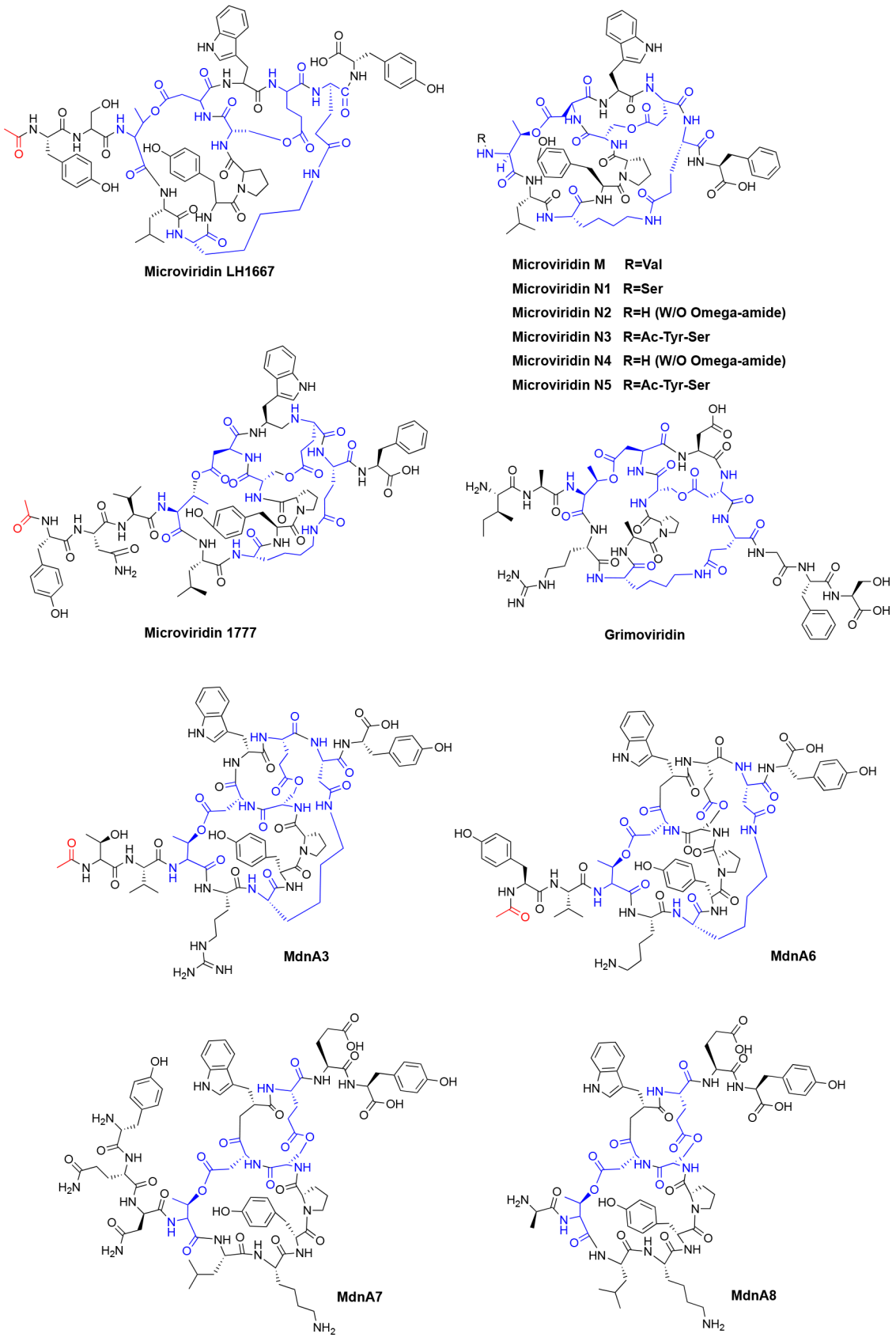

Figure 21. Structures of microviridin-like RiPPs with protease inhibitory activity. The class-defining PTMs are highlighted in blue, and other PTMs are highlighted in red.

Utilizing the minimal microviridin expression platform,[150] completely and incompletely processed microviridin N1−N5 (YSTLKYPSDWEEY, Figure 21) were detected by HPLC, while one of them, acetylated (Ac) bicyclic microviridin N3

https://doi.org/10.1021/acsbiomedchemau.2c00062
ACS Bio Med Chem Au 2023, 3, 1−31

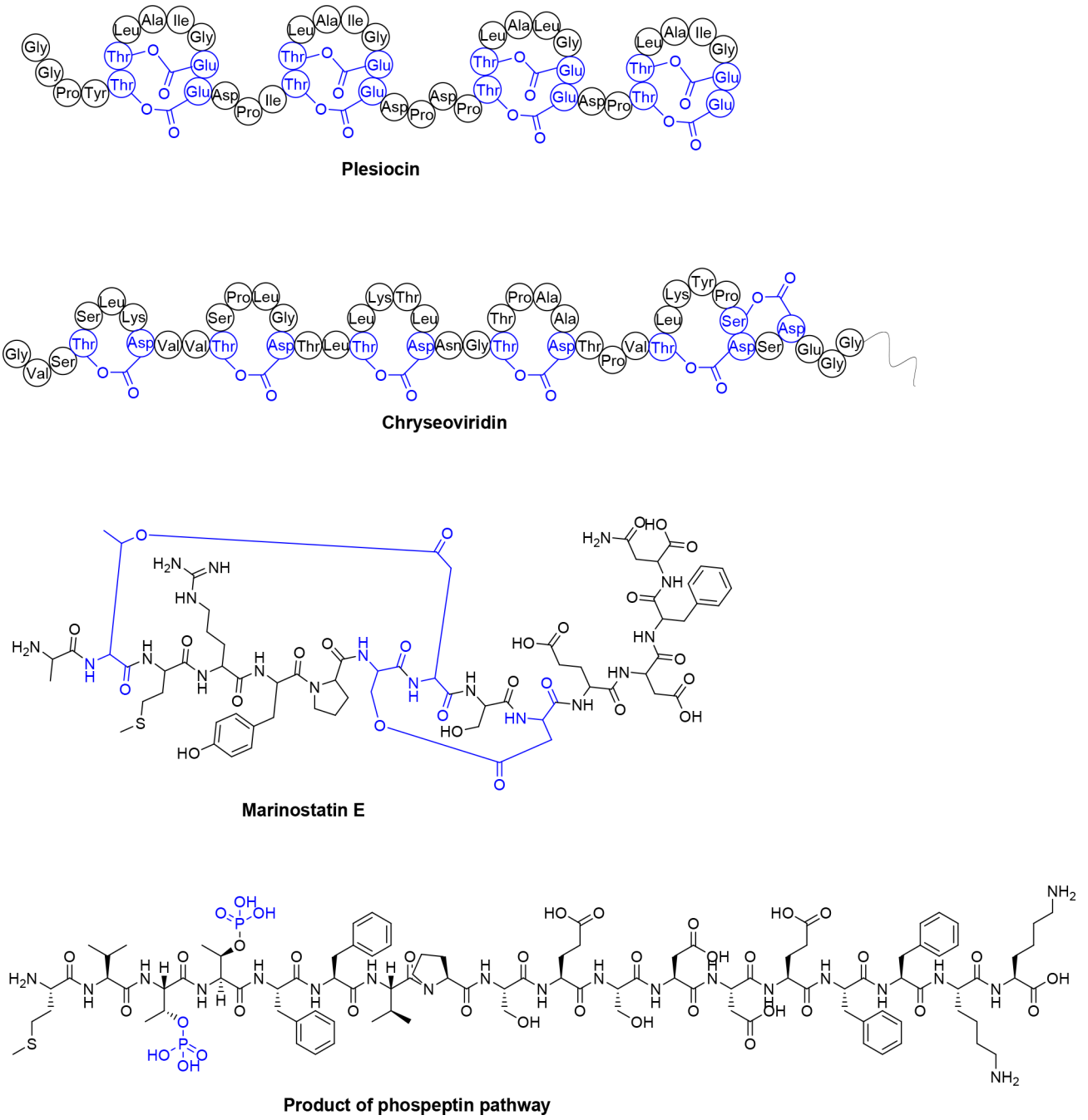

Figure 22. Structures of other RiPPs with protease inhibitory activity. The class-defining PTMs are highlighted in blue.

was isolated to test its bioactivity. It exhibited slightly higher inhibitory potential against elastase and subtilisin than microviridin M, with IC_{50} values of 2.5 and 2.0 μM, respectively.[149] Microviridin 1777 (YNVTLKYPSDWEEF, Figure 21) was isolated from cyanobacterium *Microcystis aeruginosa* by a metabologenomic approach. It displayed potent activity against elastase and chymotrypsin with IC_{50} values at 160 and 100 nM, respectively, while the IC_{50} to trypsin was more than 10 μM.[151] A microviridin-like BGC from *Grimontia marina* was expressed in heterologous host *E. coli*, and a new compound grimoviridin (IATRKAPSDDDE-GFS, Figure 21) with one isopeptide and two ester bonds was obtained. It exhibited inhibitory activity toward chymotrypsin, trypsin, and subtilisin with IC_{50} values of 5.2 μM, 238 nM, and 55 μM, respectively, while no inhibitory activity was detected to elastase.[152] Apart from the natural products, some variants of microviridins obtained by the microviridin engineering platform or chemo-enzymatic technology showed improved inhibitory activity on different types of serine proteases.[153,154] These variants enabled researchers to dissect the effect of individual amino acids for protease selectivity. The cocrystallization of microviridin J and trypsin provided more structural insights into the interaction, which would be beneficial to rationalize peptide engineering.[153]

6.2. Others

The biosynthetic gene cluster of plesiocin was identified in marine myxobacterium *Plesiocystis pacifica*, and its product was obtained by incubating precursor PsnA2 and modified enzyme

https://doi.org/10.1021/acsbiomedchemau.2c00062
ACS Bio Med Chem Au 2023, 3, 1−31

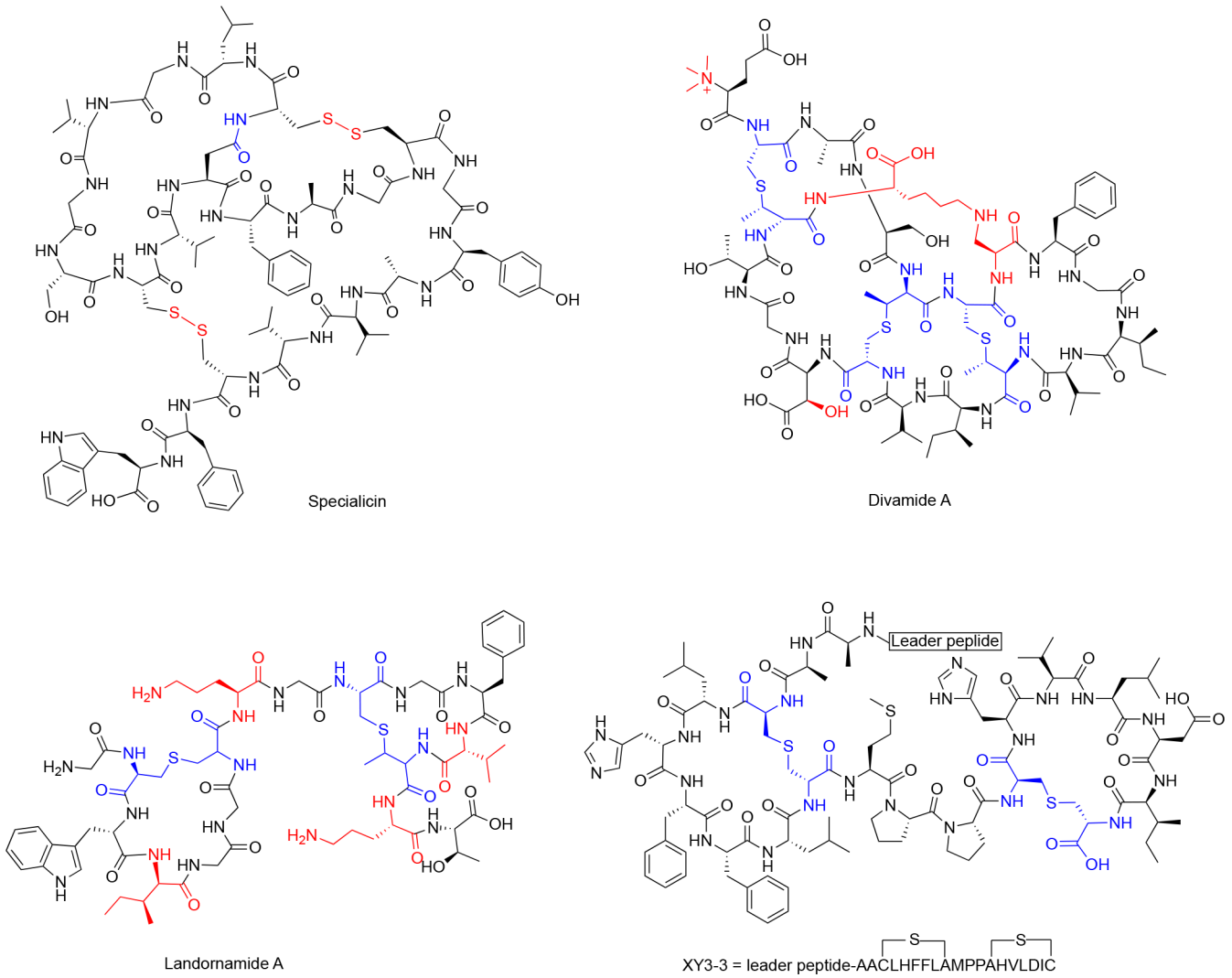

Figure 23. Structures of RiPPs with antiviral activity. The class-defining PTMs are highlighted in blue, and other PTMs are highlighted in red.

PsnB *in vitro*. Plesiocin contains four tandem hairpin-like (ring-within-a-ring, Figure 22) bicyclic repeats and showed protease inhibitory activity. The K_i values for elastase and chymotrypsin are 16 and 7.5 nM, respectively. Interestingly, the shorter fragment produced by formic acid-mediated cleavage also could inhibit the activity of the above two proteases with higher K_i values (380 and 63 nM, respectively). However, neither of them could inhibit the activity of trypsin.[155] A variant (Psn-LLLR) of plesiocin was obtained by precursor engineering and strongly inhibited both chymotrypsin and trypsin with K_i = 5.4 and 130 nM, respectively.[156]

A new multicore graspetide BGC from *Chryseobacterium gregarium* DSM 19109 was identified by genome mining. Incubation of precursor CdnA3 with ATP-grasp ligase CdnC and ATP, a modified peptide with loss of six water molecules was detected. The product without leader peptide named chryseoviridin (Figure 22) with four additional ω-esters apart from the bicyclic microviridin core. Despite the lack of ω-lactam, chryseoviridin still exhibited inhibitory activity against chymotrypsin, elastase, thrombin, and trypsin. More noteworthy is that both the chryseoviridin and its microviridin core inhibited chymotrypsin significantly with IC_{50} values of 70 nM and 100 nM, respectively.[157]

The marinostatin BGC from *Algicola sagamiensis* JCM 11461^T was cloned and expressed in heterologous host *E. coli*, which produced a new bicyclic analogue designated marinostatin E (ATMRYPSDSDEDGFN, Figure 22). It exhibited inhibitory activity to chymotrypsin and subtilisin with the IC_{50} values of 4.0 and 39.6 μM, respectively. In contrast, no activity against trypsin and elastase was detected.[158] Recently, a novel RiPP pathway (phospeptin, Figure 22) only constituted by a precursor gene and a maturase gene was identified from the deep-ocean species "*Candidatus* Eudoremicrobium malaspinii" during the investigation of the biosynthetic potential of the global ocean microbiome. The sole maturase encodes a dehydration domain homologous to lanthipeptide synthetase, and the product (Figure 22) obtained by heterologous expression and *in vitro* assay was identified as a diphosphorylated linear peptide which exhibited inhibitory activity against neutrophil elastase with an IC_{50} value of 14.3 μM.[159]

7. ANTIVIRAL RiPPs

The specialicin (CLGVGSCVDFAGCGYAVVCFW, Figure 23) is a new lasso peptide isolated from *Streptomyces specializ* by genome mining. Similar to its analogues siamycins (CLGVGSCNDFAGCGYAIVCFW),[78] specialicin showed

https://doi.org/10.1021/acsbiomedchemau.2c00062
ACS Bio Med Chem Au 2023, 3, 1−31

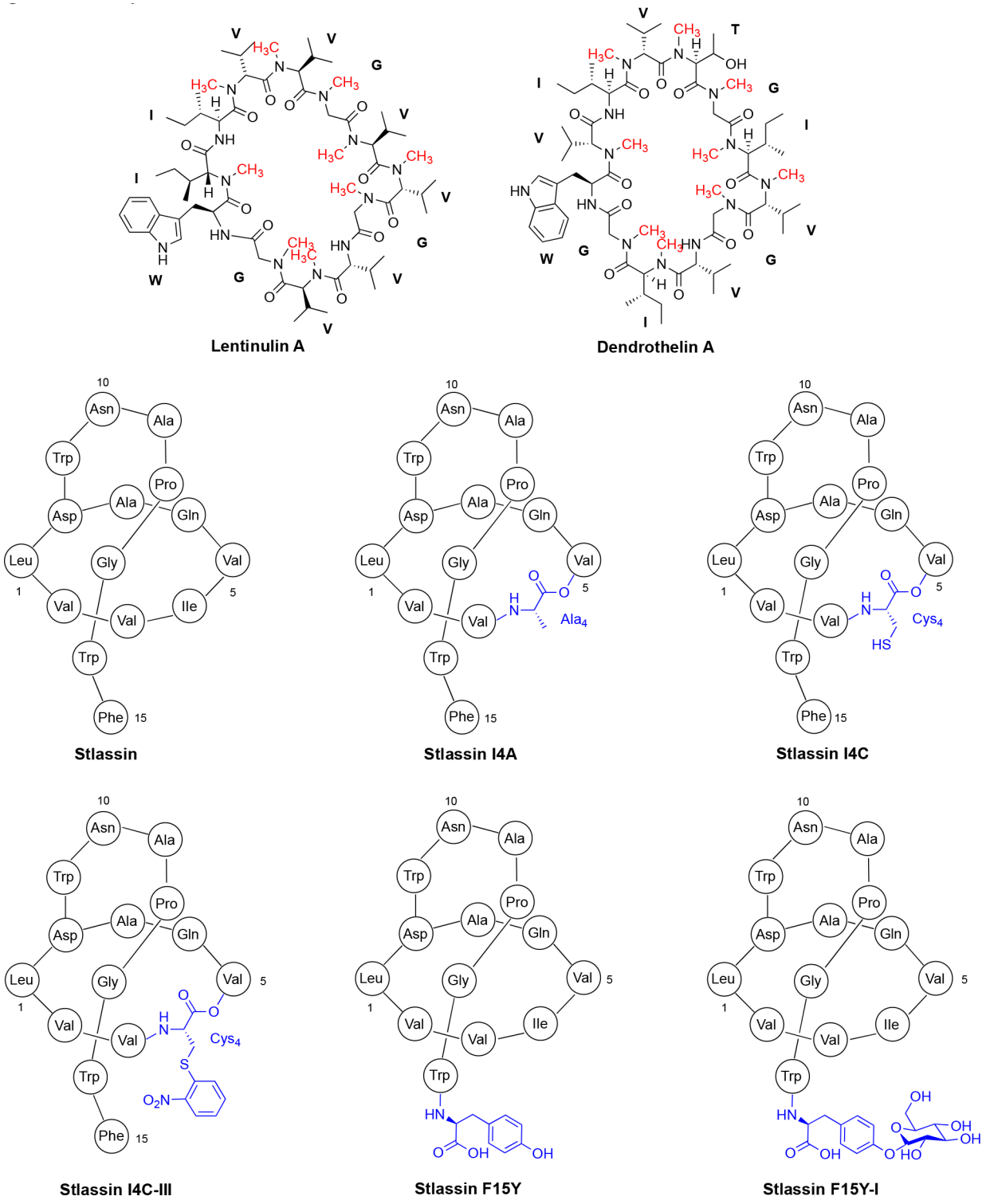

Figure 24. Structures of RiPPs with nematocidal and antagonistic activities. The amide bond *N*-methyl groups are highlighted in red. The mutations and chemical modifications in stlassin are highlighted in blue.

moderate activity against HIV-1 NL4-3 with an IC_{50} value of 7.2 ± 2.1 μM.[80] Divamides were identified from the marine tunicate *Didemnum mole* and incorporated with three methyllanthionines, one lysinoalanine, one β-hydroxy aspartic acid, and one *N*-terminal trimethylation. And one of them, divamide A (Figure 23), showed promising anti-HIV activity. To overcome the limited material, the gene cluster of divamide A was identified in the metagenome of sample E11−036, which is encoded by the symbiotic cyanobacteria *Prochloron didemnid*. The divamide A, as well as a series of intermediates, were obtained by semi−*in vivo* synthesis. All intermediates containing lysinoalamine showed similar anti-HIV activity with divamide A, which indicated the complete three-dimensional structure is essential for anti-HIV activity. The flow cytometry-based approach suggested that the antiviral and cytotoxic properties of divamide A are segregated.[160] The gene cluster of

https://doi.org/10.1021/acsbiomedchemau.2c00062
ACS Bio Med Chem Au 2023, 3, 1−31

landornamides with nitrile hydratase leader peptides (NHLPs) was identified from cyanobacterium *Kamptonema* sp. PCC 6506. The products were obtained by combining heterologous expression in *E. coli* and trypsin digestion *in vitro*. Landornamide A (Figure 23) exhibited antiviral infection activity against lymphocytic choriomeningitis virus (LCMV) at concentrations as low as 45 nM, with around 50% viral inhibition observed between 1.4 and 2.9 μM. The variant landornamide B without modification on arginine showed higher activity with about 50% inhibition at 0.18 μM; meanwhile, landornamide C without lanthionines did not show observable inhibitory activity to the tested virus which indicated the cyclic lanthionines are necessary for antiviral infection activity and unmodified arginine are favored to display inhibitory function.[161] A genetic library was constructed and coexpressed with the substrate-tolerant lanthipeptide synthetase ProcM, coupling with a bacterial reverse two-hybrid system (RTHS) for the interaction of the HIV p6 protein with the UEV domain of the human TSG101 protein, a bicyclic peptide designated XY3-3 (leader peptide-AACL-HFFLSMPPSHVLDIC, Figure 23) was identified. It could disrupt the p6-UEV interaction with an IC_{50} of 3.6 ± 0.3 μM. The variant with leader peptide truncated by Lys-C or GluC exhibited a more potent activity with IC_{50} values of 2.7 ± 0.6 and 1.9 ± 0.8 μM, respectively. XY3-3 could bind to UEV with a higher binding affinity than p6, and both rings are essential for the binding. The XY3−3 linked with a cell-permeable Tat peptide (XY3-3-Tat) showed about 65% inhibition of viral budding.[162]

8. RiPPs WITH OTHER BIOLOGICAL ACTIVITIES

Borosins are RiPPs widespread in fungi and bacteria with amide bond *N*-methylations installed on the peptide backbone. The α-amino groups are unprecedentedly automethylated by the self-sacrificing *N*-methyltransferase encoded in the *N*-terminal of precursor peptides,[163,164] albeit many borosin BGCs involving "split" precursor peptides have been unveiled very recently.[165,166] The nematicide omphalotins that exhibit toxicity to the plant pathogen *Meloidogyne incognita* are founding members of borosins. Recently, two natural variants, lentinulins and dendrothelins, were discovered from *Lentinula edodes* and *Dendrothele bispora*, respectively, via heterologous expression in the yeast *Pichia pastoris* using the promiscuous omphalotin A modification machinery. The nematotoxicity of lentinulin A (Figure 24) toward *M. incognita* is comparable to omphalotin A, while the activity of dendrothelin A (Figure 24) is significantly lower, implying that the Val to Thr mutation in dendrothelin A negatively affects the nematotoxicity.[167] In addition to omphalotin-like borosins, the *Gymnopus fusipes* derived cyclopeptides gymnopeptides with potent antiproliferative activities (mentioned in section 5.4) were classified as the second set of bioactive borosins.[142,143]

In contrast to the aforementioned lasso peptide, stlassin (Figure 24) from the marine *Streptomyces* sp. PKUMA01240 shows no antimicrobial, antitumor, or antivirus activity but antagonistic activity against the binding of lipopolysaccharides (LPS) to toll-like receptor 4 (TLR4), which may be used for preventing or treating inflammatory diseases. Several mutant-variants of stlassin, including I4A, I4C, F15Y, and the chemically modified I4C and F15Y (I4C−III and F15Y−I) exert comparable inhibitory activities, in which F15Y and F15Y−I display smaller IC_{50} values than the native peptide.[168]

Atropopeptides (atropitides) are a new family RiPPs with only four members identified up to now: tryptorubin A and B from *Streptomyces* sp. CLI2509 and amyxirubin A and B from *Amycolatopsis xylanica* (Figure 25). The cytochrome P450, the

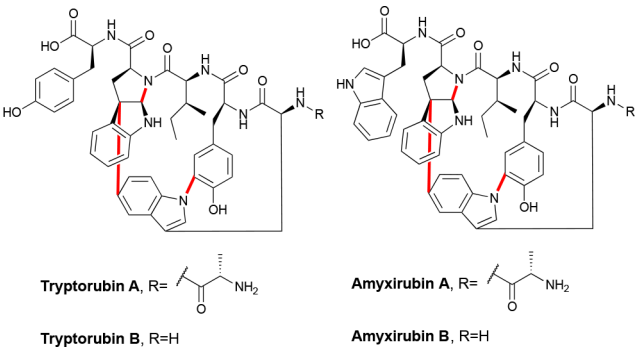

Figure 25. Structures of RiPPs with proliferative activities. The installed PTMs are highlighted in red.

exclusive modifying enzyme encoding in the BGC, atropospecifically catalyzes the generation of one carbon−carbon and two carbon−nitrogen bonds. All atropopeptides showed pro-angiogenic and pro-migratory activities for the human microvascular endothelial cell line (HMEC-1) and proliferative activities on bacterial growth (accelerating *Streptomyces* differentiation).[169−171]

9. OUTLOOK

In the past decade, advanced bioinformatic tools combined with a genome-mining approach paved the way to uncover a rapidly growing number of RiPPs. This field has not only exploded in terms of novel compound discovery, new post-translational enzymology,[6] as well as new bioinformatic tools for the prediction of RiPP biosynthetic potentials,[131,172,173] but also resulted in a broad spectrum of emerging bioactivities from antibacteria, antifungi, antiviruses to antitumor and so on. This field has exponentially expanded, and 17 new classes were discovered just between 2013 and 2020.[3] Thus, we believe that RiPPs undoubtedly tend to be promising candidates to cope with the crisis of resistance as well as other incurable diseases, given their ability to produce large libraries of chemically diverse scaffolds and various bioactivities thereof. Furthermore, many bioinformatic studies demonstrated that RiPP biosynthetic pathways are widely distributed in the prokaryotic tree of life, even in the plants and animals,[131] reflecting that the vast majority of the genetically encoded RiPP remain unknown, encouraging researchers to excavate the abundant dark matter.

However, given the increasing number of RiPPs with a variety of bioactivities will be discovered and characterized via advanced genome mining and/or bioengineering approaches in the future, the underdeveloped understanding of the mode of mechanisms might obstruct the clinical and/or commercial applications of RiPPs. Thus, we hereby attempt to collectively summarize the RiPPs uncovered during the past decade in terms of their biological activity as well as the (proposed) mode of mechanisms thereof. We hope we could sum up some disciplines of the RiPPs physiological activities to guide genome mining and drug discovery/optimization in the future.

https://doi.org/10.1021/acsbiomedchemau.2c00062
ACS Bio Med Chem Au 2023, 3, 1−31

AUTHOR INFORMATION

Corresponding Author

Liujie Huo − *Helmholtz International Laboratory for Anti-Infectives, State Key Laboratory of Microbial Technology, Shandong University, Qingdao 266237, China; Suzhou Research Institute, Shandong University, Suzhou, Jiangsu 215123, P. R. China;* orcid.org/0000-0002-1406-8466; Email: lhuo@sdu.edu.cn

Authors

Guannan Zhong − *Helmholtz International Laboratory for Anti-Infectives, State Key Laboratory of Microbial Technology, Shandong University, Qingdao 266237, China; Suzhou Research Institute, Shandong University, Suzhou, Jiangsu 215123, P. R. China;* orcid.org/0000-0002-1357-4447

Zong-Jie Wang − *Helmholtz International Laboratory for Anti-Infectives, State Key Laboratory of Microbial Technology, Shandong University, Qingdao 266237, China*

Fu Yan − *Helmholtz International Laboratory for Anti-Infectives, State Key Laboratory of Microbial Technology, Shandong University, Qingdao 266237, China*

Youming Zhang − *Helmholtz International Laboratory for Anti-Infectives, State Key Laboratory of Microbial Technology, Shandong University, Qingdao 266237, China; CAS Key Laboratory of Quantitative Engineering Biology, Shenzhen Institute of Synthetic Biology and Faculty of Synthetic Biology, Shenzhen Institute of Advanced Technology, Chinese Academy of Sciences, Shenzhen 518055, China*

Complete contact information is available at: https://pubs.acs.org/10.1021/acsbiomedchemau.2c00062

Author Contributions

†G.Z. and Z.-J.W. contributed equally.. This review was drafted by G.Z. (sections 1,−3, 8), Z.-J.W. (sections 4−7), and L.H. (section 9). All authors proofread the entire manuscript and provided suggestions for improvement in all sections.

Funding

Research in L.H.'s Lab was supported by the National Key R&D Program of China (2018YFA0900400, 2019YFA0905700), the National Natural Science Foundation of China (32161133013), the Natural Science Foundation of Jiangsu Province (BK20180228), the Shandong Provincial Natural Science Foundation (ZR2019QC001), the Youth Interdiscipline Innovative Research Group of Shandong University (2020QNQT009), and the Qilu Youth Scholar Startup Funding of Shandong University; Z.W. thanks the China Postdoctoral Science Foundation (2020M682169); G.Z. thanks the National Natural Science Foundation of China (21907057), the Natural Science Foundation of Jiangsu Province (BK20190201), the Future Plan for Young Scholars and the Fundamental Research Funds (2019GN032) of Shandong University; Y.Z. thanks the National Natural Science Foundation of China (32170038); F. Y. thanks the National Natural Science Foundation of China (82003639).

Notes

The authors declare no competing financial interest.

ACKNOWLEDGMENTS

We thank Dr. W. A. v. d. Donk (University of Illinois at Urbana−Champaign) for helpful discussions during the manuscript preparation.

REFERENCES

(1) Davies, J.; Davies, D. Origins and evolution of antibiotic resistance. *Microbiol Mol. Biol. Rev.* **2010**, *74* (3), 417−433.

(2) Newman, D. J.; Cragg, G. M. Natural Products as Sources of New Drugs over the Nearly Four Decades from 01/1981 to 09/2019. *J. Nat. Prod* **2020**, *83* (3), 770−803.

(3) Montalban-Lopez, M.; Scott, T. A.; Ramesh, S.; Rahman, I. R.; van Heel, A. J.; Viel, J. H.; Bandarian, V.; Dittmann, E.; Genilloud, O.; Goto, Y.; et al. New developments in RiPP discovery, enzymology and engineering. *Nat. Prod Rep* **2021**, *38* (1), 130−239.

(4) Arnison, P. G.; Bibb, M. J.; Bierbaum, G.; Bowers, A. A.; Bugni, T. S.; Bulaj, G.; Camarero, J. A.; Campopiano, D. J.; Challis, G. L.; Clardy, J.; et al. Ribosomally synthesized and post-translationally modified peptide natural products: overview and recommendations for a universal nomenclature. *Nat. Prod Rep* **2013**, *30* (1), 108−160.

(5) Knerr, P. J.; van der Donk, W. A. Discovery, biosynthesis, and engineering of lantipeptides. *Annu. Rev. Biochem.* **2012**, *81* (1), 479−505.

(6) Repka, L. M.; Chekan, J. R.; Nair, S. K.; van der Donk, W. A. Mechanistic Understanding of Lanthipeptide Biosynthetic Enzymes. *Chem. Rev.* **2017**, *117* (8), 5457−5520.

(7) Xu, M.; Zhang, F.; Cheng, Z.; Bashiri, G.; Wang, J.; Hong, J.; Wang, Y.; Xu, L.; Chen, X.; Huang, S. X.; et al. Functional Genome Mining Reveals a Class V Lanthipeptide Containing a d-Amino Acid Introduced by an F420 H2 -Dependent Reductase. *Angew. Chem., Int. Ed. Engl.* **2020**, *59* (41), 18029−18035.

(8) Garg, N.; Salazar-Ocampo, L. M.; van der Donk, W. A. In vitro activity of the nisin dehydratase NisB. *Proc. Natl. Acad. Sci. U. S. A.* **2013**, *110* (18), 7258−7263.

(9) Li, B.; Yu, J. P.; Brunzelle, J. S.; Moll, G. N.; van der Donk, W. A.; Nair, S. K. Structure and mechanism of the lantibiotic cyclase involved in nisin biosynthesis. *Science* **2006**, *311* (5766), 1464−1467.

(10) Ortega, M. A.; Hao, Y.; Zhang, Q.; Walker, M. C.; van der Donk, W. A.; Nair, S. K. Structure and mechanism of the tRNA-dependent lantibiotic dehydratase NisB. *Nature* **2015**, *517* (7535), 509−512.

(11) Chatterjee, C.; Miller, L. M.; Leung, Y. L.; Xie, L.; Yi, M.; Kelleher, N. L.; van der Donk, W. A. Lacticin 481 synthetase phosphorylates its substrate during lantibiotic production. *J. Am. Chem. Soc.* **2005**, *127* (44), 15332−15333.

(12) Dong, S. H.; Tang, W.; Lukk, T.; Yu, Y.; Nair, S. K.; van der Donk, W. A. The enterococcal cytolysin synthetase has an unanticipated lipid kinase fold. *Elife* **2015**, *4*, No. e07607.

(13) Meindl, K.; Schmiederer, T.; Schneider, K.; Reicke, A.; Butz, D.; Keller, S.; Gühring, H.; Vértesy, L.; Wink, J.; Hoffmann, H.; et al. Labyrinthopeptins: A New Class of Carbacyclic Lantibiotics. *Angew. Chem., Int. Ed. Engl.* **2010**, *49* (6), 1151−1154.

(14) Wang, H.; van der Donk, W. A. Biosynthesis of the class III lantipeptide catenulipeptin. *ACS Chem. Biol.* **2012**, *7* (9), 1529−1535.

(15) Chen, Y.; Wang, J.; Li, G.; Yang, Y.; Ding, W. Current Advancements in Sactipeptide Natural Products. *Front Chem.* **2021**, *9* (290), 595991.

(16) Precord, T. W.; Mahanta, N.; Mitchell, D. A. Reconstitution and Substrate Specificity of the Thioether-Forming Radical S-Adenosylmethionine Enzyme in Freyrasin Biosynthesis. *ACS Chem. Biol.* **2019**, *14* (9), 1981−1989.

(17) Zhang, Q.; Liu, W. Biosynthesis of thiopeptide antibiotics and their pathway engineering. *Nat. Prod Rep* **2013**, *30* (2), 218−226.

(18) Chan, D. C. K.; Burrows, L. L. Thiopeptides: antibiotics with unique chemical structures and diverse biological activities. *J. Antibiot (Tokyo)* **2021**, *74* (3), 161−175.

(19) Martin-Gomez, H.; Tulla-Puche, J. Lasso peptides: chemical approaches and structural elucidation. *Org. Biomol Chem.* **2018**, *16* (28), 5065−5080.
(20) Hegemann, J. D.; Zimmermann, M.; Xie, X.; Marahiel, M. A. Lasso peptides: an intriguing class of bacterial natural products. *Acc. Chem. Res.* **2015**, *48* (7), 1909−1919.
(21) Ren, H.; Biswas, S.; Ho, S.; van der Donk, W. A.; Zhao, H. Rapid Discovery of Glycocins through Pathway Refactoring in Escherichia coli. *ACS Chem. Biol.* **2018**, *13* (10), 2966−2972.
(22) Shin, J. M.; Gwak, J. W.; Kamarajan, P.; Fenno, J. C.; Rickard, A. H.; Kapila, Y. L. Biomedical applications of nisin. *J. Appl. Microbiol.* **2016**, *120* (6), 1449−1465.
(23) Song, X.; Xie, J.; Su, Y.; Martin-Esteban, A.; Qiu, J.; Li, X.; He, L. Analysis of Nosiheptide in Food Animal Tissues via Its Unique Degradation Product by Liquid Chromatography-Tandem Mass Spectrometry after Alkaline Hydrolysis. *J. Agric. Food Chem.* **2019**, *67* (38), 10791−10799.
(24) Wahyudi, H.; McAlpine, S. R. Predicting the unpredictable: Recent structure-activity studies on peptide-based macrocycles. *Bioorg Chem.* **2015**, *60*, 74−97.
(25) Mullane, K.; Lee, C.; Bressler, A.; Buitrago, M.; Weiss, K.; Dabovic, K.; Praestgaard, J.; Leeds, J. A.; Blais, J.; Pertel, P. Multicenter, randomized clinical trial to compare the safety and efficacy of LFF571 and vancomycin for Clostridium difficile infections. *Antimicrob. Agents Chemother.* **2015**, *59* (3), 1435−1440.
(26) Fabbretti, A.; He, C. G.; Gaspari, E.; Maffioli, S.; Brandi, L.; Spurio, R.; Sosio, M.; Jabes, D.; Donadio, S. A Derivative of the Thiopeptide GE2270A Highly Selective against Propionibacterium acnes. *Antimicrob. Agents Chemother.* **2015**, *59* (8), 4560−4568.
(27) Clark, K. A.; Bushin, L. B.; Seyedsayamdost, M. R. RaS-RiPPs in Streptococci and the Human Microbiome. *ACS Bio Med. Chem. Au* **2022**, *2* (4), 328−339.
(28) Lee, H.; van der Donk, W. A. Macrocyclization and Backbone Modification in RiPP Biosynthesis. *Annu. Rev. Biochem.* **2022**, *91*, 269−294.
(29) Burkhart, B. J.; Schwalen, C. J.; Mann, G.; Naismith, J. H.; Mitchell, D. A. YcaO-Dependent Posttranslational Amide Activation: Biosynthesis, Structure, and Function. *Chem. Rev.* **2017**, *117* (8), 5389−5456.
(30) Maksimov, M. O.; Pan, S. J.; James Link, A. Lasso peptides: structure, function, biosynthesis, and engineering. *Nat. Prod Rep* **2012**, *29* (9), 996−1006.
(31) Franz, L.; Kazmaier, U.; Truman, A. W.; Koehnke, J. Bottromycins - biosynthesis, synthesis and activity. *Nat. Prod Rep* **2021**, *38* (9), 1659−1683.
(32) Kessler, S. C.; Chooi, Y. H. Out for a RiPP: challenges and advances in genome mining of ribosomal peptides from fungi. *Nat. Prod Rep* **2022**, *39* (2), 222−230.
(33) Rebuffat, S. Ribosomally synthesized peptides, foreground players in microbial interactions: recent developments and unanswered questions. *Nat. Prod Rep* **2022**, *39* (2), 273−310.
(34) Li, Y.; Rebuffat, S. The manifold roles of microbial ribosomal peptide-based natural products in physiology and ecology. *J. Biol. Chem.* **2020**, *295* (1), 34−54.
(35) Ongpipattanakul, C.; Desormeaux, E. K.; DiCaprio, A.; van der Donk, W. A.; Mitchell, D. A.; Nair, S. K. Mechanism of Action of Ribosomally Synthesized and Post-Translationally Modified Peptides. *Chem. Rev.* **2022**, *122* (18), 14722−14814.
(36) Cao, L.; Do, T.; Link, A. J. Mechanisms of action of ribosomally synthesized and posttranslationally modified peptides (RiPPs). *J. Ind. Microbiol Biotechnol* **2021**, *48* (3−4), kuab005.
(37) O'Connor, P. M.; O'Shea, E. F.; Guinane, C. M.; O'Sullivan, O.; Cotter, P. D.; Ross, R. P.; Hill, C. Nisin H Is a New Nisin Variant Produced by the Gut-Derived Strain Streptococcus hyointestinalis DPC6484. *Appl. Environ. Microbiol.* **2015**, *81* (12), 3953−3960.
(38) Hatziioanou, D.; Gherghisan-Filip, C.; Saalbach, G.; Horn, N.; Wegmann, U.; Duncan, S. H.; Flint, H. J.; Mayer, M. J.; Narbad, A. Discovery of a novel lantibiotic nisin O from Blautia obeum A2−162, isolated from the human gastrointestinal tract. *Microbiology (Reading)* **2017**, *163* (9), 1292−1305.
(39) Gherghisan-Filip, C.; Saalbach, G.; Hatziioanou, D.; Narbad, A.; Mayer, M. J. Processing and Structure of the Lantibiotic Peptide Nso From the Human Gut Bacterium Blautia obeum A2−162 analysed by Mass Spectrometry. *Sci. Rep* **2018**, *8* (1), 10077.
(40) van Heel, A. J.; Kloosterman, T. G.; Montalban-Lopez, M.; Deng, J.; Plat, A.; Baudu, B.; Hendriks, D.; Moll, G. N.; Kuipers, O. P. Discovery, Production and Modification of Five Novel Lantibiotics Using the Promiscuous Nisin Modification Machinery. *ACS Synth. Biol.* **2016**, *5* (10), 1146−1154.
(41) Liu, R.; Zhang, Y.; Zhai, G.; Fu, S.; Xia, Y.; Hu, B.; Cai, X.; Zhang, Y.; Li, Y.; Deng, Z.; et al. A Cell-Free Platform Based on Nisin Biosynthesis for Discovering Novel Lanthipeptides and Guiding their Overproduction In Vivo. *Adv. Sci. (Weinh)* **2020**, *7* (17), 2001616.
(42) Schmitt, S.; Montalban-Lopez, M.; Peterhoff, D.; Deng, J.; Wagner, R.; Held, M.; Kuipers, O. P.; Panke, S. Analysis of modular bioengineered antimicrobial lanthipeptides at nanoliter scale. *Nat. Chem. Biol.* **2019**, *15* (5), 437−443.
(43) Grigoreva, A.; Andreeva, J.; Bikmetov, D.; Rusanova, A.; Serebryakova, M.; Garcia, A. H.; Slonova, D.; Nair, S. K.; Lippens, G.; Severinov, K.; et al. Identification and characterization of andalusicin: N-terminally dimethylated class III lantibiotic from Bacillus thuringiensis sv. andalousiensis. *iScience* **2021**, *24* (5), 102480.
(44) Zhang, Y.; Hong, Z.; Zhou, L.; Zhang, Z.; Tang, T.; Guo, E.; Zheng, J.; Wang, C.; Dai, L.; Si, T.; et al. Biosynthesis of Gut-Microbiota-Derived Lantibiotics Reveals a Subgroup of S8 Family Proteases for Class III Leader Removal. *Angew. Chem., Int. Ed. Engl.* **2022**, *61* (6), No. e202114414.
(45) Kloosterman, A. M.; Cimermancic, P.; Elsayed, S. S.; Du, C.; Hadjithomas, M.; Donia, M. S.; Fischbach, M. A.; van Wezel, G. P.; Medema, M. H. Expansion of RiPP biosynthetic space through integration of pan-genomics and machine learning uncovers a novel class of lanthipeptides. *PLoS Biol.* **2020**, *18* (12), No. e3001026.
(46) Aftab Uddin, M.; Akter, S.; Ferdous, M.; Haidar, B.; Amin, A.; Shofiul Islam Molla, A. H. M.; Khan, H.; Islam, M. R. A plant endophyte Staphylococcus hominis strain MBL_AB63 produces a novel lantibiotic, homicorcin and a position one variant. *Sci. Rep* **2021**, *11* (1), 11211.
(47) Shi, J.; Ma, J. Q.; Wang, Y. C.; Xu, Z. F.; Zhang, B.; Jiao, R. H.; Tan, R. X.; Ge, H. M. Discovery of daspyromycins A and B, 2-aminovinyl-cysteine containing lanthipeptides, through a genomics-based approach. *Chin. Chem. Lett.* **2022**, *33* (1), 511−515.
(48) McClerren, A. L.; Cooper, L. E.; Quan, C.; Thomas, P. M.; Kelleher, N. L.; van der Donk, W. A. Discovery and in vitro biosynthesis of haloduracin, a two-component lantibiotic. *Proc. Natl. Acad. Sci. U. S. A.* **2006**, *103* (46), 17243−17248.
(49) Huo, L.; van der Donk, W. A. Discovery and Characterization of Bicereucin, an Unusual d-Amino Acid-Containing Mixed Two-Component Lantibiotic. *J. Am. Chem. Soc.* **2016**, *138* (16), 5254−5257.
(50) Zhao, X.; van der Donk, W. A. Structural Characterization and Bioactivity Analysis of the Two-Component Lantibiotic Flv System from a Ruminant Bacterium. *Cell Chem. Biol.* **2016**, *23* (2), 246−256.
(51) Singh, M.; Chaudhary, S.; Sareen, D. Roseocin, a novel two-component lantibiotic from an actinomycete. *Mol. Microbiol.* **2020**, *113* (2), 326−337.
(52) Walker, M. C.; Eslami, S. M.; Hetrick, K. J.; Ackenhusen, S. E.; Mitchell, D. A.; van der Donk, W. A. Precursor peptide-targeted mining of more than one hundred thousand genomes expands the lanthipeptide natural product family. *BMC Genomics* **2020**, *21* (1), 387.
(53) Nakatsuji, T.; Chen, T. H.; Narala, S.; Chun, K. A.; Two, A. M.; Yun, T.; Shafiq, F.; Kotol, P. F.; Bouslimani, A.; Melnik, A. V.; et al. Antimicrobials from human skin commensal bacteria protect against Staphylococcus aureus and are deficient in atopic dermatitis. *Sci. Transl Med.* **2017**, *9* (378), No. eaah4680.
(54) Kim, S. G.; Becattini, S.; Moody, T. U.; Shliaha, P. V.; Littmann, E. R.; Seok, R.; Gjonbalaj, M.; Eaton, V.; Fontana, E.;

Amoretti, L.; et al. Microbiota-derived lantibiotic restores resistance against vancomycin-resistant Enterococcus. *Nature* **2019**, *572* (7771), 665−669.
(55) Chen, E.; Chen, Q.; Chen, S.; Xu, B.; Ju, J.; Wang, H. Mathermycin, a Lantibiotic from the Marine Actinomycete Marinactinospora thermotolerans SCSIO 00652. *Appl. Environ. Microbiol.* **2017**, *83* (15), e00926-17.
(56) Ongey, E. L.; Giessmann, R. T.; Fons, M.; Rappsilber, J.; Adrian, L.; Neubauer, P. Heterologous Biosynthesis, Modifications and Structural Characterization of Ruminococcin-A, a Lanthipeptide From the Gut Bacterium Ruminococcus gnavus E1, in Escherichia coli. *Front Microbiol* **2018**, *9*, 1688.
(57) Kers, J. A.; Sharp, R. E.; Defusco, A. W.; Park, J. H.; Xu, J.; Pulse, M. E.; Weiss, W. J.; Handfield, M. Mutacin 1140 Lantibiotic Variants Are Efficacious Against Clostridium difficile Infection. *Front Microbiol* **2018**, *9*, 415.
(58) Hussein, W. E.; Huang, E.; Ozturk, I.; Somogyi, A.; Yang, X.; Liu, B.; Yousef, A. E. Genome-Guided Mass Spectrometry Expedited the Discovery of Paraplantaricin TC318, a Lantibiotic Produced by Lactobacillus paraplantarum Strain Isolated From Cheese. *Front Microbiol* **2020**, *11*, 1381.
(59) Wiebach, V.; Mainz, A.; Schnegotzki, R.; Siegert, M. J.; Hugelland, M.; Pliszka, N.; Sussmuth, R. D. An Amphipathic Alpha-Helix Guides Maturation of the Ribosomally-Synthesized Lipolanthines. *Angew. Chem., Int. Ed. Engl.* **2020**, *59* (38), 16777−16785.
(60) Wiebach, V.; Mainz, A.; Siegert, M. J.; Jungmann, N. A.; Lesquame, G.; Tirat, S.; Dreux-Zigha, A.; Aszodi, J.; Le Beller, D.; Sussmuth, R. D. The anti-staphylococcal lipolanthines are ribosomally synthesized lipopeptides. *Nat. Chem. Biol.* **2018**, *14* (7), 652−654.
(61) Kozakai, R.; Ono, T.; Hoshino, S.; Takahashi, H.; Katsuyama, Y.; Sugai, Y.; Ozaki, T.; Teramoto, K.; Teramoto, K.; Tanaka, K.; et al. Acyltransferase that catalyses the condensation of polyketide and peptide moieties of goadvionin hybrid lipopeptides. *Nat. Chem.* **2020**, *12* (9), 869−877.
(62) Balty, C.; Guillot, A.; Fradale, L.; Brewee, C.; Boulay, M.; Kubiak, X.; Benjdia, A.; Berteau, O. Ruminococcin C, an anti-clostridial sactipeptide produced by a prominent member of the human microbiota Ruminococcus gnavus. *J. Biol. Chem.* **2019**, *294* (40), 14512−14525.
(63) Chiumento, S.; Roblin, C.; Kieffer-Jaquinod, S.; Tachon, S.; Lepretre, C.; Basset, C.; Aditiyarini, D.; Olleik, H.; Nicoletti, C.; Bornet, O.; et al. Ruminococcin C, a promising antibiotic produced by a human gut symbiont. *Sci. Adv.* **2019**, *5* (9), No. eaaw9969.
(64) Roblin, C.; Chiumento, S.; Bornet, O.; Nouailler, M.; Müller, C. S.; Jeannot, K.; Basset, C.; Kieffer-Jaquinod, S.; Coute, Y.; Torelli, S.; et al. The unusual structure of Ruminococcin C1 antimicrobial peptide confers clinical properties. *Proc. Natl. Acad. Sci. U. S. A.* **2020**, *117* (32), 19168−19177.
(65) Roblin, C.; Chiumento, S.; Jacqueline, C.; Pinloche, E.; Nicoletti, C.; Olleik, H.; Courvoisier-Dezord, E.; Amouric, A.; Basset, C.; Dru, L.; et al. The Multifunctional Sactipeptide Ruminococcin C1 Displays Potent Antibacterial Activity In Vivo as Well as Other Beneficial Properties for Human Health. *Int. J. Mol. Sci.* **2021**, *22* (6), 3253.
(66) Hudson, G. A.; Burkhart, B. J.; DiCaprio, A. J.; Schwalen, C. J.; Kille, B.; Pogorelov, T. V.; Mitchell, D. A. Bioinformatic Mapping of Radical S-Adenosylmethionine-Dependent Ribosomally Synthesized and Post-Translationally Modified Peptides Identifies New Calpha, Cbeta, and Cgamma-Linked Thioether-Containing Peptides. *J. Am. Chem. Soc.* **2019**, *141* (20), 8228−8238.
(67) Mo, T.; Ji, X.; Yuan, W.; Mandalapu, D.; Wang, F.; Zhong, Y.; Li, F.; Chen, Q.; Ding, W.; Deng, Z.; et al. Thuricin Z: A Narrow-Spectrum Sactibiotic that Targets the Cell Membrane. *Angew. Chem., Int. Ed. Engl.* **2019**, *58* (52), 18793−18797.
(68) Rea, M. C.; Sit, C. S.; Clayton, E.; O'Connor, P. M.; Whittal, R. M.; Zheng, J.; Vederas, J. C.; Ross, R. P.; Hill, C. Thuricin CD, a posttranslationally modified bacteriocin with a narrow spectrum of activity against Clostridium difficile. *Proc. Natl. Acad. Sci. U. S. A.* **2010**, *107* (20), 9352−9357.
(69) Bushin, L. B.; Covington, B. C.; Rued, B. E.; Federle, M. J.; Seyedsayamdost, M. R. Discovery and Biosynthesis of Streptosactin, a Sactipeptide with an Alternative Topology Encoded by Commensal Bacteria in the Human Microbiome. *J. Am. Chem. Soc.* **2020**, *142* (38), 16265−16275.
(70) Duarte, A. F. S.; Ceotto-Vigoder, H.; Barrias, E. S.; Souto-Padron, T.; Nes, I. F.; Bastos, M. Hyicin 4244, the first sactibiotic described in staphylococci, exhibits an anti-staphylococcal biofilm activity. *Int. J. Antimicrob. Agents* **2018**, *51* (3), 349−356.
(71) Schwalen, C. J.; Hudson, G. A.; Kille, B.; Mitchell, D. A. Bioinformatic Expansion and Discovery of Thiopeptide Antibiotics. *J. Am. Chem. Soc.* **2018**, *140* (30), 9494−9501.
(72) Santos-Aberturas, J.; Chandra, G.; Frattaruolo, L.; Lacret, R.; Pham, T. H.; Vior, N. M.; Eyles, T. H.; Truman, A. W. Uncovering the unexplored diversity of thioamidated ribosomal peptides in Actinobacteria using the RiPPER genome mining tool. *Nucleic Acids Res.* **2019**, *47* (9), 4624−4637.
(73) Eyles, T. H.; Vior, N. M.; Lacret, R.; Truman, A. W. Understanding thioamitide biosynthesis using pathway engineering and untargeted metabolomics. *Chem. Sci.* **2021**, *12* (20), 7138−7150.
(74) Liu, A.; Si, Y.; Dong, S. H.; Mahanta, N.; Penkala, H. N.; Nair, S. K.; Mitchell, D. A. Functional elucidation of TfuA in peptide backbone thioamidation. *Nat. Chem. Biol.* **2021**, *17* (5), 585−592.
(75) Claesen, J.; Spagnolo, J. B.; Ramos, S. F.; Kurita, K. L.; Byrd, A. L.; Aksenov, A. A.; Melnik, A. V.; Wong, W. R.; Wang, S.; Hernandez, R. D.; et al. A Cutibacterium acnes antibiotic modulates human skin microbiota composition in hair follicles. *Sci. Transl Med.* **2020**, *12* (570), No. eaay5445.
(76) Schneider, O.; Simic, N.; Aachmann, F. L.; Ruckert, C.; Kristiansen, K. A.; Kalinowski, J.; Jiang, Y.; Wang, L.; Jiang, C. L.; Lale, R.; et al. Genome Mining of Streptomyces sp. YIM 130001 Isolated From Lichen Affords New Thiopeptide Antibiotic. *Front Microbiol* **2018**, *9*, 3139.
(77) Tietz, J. I.; Schwalen, C. J.; Patel, P. S.; Maxson, T.; Blair, P. M.; Tai, H. C.; Zakai, U. I.; Mitchell, D. A. A new genome-mining tool redefines the lasso peptide biosynthetic landscape. *Nat. Chem. Biol.* **2017**, *13* (5), 470−478.
(78) Detlefsen, D. J.; Hill, S. E.; Volk, K. J.; Klohr, S. E.; Tsunakawa, M.; Furumai, T.; Lin, P. F.; Nishio, M.; Kawano, K.; Oki, T.; et al. Siamycins I and II, new anti-HIV-1 peptides: II. Sequence analysis and structure determination of siamycin I. *J. Antibiot (Tokyo)* **1995**, *48* (12), 1515−1517.
(79) Nakayama, J.; Tanaka, E.; Kariyama, R.; Nagata, K.; Nishiguchi, K.; Mitsuhata, R.; Uemura, Y.; Tanokura, M.; Kumon, H.; Sonomoto, K. Siamycin attenuates fsr quorum sensing mediated by a gelatinase biosynthesis-activating pheromone in Enterococcus faecalis. *J. Bacteriol.* **2007**, *189* (4), 1358−1365.
(80) Kaweewan, I.; Hemmi, H.; Komaki, H.; Harada, S.; Kodani, S. Isolation and structure determination of a new lasso peptide specialicin based on genome mining. *Bioorg. Med. Chem.* **2018**, *26* (23−24), 6050−6055.
(81) Feng, Z.; Ogasawara, Y.; Dairi, T. Identification of the peptide epimerase MslH responsible for d-amino acid introduction at the C-terminus of ribosomal peptides. *Chem. Sci.* **2021**, *12* (7), 2567−2574.
(82) Kaweewan, I.; Ohnishi-Kameyama, M.; Kodani, S. Isolation of a new antibacterial peptide achromosin from Streptomyces achromogenes subsp. achromogenes based on genome mining. *J. Antibiot (Tokyo)* **2017**, *70* (2), 208−211.
(83) Stariha, L. M.; McCafferty, D. G. Discovery of the Class I Antimicrobial Lasso Peptide Arcumycin. *Chembiochem* **2021**, *22* (16), 2632−2640.
(84) Wang, S.; Zeng, X. F.; Wang, Q. W.; Zhu, J. L.; Peng, Q.; Hou, C. L.; Thacker, P.; Qiao, S. Y. The antimicrobial peptide sublancin ameliorates necrotic enteritis induced by Clostridium perfringens in broilers. *J. Anim Sci.* **2015**, *93* (10), 4750−4760.
(85) Wang, S.; Wang, Q.; Zeng, X.; Ye, Q.; Huang, S.; Yu, H.; Yang, T.; Qiao, S. Use of the Antimicrobial Peptide Sublancin with Combined Antibacterial and Immunomodulatory Activities To

Protect against Methicillin-Resistant Staphylococcus aureus Infection in Mice. *J. Agric. Food Chem.* **2017**, *65* (39), 8595−8605.
(86) Lobstein, J.; Emrich, C. A.; Jeans, C.; Faulkner, M.; Riggs, P.; Berkmen, M. SHuffle, a novel Escherichia coli protein expression strain capable of correctly folding disulfide bonded proteins in its cytoplasm. *Microb Cell Fact* **2012**, *11* (1), 56.
(87) Biswas, S.; Garcia De Gonzalo, C. V.; Repka, L. M.; van der Donk, W. A. Structure-Activity Relationships of the S-Linked Glycocin Sublancin. *ACS Chem. Biol.* **2017**, *12* (12), 2965−2969.
(88) Kaunietis, A.; Buivydas, A.; Citavicius, D. J.; Kuipers, O. P. Heterologous biosynthesis and characterization of a glycocin from a thermophilic bacterium. *Nat. Commun.* **2019**, *10* (1), 1115.
(89) Main, P.; Hata, T.; Loo, T. S.; Man, P.; Novak, P.; Havlicek, V.; Norris, G. E.; Patchett, M. L. Bacteriocin ASM1 is an O/S-diglycosylated, plasmid-encoded homologue of glycocin F. *FEBS Lett.* **2020**, *594* (7), 1196−1206.
(90) Ma, S.; Zhang, Q. Linaridin natural products. *Nat. Prod Rep* **2020**, *37* (9), 1152−1163.
(91) Komiyama, K.; Otoguro, K.; Segawa, T.; Shiomi, K.; Yang, H.; Takahashi, Y.; Hayashi, M.; Oxani, T.; Omura, S. A new antibiotic, cypemycin. Taxonomy, fermentation, isolation and biological characteristics. *J. Antibiot (Tokyo)* **1993**, *46* (11), 1666−1671.
(92) Shang, Z.; Winter, J. M.; Kauffman, C. A.; Yang, I.; Fenical, W. Salinipeptins: Integrated Genomic and Chemical Approaches Reveal Unusual d-Amino Acid-Containing Ribosomally Synthesized and Post-Translationally Modified Peptides (RiPPs) from a Great Salt Lake Streptomyces sp. *ACS Chem. Biol.* **2019**, *14* (3), 415−425.
(93) Ortiz-Lopez, F. J.; Carretero-Molina, D.; Sanchez-Hidalgo, M.; Martin, J.; Gonzalez, I.; Roman-Hurtado, F.; de la Cruz, M.; Garcia-Fernandez, S.; Reyes, F.; Deisinger, J. P.; et al. Cacaoidin, First Member of the New Lanthidin RiPP Family. *Angew. Chem., Int. Ed. Engl.* **2020**, *59* (31), 12654−12658.
(94) Mascher, T.; Margulis, N. G.; Wang, T.; Ye, R. W.; Helmann, J. D. Cell wall stress responses in Bacillus subtilis: the regulatory network of the bacitracin stimulon. *Mol. Microbiol.* **2003**, *50* (5), 1591−1604.
(95) Benjdia, A.; Guillot, A.; Ruffie, P.; Leprince, J.; Berteau, O. Post-translational modification of ribosomally synthesized peptides by a radical SAM epimerase in Bacillus subtilis. *Nat. Chem.* **2017**, *9* (7), 698−707.
(96) Popp, P. F.; Benjdia, A.; Strahl, H.; Berteau, O.; Mascher, T. The Epipeptide YydF Intrinsically Triggers the Cell Envelope Stress Response of Bacillus subtilis and Causes Severe Membrane Perturbations. *Front Microbiol* **2020**, *11*, 151.
(97) Bushin, L. B.; Clark, K. A.; Pelczer, I.; Seyedsayamdost, M. R. Charting an Unexplored Streptococcal Biosynthetic Landscape Reveals a Unique Peptide Cyclization Motif. *J. Am. Chem. Soc.* **2018**, *140* (50), 17674−17684.
(98) Rued, B. E.; Covington, B. C.; Bushin, L. B.; Szewczyk, G.; Laczkovich, I.; Seyedsayamdost, M. R.; Federle, M. J. Quorum Sensing in Streptococcus mutans Regulates Production of Tryglysin, a Novel RaS-RiPP Antimicrobial Compound. *mBio* **2021**, *12* (2), e02688-20.
(99) Xin, B.; Liu, H.; Zheng, J.; Xie, C.; Gao, Y.; Dai, D.; Peng, D.; Ruan, L.; Chen, H.; Sun, M. In Silico Analysis Highlights the Diversity and Novelty of Circular Bacteriocins in Sequenced Microbial Genomes. *mSystems* **2020**, *5* (3), No. e00047-20.
(100) Xin, B. Y.; Xu, H. T.; Liu, H. L.; Liu, S.; Wang, J. J.; Xue, J. P.; Zhang, F.; Deng, S. L.; Zeng, H. W.; Zeng, X.; et al. Identification and characterization of a novel circular bacteriocin, bacicyclicin XIN-1, from Bacillus sp. Xin1. *Food Control* **2021**, *121*, 107696.
(101) Liu, G.; Wang, Y.; Li, X.; Hao, X.; Xu, D.; Zhou, Y.; Mehmood, A.; Wang, C. Genetic and Biochemical Evidence That Enterococcus faecalis Gr17 Produces a Novel and Sec-Dependent Bacteriocin, Enterocin Gr17. *Front Microbiol* **2019**, *10*, 1806.
(102) Lozo, J.; Mirkovic, N.; O'Connor, P. M.; Malesevic, M.; Miljkovic, M.; Polovic, N.; Jovcic, B.; Cotter, P. D.; Kojic, M. Lactolisterin BU, a Novel Class II Broad-Spectrum Bacteriocin from Lactococcus lactis subsp. lactis bv. diacetylactis BGBU1−4. *Appl. Environ. Microbiol.* **2017**, *83* (21), No. e01519-17.
(103) Imai, Y.; Meyer, K. J.; Iinishi, A.; Favre-Godal, Q.; Green, R.; Manuse, S.; Caboni, M.; Mori, M.; Niles, S.; Ghiglieri, M.; et al. A new antibiotic selectively kills Gram-negative pathogens. *Nature* **2019**, *576* (7787), 459−464.
(104) Kaur, H.; Jakob, R. P.; Marzinek, J. K.; Green, R.; Imai, Y.; Bolla, J. R.; Agustoni, E.; Robinson, C. V.; Bond, P. J.; Lewis, K.; et al. The antibiotic darobactin mimics a beta-strand to inhibit outer membrane insertase. *Nature* **2021**, *593* (7857), 125−129.
(105) Ritzmann, N.; Manioglu, S.; Hiller, S.; Müller, D. J. Monitoring the antibiotic darobactin modulating the beta-barrel assembly factor BamA. *Structure* **2022**, *30* (3), 350−359.
(106) Gross, S.; Panter, F.; Pogorevc, D.; Seyfert, C. E.; Deckarm, S.; Bader, C. D.; Herrmann, J.; Müller, R. Improved broad-spectrum antibiotics against Gram-negative pathogens via darobactin biosynthetic pathway engineering. *Chem. Sci.* **2021**, *12* (35), 11882−11893.
(107) Bohringer, N.; Green, R.; Liu, Y.; Mettal, U.; Marner, M.; Modaresi, S. M.; Jakob, R. P.; Wuisan, Z. G.; Maier, T.; Iinishi, A.; et al. Mutasynthetic Production and Antimicrobial Characterization of Darobactin Analogs. *Microbiol Spectr* **2021**, *9* (3), No. e0153521.
(108) Seyfert, C. E.; Porten, C.; Yuan, B.; Deckarm, S.; Panter, F.; Bader, C.; Coetzee, J.; Deschner, F.; Tehrani, K.; Higgins, P. G. Darobactins Exhibiting Superior Antibiotic Activity by Cryo-EM Structure Guided Biosynthetic Engineering. *Angew. Chem., Int. Ed. Engl.* **2022**, DOI: 10.1002/anie.202214094.
(109) Miller, R. D.; Iinishi, A.; Modaresi, S. M.; Yoo, B. K.; Curtis, T. D.; Lariviere, P. J.; Liang, L.; Son, S.; Nicolau, S.; Bargabos, R.; et al. Computational identification of a systemic antibiotic for gram-negative bacteria. *Nat. Microbiol* **2022**, *7* (10), 1661−1672.
(110) Moon, K.; Xu, F.; Seyedsayamdost, M. R. Cebulantin, a Cryptic Lanthipeptide Antibiotic Uncovered Using Bioactivity-Coupled HiTES. *Angew. Chem., Int. Ed. Engl.* **2019**, *58* (18), 5973−5977.
(111) Metelev, M.; Osterman, I. A.; Ghilarov, D.; Khabibullina, N. F.; Yakimov, A.; Shabalin, K.; Utkina, I.; Travin, D. Y.; Komarova, E. S.; Serebryakova, M.; et al. Klebsazolicin inhibits 70S ribosome by obstructing the peptide exit tunnel. *Nat. Chem. Biol.* **2017**, *13* (10), 1129−1136.
(112) Travin, D. Y.; Watson, Z. L.; Metelev, M.; Ward, F. R.; Osterman, I. A.; Khven, I. M.; Khabibullina, N. F.; Serebryakova, M.; Mergaert, P.; Polikanov, Y. S.; et al. Structure of ribosome-bound azole-modified peptide phazolicin rationalizes its species-specific mode of bacterial translation inhibition. *Nat. Commun.* **2019**, *10* (1), 4563.
(113) Cheung-Lee, W. L.; Parry, M. E.; Jaramillo Cartagena, A.; Darst, S. A.; Link, A. J. Discovery and structure of the antimicrobial lasso peptide citrocin. *J. Biol. Chem.* **2019**, *294* (17), 6822−6830.
(114) Cheung-Lee, W. L.; Parry, M. E.; Zong, C.; Cartagena, A. J.; Darst, S. A.; Connell, N. D.; Russo, R.; Link, A. J. Discovery of Ubonodin, an Antimicrobial Lasso Peptide Active against Members of the Burkholderia cepacia Complex. *Chembiochem* **2020**, *21* (9), 1335−1340.
(115) Metelev, M.; Arseniev, A.; Bushin, L. B.; Kuznedelov, K.; Artamonova, T. O.; Kondratenko, R.; Khodorkovskii, M.; Seyedsayamdost, M. R.; Severinov, K. Acinetodin and Klebsidin, RNA Polymerase Targeting Lasso Peptides Produced by Human Isolates of Acinetobacter gyllenbergii and Klebsiella pneumoniae. *ACS Chem. Biol.* **2017**, *12* (3), 814−824.
(116) Mohr, K. I.; Volz, C.; Jansen, R.; Wray, V.; Hoffmann, J.; Bernecker, S.; Wink, J.; Gerth, K.; Stadler, M.; Müller, R. Pinensins: the first antifungal lantibiotics. *Angew. Chem., Int. Ed. Engl.* **2015**, *54* (38), 11254−11258.
(117) Hayakawa, Y.; Sasaki, K.; Adachi, H.; Furihata, K.; Nagai, K.; Shin-ya, K. Thioviridamide, a novel apoptosis inducer in transformed cells from Streptomyces olivoviridis. *J. Antibiot (Tokyo)* **2006**, *59* (1), 1−5.

(118) Hayakawa, Y.; Sasaki, K.; Nagai, K.; Shin-ya, K.; Furihata, K. Structure of thioviridamide, a novel apoptosis inducer from Streptomyces olivoviridis. *J. Antibiot (Tokyo)* **2006**, *59* (1), 6−10.
(119) Izumikawa, M.; Kozone, I.; Hashimoto, J.; Kagaya, N.; Takagi, M.; Koiwai, H.; Komatsu, M.; Fujie, M.; Satoh, N.; Ikeda, H.; et al. Novel thioviridamide derivative-JBIR-140: heterologous expression of the gene cluster for thioviridamide biosynthesis. *J. Antibiot (Tokyo)* **2015**, *68* (8), 533−536.
(120) Kawahara, T.; Izumikawa, M.; Kozone, I.; Hashimoto, J.; Kagaya, N.; Koiwai, H.; Komatsu, M.; Fujie, M.; Sato, N.; Ikeda, H.; et al. Neothioviridamide, a Polythioamide Compound Produced by Heterologous Expression of a Streptomyces sp. Cryptic RiPP Biosynthetic Gene Cluster. *J. Nat. Prod* **2018**, *81* (2), 264−269.
(121) Frattaruolo, L.; Lacret, R.; Cappello, A. R.; Truman, A. W. A Genomics-Based Approach Identifies a Thioviridamide-Like Compound with Selective Anticancer Activity. *ACS Chem. Biol.* **2017**, *12* (11), 2815−2822.
(122) Frattaruolo, L.; Fiorillo, M.; Brindisi, M.; Curcio, R.; Dolce, V.; Lacret, R.; Truman, A. W.; Sotgia, F.; Lisanti, M. P.; Cappello, A. R. Thioalbamide, A Thioamidated Peptide from Amycolatopsis alba, Affects Tumor Growth and Stemness by Inducing Metabolic Dysfunction and Oxidative Stress. *Cells* **2019**, *8* (11), 1408.
(123) Kjaerulff, L.; Sikandar, A.; Zaburannyi, N.; Adam, S.; Herrmann, J.; Koehnke, J.; Müller, R. Thioholgamides: Thioamide-Containing Cytotoxic RiPP Natural Products. *ACS Chem. Biol.* **2017**, *12* (11), 2837−2841.
(124) Li, Y. Q.; Liu, J. Y.; Tang, H. Y.; Qiu, Y. P.; Chen, D. D.; Liu, W. Discovery of New Thioviridamide-Like Compounds with Antitumor Activities. *Chin. J. Chem.* **2019**, *37* (10), 1015−1020.
(125) Shin-ya, K.; Wierzba, K.; Matsuo, K.; Ohtani, T.; Yamada, Y.; Furihata, K.; Hayakawa, Y.; Seto, H. Telomestatin, a novel telomerase inhibitor from Streptomyces anulatus. *J. Am. Chem. Soc.* **2001**, *123* (6), 1262−1263.
(126) Sohda, K. Y.; Nagai, K.; Yamori, T.; Suzuki, K.; Tanaka, A. YM-216391, a novel cytotoxic cyclic peptide from Streptomyces nobilis. I. fermentation, isolation and biological activities. *J. Antibiot (Tokyo)* **2005**, *58* (1), 27−31.
(127) Sohda, K. Y.; Hiramoto, M.; Suzumura, K.; Takebayashi, Y.; Suzuki, K.; Tanaka, A. YM-216391, a novel cytotoxic cyclic peptide from Streptomyces nobilis. II. Physico-chemical properties and structure elucidation. *J. Antibiot (Tokyo)* **2005**, *58* (1), 32−36.
(128) Kanoh, K.; Matsuo, Y.; Adachi, K.; Imagawa, H.; Nishizawa, M.; Shizuri, Y. Mechercharmycins A and B, cytotoxic substances from marine-derived Thermoactinomyces sp. YM3−251. *J. Antibiot (Tokyo)* **2005**, *58* (4), 289−292.
(129) Matsuo, Y.; Kanoh, K.; Yamori, T.; Kasai, H.; Katsuta, A.; Adachi, K.; Shin-Ya, K.; Shizuri, Y. Urukthapelstatin A, a novel cytotoxic substance from marine-derived Mechercharimyces asporophorigenens YM11−542. I. Fermentation, isolation and biological activities. *J. Antibiot (Tokyo)* **2007**, *60* (4), 251−255.
(130) Matsuo, Y.; Kanoh, K.; Imagawa, H.; Adachi, K.; Nishizawa, M.; Shizuri, Y. Urukthapelstatin A, a novel cytotoxic substance from marine-derived Mechercharimyces asporophorigenens YM11−542. II. Physico-chemical properties and structural elucidation. *J. Antibiot (Tokyo)* **2007**, *60* (4), 256−260.
(131) Skinnider, M. A.; Johnston, C. W.; Edgar, R. E.; Dejong, C. A.; Merwin, N. J.; Rees, P. N.; Magarvey, N. A. Genomic charting of ribosomally synthesized natural product chemical space facilitates targeted mining. *Proc. Natl. Acad. Sci. U. S. A.* **2016**, *113* (42), E6343−E6351.
(132) Pei, Z. F.; Yang, M. J.; Li, L.; Jian, X. H.; Yin, Y.; Li, D.; Pan, H. X.; Lu, Y.; Jiang, W.; Tang, G. L. Directed production of aurantizolicin and new members based on a YM-216391 biosynthetic system. *Org. Biomol Chem.* **2018**, *16* (48), 9373−9376.
(133) Kaweewan, I.; Komaki, H.; Hemmi, H.; Hoshino, K.; Hosaka, T.; Isokawa, G.; Oyoshi, T.; Kodani, S. Isolation and structure determination of a new cytotoxic peptide, curacozole, from Streptomyces curacoi based on genome mining. *J. Antibiot (Tokyo)* **2019**, *72* (1), 1−7.
(134) Pei, Z. F.; Yang, M. J.; Zhang, K.; Jian, X. H.; Tang, G. L. Heterologous characterization of mechercharmycin A biosynthesis reveals alternative insights into post-translational modifications for RiPPs. *Cell Chem. Biol.* **2022**, *29* (4), 650−659.
(135) Freeman, M. F.; Gurgui, C.; Helf, M. J.; Morinaka, B. I.; Uria, A. R.; Oldham, N. J.; Sahl, H. G.; Matsunaga, S.; Piel, J. Metagenome mining reveals polytheonamides as posttranslationally modified ribosomal peptides. *Science* **2012**, *338* (6105), 387−390.
(136) Hamada, T.; Sugawara, T.; Matsunaga, S.; Fusetani, N. Polytheonamides, unprecedented highly cytotoxic polypeptides, from the marine sponge theonella swinhoei. *Tetrahedron Lett.* **1994**, *35* (5), 719−720.
(137) Iwamoto, M.; Shimizu, H.; Muramatsu, I.; Oiki, S. A cytotoxic peptide from a marine sponge exhibits ion channel activity through vectorial-insertion into the membrane. *FEBS Lett.* **2010**, *584* (18), 3995−3999.
(138) Bhushan, A.; Egli, P. J.; Peters, E. E.; Freeman, M. F.; Piel, J. Genome mining- and synthetic biology-enabled production of hypermodified peptides. *Nat. Chem.* **2019**, *11* (10), 931−939.
(139) Son, S.; Jang, M.; Lee, B.; Hong, Y. S.; Ko, S. K.; Jang, J. H.; Ahn, J. S. Ulleungdin, a Lasso Peptide with Cancer Cell Migration Inhibitory Activity Discovered by the Genome Mining Approach. *J. Nat. Prod* **2018**, *81* (10), 2205−2211.
(140) Hanahan, D.; Weinberg, R. A. Hallmarks of cancer: the next generation. *Cell* **2011**, *144* (5), 646−674.
(141) Guerrero-Garzon, J. F.; Madland, E.; Zehl, M.; Singh, M.; Rezaei, S.; Aachmann, F. L.; Courtade, G.; Urban, E.; Ruckert, C.; Busche, T.; et al. Class IV Lasso Peptides Synergistically Induce Proliferation of Cancer Cells and Sensitize Them to Doxorubicin. *iScience* **2020**, *23* (12), 101785.
(142) Vanyolos, A.; Dekany, M.; Kovacs, B.; Kramos, B.; Berdi, P.; Zupko, I.; Hohmann, J.; Beni, Z. Gymnopeptides A and B, Cyclic Octadecapeptides from the Mushroom Gymnopus fusipes. *Org. Lett.* **2016**, *18* (11), 2688−2691.
(143) Quijano, M. R.; Zach, C.; Miller, F. S.; Lee, A. R.; Imani, A. S.; Kunzler, M.; Freeman, M. F. Distinct Autocatalytic alpha- N-Methylating Precursors Expand the Borosin RiPP Family of Peptide Natural Products. *J. Am. Chem. Soc.* **2019**, *141* (24), 9637−9644.
(144) Cegłowska, M.; Szubert, K.; Wieczerzak, E.; Kosakowska, A.; Mazur-Marzec, H. Eighteen New Aeruginosamide Variants Produced by the Baltic Cyanobacterium Limnoraphis CCNP1324. *Mar Drugs* **2020**, *18* (9), 446.
(145) Ishitsuka, M. O.; Kusumi, T.; Kakisawa, H.; Kaya, K.; Watanabe, M. M. Microviridin. A novel tricyclic depsipeptide from the toxic cyanobacterium Microcystis viridis. *J. Am. Chem. Soc.* **1990**, *112* (22), 8180−8182.
(146) Vegman, M.; Carmeli, S. Three aeruginosins and a microviridin from a bloom assembly of Microcystis spp. collected from a fishpond near Kibbutz Lehavot HaBashan, Israel. *Tetrahedron* **2014**, *70* (38), 6817−6824.
(147) Murakami, M.; Sun, Q.; Ishida, K.; Matsuda, H.; Okino, T.; Yamaguchi, K. Microviridins, elastase inhibitors from the cyanobacterium Nostoc minutum (NIES-26). *Phytochemistry* **1997**, *45* (6), 1197−1202.
(148) Ahmed, M. N.; Reyna-Gonzalez, E.; Schmid, B.; Wiebach, V.; Sussmuth, R. D.; Dittmann, E.; Fewer, D. P. Phylogenomic Analysis of the Microviridin Biosynthetic Pathway Coupled with Targeted Chemo-Enzymatic Synthesis Yields Potent Protease Inhibitors. *ACS Chem. Biol.* **2017**, *12* (6), 1538−1546.
(149) Gatte-Picchi, D.; Weiz, A.; Ishida, K.; Hertweck, C.; Dittmann, E. Functional analysis of environmental DNA-derived microviridins provides new insights into the diversity of the tricyclic peptide family. *Appl. Environ. Microbiol.* **2014**, *80* (4), 1380−1387.
(150) Weiz, A. R.; Ishida, K.; Makower, K.; Ziemert, N.; Hertweck, C.; Dittmann, E. Leader peptide and a membrane protein scaffold guide the biosynthesis of the tricyclic peptide microviridin. *Chem. Biol.* **2011**, *18* (11), 1413−1421.
(151) Sieber, S.; Grendelmeier, S. M.; Harris, L. A.; Mitchell, D. A.; Gademann, K. Microviridin 1777: A Toxic Chymotrypsin Inhibitor

Discovered by a Metabologenomic Approach. *J. Nat. Prod* **2020**, *83* (2), 438−446.
(152) Unno, K.; Kaweewan, I.; Nakagawa, H.; Kodani, S. Heterologous expression of a cryptic gene cluster from Grimontia marina affords a novel tricyclic peptide grimoviridin. *Appl. Microbiol. Biotechnol.* **2020**, *104* (12), 5293−5302.
(153) Weiz, A. R.; Ishida, K.; Quitterer, F.; Meyer, S.; Kehr, J. C.; Müller, K. M.; Groll, M.; Hertweck, C.; Dittmann, E. Harnessing the evolvability of tricyclic microviridins to dissect protease-inhibitor interactions. *Angew. Chem., Int. Ed. Engl.* **2014**, *53* (14), 3735−3738.
(154) Reyna-Gonzalez, E.; Schmid, B.; Petras, D.; Sussmuth, R. D.; Dittmann, E. Leader Peptide-Free In Vitro Reconstitution of Microviridin Biosynthesis Enables Design of Synthetic Protease-Targeted Libraries. *Angew. Chem., Int. Ed. Engl.* **2016**, *55* (32), 9398−9401.
(155) Lee, H.; Park, Y.; Kim, S. Enzymatic Cross-Linking of Side Chains Generates a Modified Peptide with Four Hairpin-like Bicyclic Repeats. *Biochemistry* **2017**, *56* (37), 4927−4930.
(156) Lee, C.; Lee, H.; Park, J. U.; Kim, S. Introduction of Bifunctionality into the Multidomain Architecture of the omega-Ester-Containing Peptide Plesiocin. *Biochemistry* **2020**, *59* (3), 285−289.
(157) Zhao, G.; Kosek, D.; Liu, H. B.; Ohlemacher, S. I.; Blackburne, B.; Nikolskaya, A.; Makarova, K. S.; Sun, J.; Barry Iii, C. E.; Koonin, E. V.; et al. Structural Basis for a Dual Function ATP Grasp Ligase That Installs Single and Bicyclic omega-Ester Macrocycles in a New Multicore RiPP Natural Product. *J. Am. Chem. Soc.* **2021**, *143* (21), 8056−8068.
(158) Unno, K.; Nakagawa, H.; Kodani, S. Heterologous production of new protease inhibitory peptide marinostatin E. *Biosci Biotechnol Biochem* **2021**, *85* (1), 97−102.
(159) Paoli, L.; Ruscheweyh, H. J.; Forneris, C. C.; Hubrich, F.; Kautsar, S.; Bhushan, A.; Lotti, A.; Clayssen, Q.; Salazar, G.; Milanese, A.; et al. Biosynthetic potential of the global ocean microbiome. *Nature* **2022**, *607* (7917), 111−118.
(160) Smith, T. E.; Pond, C. D.; Pierce, E.; Harmer, Z. P.; Kwan, J.; Zachariah, M. M.; Harper, M. K.; Wyche, T. P.; Matainaho, T. K.; Bugni, T. S.; et al. Accessing chemical diversity from the uncultivated symbionts of small marine animals. *Nat. Chem. Biol.* **2018**, *14* (2), 179−185.
(161) Bosch, N. M.; Borsa, M.; Greczmiel, U.; Morinaka, B. I.; Gugger, M.; Oxenius, A.; Vagstad, A. L.; Piel, J. Landornamides: Antiviral Ornithine-Containing Ribosomal Peptides Discovered through Genome Mining. *Angew. Chem., Int. Ed. Engl.* **2020**, *59* (29), 11763−11768.
(162) Yang, X.; Lennard, K. R.; He, C.; Walker, M. C.; Ball, A. T.; Doigneaux, C.; Tavassoli, A.; van der Donk, W. A. A lanthipeptide library used to identify a protein-protein interaction inhibitor. *Nat. Chem. Biol.* **2018**, *14* (4), 375−380.
(163) van der Velden, N. S.; Kalin, N.; Helf, M. J.; Piel, J.; Freeman, M. F.; Kunzler, M. Autocatalytic backbone N-methylation in a family of ribosomal peptide natural products. *Nat. Chem. Biol.* **2017**, *13* (8), 833−835.
(164) Ramm, S.; Krawczyk, B.; Muhlenweg, A.; Poch, A.; Mosker, E.; Sussmuth, R. D. A Self-Sacrificing N-Methyltransferase Is the Precursor of the Fungal Natural Product Omphalotin. *Angew. Chem., Int. Ed. Engl.* **2017**, *56* (33), 9994−9997.
(165) Miller, F. S.; Crone, K. K.; Jensen, M. R.; Shaw, S.; Harcombe, W. R.; Elias, M. H.; Freeman, M. F. Conformational rearrangements enable iterative backbone N-methylation in RiPP biosynthesis. *Nat. Commun.* **2021**, *12* (1), 5355.
(166) Imani, A. S.; Lee, A. R.; Vishwanathan, N.; de Waal, F.; Freeman, M. F. Diverse Protein Architectures and alpha-N-Methylation Patterns Define Split Borosin RiPP Biosynthetic Gene Clusters. *ACS Chem. Biol.* **2022**, *17* (4), 908−917.
(167) Matabaro, E.; Kaspar, H.; Dahlin, P.; Bader, D. L. V.; Murar, C. E.; Staubli, F.; Field, C. M.; Bode, J. W.; Künzler, M. Identification, heterologous production and bioactivity of lentinulin A and dendrothelin A, two natural variants of backbone N-methylated peptide macrocycle omphalotin A. *Sci. Rep* **2021**, *11* (1), 3541.
(168) Liu, T.; Ma, X.; Yu, J.; Yang, W.; Wang, G.; Wang, Z.; Ge, Y.; Song, J.; Han, H.; Zhang, W.; et al. Rational generation of lasso peptides based on biosynthetic gene mutations and site-selective chemical modifications. *Chem. Sci.* **2021**, *12* (37), 12353−12364.
(169) Wyche, T. P.; Ruzzini, A. C.; Schwab, L.; Currie, C. R.; Clardy, J. Tryptorubin A: A Polycyclic Peptide from a Fungus-Derived Streptomycete. *J. Am. Chem. Soc.* **2017**, *139* (37), 12899−12902.
(170) Reisberg, S. H.; Gao, Y.; Walker, A. S.; Helfrich, E. J. N.; Clardy, J.; Baran, P. S. Total synthesis reveals atypical atropisomerism in a small-molecule natural product, tryptorubin A. *Science* **2020**, *367* (6476), 458−463.
(171) Nanudorn, P.; Thiengmag, S.; Biermann, F.; Erkoc, P.; Dirnberger, S. D.; Phan, T. N.; Fürst, R.; Ueoka, R.; Helfrich, E. J. N. Atropopeptides are a Novel Family of Ribosomally Synthesized and Posttranslationally Modified Peptides with a Complex Molecular Shape. *Angew. Chem., Int. Ed. Engl.* **2022**, *61* (41), No. e202208361.
(172) van Heel, A. J.; de Jong, A.; Song, C.; Viel, J. H.; Kok, J.; Kuipers, O. P. BAGEL4: a user-friendly web server to thoroughly mine RiPPs and bacteriocins. *Nucleic Acids Res.* **2018**, *46* (W1), W278−W281.
(173) Blin, K.; Wolf, T.; Chevrette, M. G.; Lu, X.; Schwalen, C. J.; Kautsar, S. A.; Suarez Duran, H. G.; de Los Santos, E. L. C.; Kim, H. U.; Nave, M.; et al. antiSMASH 4.0-improvements in chemistry prediction and gene cluster boundary identification. *Nucleic Acids Res.* **2017**, *45* (W1), W36−W41.